

Handbook T-I

Engineering and Architecture in the northern part of the State of Mexico

LÓPEZ-RAMÍREZ, Roberto

Coordinator

ECORFAN®

ECORFAN®

Coordinators

LÓPEZ-RAMÍREZ, Roberto. PhD

Editor in Chief

VARGAS-DELGADO, Oscar. PhD

Executive Director

RAMOS-ESCAMILLA, María. PhD

Editorial Director

PERALTA-CASTRO, Enrique. MsC

Web Designer

ESCAMILLA-BOUCHAN, Imelda. PhD

Web Diagrammer

LUNA-SOTO, Vladimir. PhD

Editorial Assistant

SORIANO-VELASCO, Jesús. BsC

Philologist

RAMOS-ARANCIBIA, Alejandra. BsC

ISBN: 978-607-8948-04-8

ECORFAN Publishing Label: 607-8948

HEA Control Number: 2023-05

HEA Classification (2023): 280923-0005

©ECORFAN-México, S.C.

No part of this writing protected by the Federal Copyright Law may be reproduced, transmitted or used in any form or by any means, graphic, electronic or mechanical, including, but not limited to, the following: Quotations in radio or electronic journalistic data compilation articles and bibliographic commentaries. For the purposes of articles 13, 162,163 fraction I, 164 fraction I, 168, 169,209 fraction III and other relative articles of the Federal Copyright Law. Infringements: Being compelled to prosecute under Mexican copyright law. The use of general descriptive names, registered names, trademarks, or trade names in this publication does not imply, even in the absence of a specific statement, that such names are exempt from the relevant protection in laws and regulations of Mexico and therefore free for general use by the international scientific community. HEA is part of ECORFAN Media (www.ecorfan.org)

Handbooks

Definition of Handbooks

Scientific Objectives

To support the International Scientific Community in its written production of Science, Technology and Innovation in the CONAHCYT and PRODEP research areas.

ECORFAN-Mexico, S.C. is a Scientific and Technological Company in contribution to the formation of Human Resources focused on the continuity in the critical analysis of International Research and is attached to the RENIECYT of CONAHCYT with number 1702902, its commitment is to disseminate research and contributions of the International Scientific Community, academic institutions, agencies and entities of the public and private sectors and contribute to the linkage of researchers who perform scientific activities, technological developments and training of specialized human resources with governments, businesses and social organizations.

To encourage the interlocution of the International Scientific Community with other study centres in Mexico and abroad and to promote a wide incorporation of academics, specialists and researchers to the serial publication in Science Niches of Autonomous Universities - State Public Universities - Federal IES - Polytechnic Universities - Technological Universities - Federal Technological Institutes - Teacher Training Colleges - Decentralised Technological Institutes - Intercultural Universities - S&T Councils - CONAHCYT Research Centres.

Scope, Coverage and Audience

Handbooks is a product edited by ECORFAN-Mexico S.C. in its Holding with repository in Mexico, it is a refereed and indexed scientific publication. It admits a wide range of contents that are evaluated by academic peers by the double-blind method, on topics related to the theory and practice of the CONAHCYT and PRODEP research areas respectively with diverse approaches and perspectives, which contribute to the dissemination of the development of Science, Technology and Innovation that allow arguments related to decision-making and influence the formulation of international policies in the field of Science. The editorial horizon of ECORFAN-Mexico® extends beyond academia and integrates other segments of research and analysis outside that field, as long as they meet the requirements of argumentative and scientific rigour, in addition to addressing issues of general and current interest of the International Scientific Society.

Editorial Board

ROCHA - RANGEL, Enrique. PhD
Oak Ridge National Laboratory

CARBAJAL - DE LA TORRE, Georgina. PhD
Université des Sciences et Technologies de Lille

GUZMÁN - ARENAS, Adolfo. PhD
Institute of Technology

CASTILLO - TÉLLEZ, Beatriz. PhD
University of La Rochelle

FERNANDEZ - ZAYAS, José Luis. PhD
University of Bristol

DECTOR - ESPINOZA, Andrés. PhD
Centro de Microelectrónica de Barcelona

TELOXA - REYES, Julio. PhD
Advanced Technology Center

HERNÁNDEZ - PRIETO, María de Lourdes. PhD
Universidad Gestalt

CENDEJAS - VALDEZ, José Luis. PhD
Universidad Politécnica de Madrid

HERNANDEZ - ESCOBEDO, Quetzalcoatl Cruz. PhD
Universidad Central del Ecuador

Arbitration Committee

VALERDI, Ricardo. PhD
Universidad de Arizona

RODRIGUEZ - ROBLEDO, Gricelda. PhD
Universidad Tecnológica de Morelia

CENDEJAS José. PhD
Universidad Tecnológica de Morelia

CORTES - MORALES, Griselda. PhD
Universidad Autónoma de Coahuila

FERREIRA - MEDINA, Heberto. PhD
Institute of Research in Ecosystems - UNAM Campus Morelia

GONZÁLEZ - SILVA, Marco Antonio. PhD
Universidad Politécnica Metropolitana de Hidalgo

CRUZ - BARRAGÁN, Aidee. PhD
Universidad de la Sierra Sur

PALMA, Oscar. PhD
Instituto Tecnológico de Conkal

BARRON, Juan. PhD
Universidad Tecnológica de Jalisco

SANDOVAL - GUTIÉRREZ, Jacobo. PhD
Universidad Autónoma Metropolitana

Assignment of Rights

By submitting a Scientific Work to ECORFAN Handbooks, the author undertakes not to submit it simultaneously to other scientific publications for consideration. To do so, the author must complete the Originality Form for his or her Scientific Work.

The authors sign the Authorisation Form for their Scientific Work to be disseminated by the means that ECORFAN-Mexico, S.C. in its Holding Mexico considers pertinent for the dissemination and diffusion of their Scientific Work, ceding their Scientific Work Rights.

Declaration of Authorship

Indicate the name of 1 Author and a maximum of 3 Co-authors in the participation of the Scientific Work and indicate in full the Institutional Affiliation indicating the Unit.

Identify the name of 1 author and a maximum of 3 co-authors with the CVU number -PNPC or SNI-CONAHCYT- indicating the level of researcher and their Google Scholar profile to verify their citation level and H index.

Identify the Name of 1 Author and 3 Co-authors maximum in the Science and Technology Profiles widely accepted by the International Scientific Community ORC ID - Researcher ID Thomson - arXiv Author ID - PubMed Author ID - Open ID respectively.

Indicate the contact for correspondence to the Author (Mail and Telephone) and indicate the Contributing Researcher as the first Author of the Scientific Work.

Plagiarism Detection

All Scientific Works will be tested by the PLAGSCAN plagiarism software. If a Positive plagiarism level is detected, the Scientific Work will not be sent to arbitration and the receipt of the Scientific Work will be rescinded, notifying the responsible Authors, claiming that academic plagiarism is typified as a crime in the Penal Code.

Refereeing Process

All Scientific Works will be evaluated by academic peers using the Double Blind method. Approved refereeing is a requirement for the Editorial Board to make a final decision which will be final in all cases. MARVID® is a spin-off brand of ECORFAN® specialised in providing expert reviewers all of them with PhD degree and distinction of International Researchers in the respective Councils of Science and Technology and the counterpart of CONAHCYT for the chapters of America-Europe-Asia-Africa and Oceania. The identification of authorship should only appear on a first page, which can be removed, in order to ensure that the refereeing process is anonymous and covers the following stages: Identification of ECORFAN Handbooks with their author occupancy rate - Identification of Authors and Co-authors - PLAGSCAN Plagiarism Detection - Review of Authorisation and Originality Forms-Assignment to the Editorial Board - Assignment of the pair of Expert Referees - Notification of Opinion - Statement of Observations to the Author - Modified Scientific Work Package for Editing - Publication.

ECORFAN Engineering and architecture in the northern part of the State of Mexico

Volume I

The Handbook will offer volumes of selected contributions from researchers who contribute to the scientific dissemination activity of the Tecnológico de Estudios Superiores de Jocotitlán in their areas of research in Social Sciences. In addition to having a total evaluation, in the hands of the directors of the Tecnológico de Estudios Superiores de Jocotitlán, the quality and timeliness of its chapters, each individual contribution was refereed to international standards (RESEARCH GATE, MENDELEY, GOOGLE SCHOLAR and REDIB), the Handbook thus proposes to the academic community, recent reports on new developments in the most interesting and promising areas of research in the Social Sciences.

López-Ramírez, Roberto

Coordinator

Engineering and architecture in the northern part of the State of Mexico T-I *Handbooks*

Tecnológico de Estudios Superiores de Jocotitlán

September, 2023

DOI: 10.35429/H.2023.5.1.142

Preface

The handbook “Engineering and Architecture in the northern part of the State of Mexico” aims to disseminate works in the areas of Engineering (Electronics, Mechanics, Chemistry and Materials) and architecture, generated by academics from the Tecnológico de Estudios Superiores de Jocotitlan. As in all higher education institutions, the documentation and publication of the most outstanding results of recent work that are the result of the natural and daily work of academic life, are part of the continuous work that is carried out, in addition to the already so well-known teaching. Student participation is reflected in the presence of their authorship in several chapters that are integrated into this Handbook; supporting the professional training of those who are the origin of education. It can also be mentioned that the participation of collegiate bodies, identified as professors with a PRODEP profile and members of academic bodies within this Handbook, allows contributing to the institutional strengthening of the Tecnológico de Estudios Superiores de Jocotitlán. The content is intended for general and technical reading by anyone who is interested in the topic and also by those who can learn what this technology produces for the educational, industrial and research sectors. We sincerely hope that this text can also serve as a stimulus to those who have the idea of training in the areas of engineering and architecture, which are integrated in this Handbook.

Oguri, Escobar and Pretel, provide a sustainable and responsible solution to the current challenges facing construction, offering an ecological solution in the form of lattices made from recycled clothing. The importance of this proposal lies in its commitment to sustainability, addressing the need for learning to reduce environmental impact and advocating for a responsible approach to construction practices, *De La Cruz, Alberto, Mastache and Namigtle*, present a class E voltage amplifier, this is capable of generating an electric arc, thus producing a dielectric barrier discharge, *Garcia & Garcia* studied different filtration media such as zeolite, pumicite, tezontle, dolomite, ground corn straw, coconut fiber and biocalcium to analyze the physical-chemical interaction of these materials and the components of laundry gray water in a simple filtration process, *Soto, Martínez and Coutiño* carried out a comparative analysis between the results analytical and those obtained numerically from the stress concentration factor of a stepped flat bar subjected to traction, *Soriano, Mendoza, Lopez and Garcia* analyze electrically conductive adhesives for use in the manufacture of photovoltaic modules to propose a technological development to obtain greater efficiency In energy capture, they also studied polycrystalline cells and monocrystalline cells, *Corona, Namigtle, Mastache and López*, addressed the use of different Grove modules, with this it was possible to implement both control and visualization through simple graphical interfaces taking advantage of the Benefits offered by Python, *Salazar, Bernal and Sánchez*, carried out an analysis of the studies using sustainable materials with terms of biosorbents and biomaterials, mainly those applied in water, with the purpose of carrying out an analysis on the removal of different types of contaminants, both organic . as inorganic.

LÓPEZ-RAMÍREZ, Roberto

Content

	Page
1 Latticework based on epoxy resin and recycled clothing OGURI, Leticia, ESCOBAR, Marlem Guadalupe and PRETEL, Ana María	1-17
2 Design and Implement of a Class E Source for possible sputtering application and dielectric barrier discharge DE LA CRUZ-ESCOBAR Jorge, ALBERTO-SERRANO, Alejandro, MASTACHE-MASTACHE, Jorge Edmundo and NAMIGTLE-JIMENEZ, Jesús	18-28
3 Filtration as gray water treatment using conventional and unconventional adsorbent beds GARCIA-SANCHEZ, José Juan & GARCIA-GARCIA, Eduardo	29-46
4 Theoretical-numerical analysis of the stress concentration factor in a stepped bar in tension SOTO-MENDOZA, Gilberto, MARTÍNEZ-GARCÍA, José and COUTIÑO-MORENO, Elvis	47-60
5 Study of electrically conductive adhesives in the manufacture of photovoltaic modules SORIANO-VARGAS, Orlando, MENDOZA-HERNÁNDEZ, Raúl, LOPEZ, Roberto and GARCIA-SANCHEZ, José Juan	61-85
6 Raspberry Pi and grovepi with Python: Sensors, actuators and interfaces CORONA-SÁNCHEZ, Ernesto, NAMIGTLE-JIMENEZ, Jesús, MASTACHE-MASTACHE, Jorge Edmundo and LÓPEZ-RAMÍREZ, Roberto	86-110
7 Biosorbents and biomaterials: Application in the environment and in the health sector SALAZAR-PERALTA Araceli, BERNAL-MARTÍNEZ Lina Agustina and SÁNCHEZ-OROZCO Raymundo	111-122

Chapter 1 Latticework based on epoxy resin and recycled clothing

Capítulo 1 Celosias a base de resina epoxica y ropa reciclada

OGURI, Leticia†*, ESCOBAR, Marlem Guadalupe and PRETEL, Ana María

TecNM/Tecnológico de Estudios Superiores de Jocotitlán, Licenciatura en Arquitectura

ID 1st Author: *Leticia, Oguri* / **ORC ID:** 0000-0003-3723-9202, **Researcher ID Thomson:** AAX-2427-2021

ID 1st Co-author: *Marlem Guadalupe, Escobar* / **ORC ID:** 0000-0003-3079-3462

ID 2nd Co-author: *Ana María, Pretel* / **ORC ID:** 0000-0002-8508-8114

DOI: 10.35429/H.2023.5.1.17

L. Oguri, M. Escobar and A. Pretel

*leticia.oguri@tesjo.edu.mx

R. López (AA.) Engineering and Architecture in the Northern part of the State of Mexico. Handbooks-TI-©ECORFAN-Mexico, Estado de México, 2023

Abstract

This innovation project within the construction industry introduces a captivating and eco-friendly concept: the development of lattices using recycled materials, specifically recycled clothing. The aim of this initiative is to provide a sustainable and responsible solution to the current challenges faced in construction, with a particular focus on mitigating the industry's ecological footprint.

In the 21st century, the construction sector grapples with a pivotal challenge: to achieve sustainable and responsible production, while adhering to society's quality standards and demands, all the while minimizing environmental impact. Crucial to this endeavor is the integration of material recycling and the promotion of responsible construction practices that not only benefit the environment but also the local communities.

The primary value added by this proposal lies in its innovative and eco-conscious approach. By harnessing the potential of recycled clothing for the fabrication of lattices and ceiling lights, an environmentally sustainable alternative is presented, reducing reliance on finite natural resources, and curbing the accumulation of textile waste in landfills.

Among the noteworthy features of this project is its utilization of recycled materials in the manufacturing of construction elements. Additionally, it emphasizes the optimal use and efficiency of lattices and ceiling lights, ensuring long-lasting and durable performance.

Overall, this project highlights a promising avenue for the construction industry, offering an eco-friendly solution in the form of lattices made from recycled clothing. The significance of this proposal lies in its commitment to sustainability, addressing the pressing need to reduce environmental impact and championing a responsible approach to construction practices.

Textiles, Epoxy Resin, Innovation, Experimentation, Constructive Elements

Resumen

Este proyecto de innovación dentro de la industria de la construcción introduce un concepto cautivador y ecológico: el desarrollo de celosías utilizando materiales reciclados, específicamente ropa reciclada. El objetivo de esta iniciativa es proporcionar una solución sostenible y responsable a los desafíos actuales que enfrenta la construcción, con un enfoque en mitigar la huella ecológica de la industria.

En el siglo XXI, el sector de la construcción se enfrenta a un desafío fundamental: lograr una producción sostenible y responsable, al tiempo que se adhiere a los estándares y demandas de calidad de la sociedad, al tiempo que minimiza el impacto ambiental. Crucial para este esfuerzo es la integración del reciclaje de materiales y la promoción de prácticas de construcción responsables que no solo beneficien al medio ambiente sino también a las comunidades locales.

El principal valor añadido de esta propuesta reside en su enfoque innovador y respetuoso con el medio ambiente. Al aprovechar el potencial de la ropa reciclada para la fabricación de celosías y luces de techo, se presenta una alternativa ambientalmente sostenible, reduciendo la dependencia de recursos naturales finitos y frenando la acumulación de residuos textiles en vertederos.

Entre las características destacables de este proyecto destaca su utilización de materiales reciclados en la fabricación de elementos constructivos. Además, enfatiza el uso óptimo y la eficiencia de las celosías y las luces de techo, asegurando un rendimiento duradero y duradero.

En general, este proyecto destaca una vía prometedora para la industria de la construcción, ofreciendo una solución ecológica en forma de celosías hechas de ropa reciclada. La importancia de esta propuesta radica en su compromiso con la sostenibilidad, abordando la necesidad apremiante de reducir el impacto ambiental y defendiendo un enfoque responsable de las prácticas de construcción.

Textiles, Resina Epoxi, Innovación, Experimentación, Elementos Constructivos

1. Introduction

In this innovation project in the construction industry, a fascinating and eco-friendly proposal is addressed: the development of lattices and ceiling lights made from recycled materials, specifically, recycled clothing. This initiative seeks to offer a sustainable and responsible solution to current construction challenges, focusing on reducing the ecological footprint that this industry generates.

The construction industry faces a crucial challenge in the 21st century: to produce in a sustainable and responsible manner, complying with the quality standards and demands of society, while minimizing environmental impact. It is essential that buildings and infrastructures are built considering the recycling of materials and promoting responsible construction practices that benefit the environment and the community.

The added value of this proposal lies in its innovative and environmentally conscious approach. By taking advantage of recycled clothing to manufacture lattices, a sustainable alternative to conventional materials is offered, reducing dependence on natural resources, and reducing the amount of textile waste that ends up in landfills.

Among the key characteristics of this proposal, the use of recycled materials for the preparation of the construction elements stands out. In addition, it focuses on the correct use and operation of the lattices, guaranteeing their efficiency and durability.

The problem to be solved is the high pollution generated by the construction industry by producing the traditional materials used in lattices and the textile industry. By adopting more sustainable construction practices, such as textile recycling, it seeks to mitigate this negative impact and move towards a more environmentally responsible industry.

The central hypothesis of this project is that, using recycled materials in the manufacture of lattices, it will be possible to significantly reduce the ecological footprint of the construction industry, thus contributing to the development of a more sustainable and respectful environment with the environment.

In summary, this innovative project proposes a promising solution for the construction industry, by offering lattices made from recycled clothing. The importance of this proposal lies in its sustainable approach, which seeks to reduce pollution and preserve the economic, social, and environmental values of the environment. By focusing on the recycling of materials and the reduction of the ecological footprint, this initiative represents a significant step towards a more conscious and responsible construction with the planet.

2. Development

Today, the reuse of clothing stands out to contribute to the environment by taking advantage of products with a longer useful life. Fashion, being a major industry, often wastes clothes that could meet people's needs. The textile industry, in constant growth, can generate income and recognition in the international market, being essential to consider options that promote care for the environment. Unfortunately, SEMARNAT (Ministry of the Environment and Natural Resources) indicated that in Mexico about 3.7 billion tons of textile waste are discarded per year and of that amount, only 1% is recycled. (See Fig.1)

Figure 1. Thousands of tons of textile waste



Reference Source: (Martell, 2022)

The textile industry has been identified by organizations such as the UN and Greenpeace as one of the main sources of environmental pollution, due to its high consumption of water, carbon emissions and generation of microplastics that affect the oceans and marine life. The incineration and accumulation of clothing in landfills aggravate soil and air pollution, accentuating environmental problems.

Faced with this problem, circular fashion has gained relevance, promoting giving a second, third and even fourth life to clothing to maximize its usefulness and reduce the mass consumption of textiles. (UN, 2022)

The promotion of alternatives to give garments a second use and support innovation projects that encourage reuse and sustainability in the construction industry is of the utmost importance today. The problem of textile waste and its environmental impact requires joint action by all social actors, including manufacturers, consumers, and the educational system.

The purpose of this article is to promote a deep reflection on the topic addressed, while presenting an innovative research project developed in the academic context of the degree in Architecture.

The research project focuses on the conception and creation of a Lattice made from textile waste, such as garments and fabrics.

The main objective of this proposal is to take optimal advantage of textile waste, investigating and evaluating its suitability as constructive elements. It seeks to verify their effectiveness and feasibility, with the intention of considering them as a friendly alternative to the environment and the process of recycling textiles in the field of construction.

The initiative is based on a scientific and rigorous approach, carried out from university classrooms, where research principles and analytical methods are applied to evaluate the feasibility and potential benefits of the Textile Lattice in the field of sustainable architecture.

By using terms from the scientific field, we proceed to the detailed characterization of the selected textile materials, analyzing their physical and mechanical properties, as well as their behavior in various environmental conditions. Likewise, the feasibility of integrating these textile elements in the construction process is examined, considering criteria of structural resistance, durability, and compatibility with other architectural components.

The approach is based on the premise of promoting eco-sustainable practices in the field of construction and explores how the use of these textile lattices could reduce waste generation and reduce the environmental footprint associated with the textile industry and traditional construction.

It is relevant to highlight that the project not only seeks to provide an environmentally friendly constructive alternative, but also to contribute to the promotion of the circular economy, promoting the reuse and recycling of textiles, which could have a positive impact on the textile industry and on waste management.

This research aims to provide a solid scientific and academic analysis that supports the use of textile trusses as a viable and efficient option in the field of sustainable construction. In this way, it seeks to encourage the adoption of architectural practices that are respectful of the environment and contribute to the development of a more conscious and responsible built environment.

Concepts

Lattice

It is an openwork decorative architectural element, which partially protects the views of lighting and ventilation where we usually place the windows or windows, but also, they work to give the project a style, this can be made of stucco, wood, stone, iron, clay, or any other material.

"Enclosure door, perforated, made of wood or iron, formed by a frame in which horizontal slats fit, spaced and inclined, in such a way that they allow one to look from the inside to the outside of an apartment without being able to see it from the outside." (Lajo and Surroca, 1997).

"Openwork board (wood or other material) that placed on a door or window makes it difficult to see inside a room" (Caballero, 2020).

Figure 2 Clay, metal, and wood lattices



Reference Source: (Ceramicaamanoalzada.com, Terrazacym.comConsumer.es, 2023)

Textile material

It is a solid and flexible material composed of filaments known as fibers, which are found vertically and horizontally intertwining with each other, which can be natural or synthetic, being the raw material for the manufacture of products (Warshaw, 2006).

“A flat structure, flexible enough to be able to be transformed into garments and textiles for domestic use, as well as for industrial uses where some flexibility is required (Hollen & Saddler, 2006)

Textile waste

They are fragments, scraps or pieces of fabric that are left over after the creation of a product in this case of design, and a large part of these are discarded, and another quantity is destined for sale.

“Those leftovers are more than just a physical manifestation of a chain of development and a segmented pattern cutting method” (Fletcher and Grose, 2012).

Resin

Also called liquid glass, it is a viscous substance, with a high density and solubility, with an intense odor and that reacts to the effect of heat. It is naturally obtained from the secretion of certain species of coniferous plants. (definicion.com, 2023).

Eco-friendly

Respectful of the environment (Neoma, 2023).

Eco-design

“It is a philosophy that seeks to design sustainable products and services that minimize the environmental impact throughout the product's life cycle from its design itself to production, use and withdrawal. To do this, environmental criteria are added to the conventional criteria of any design process (cost, utility, manufacturability, safety, etc.).

Eco-design then tries to identify the possible environmental aspects and impacts of a product/service based on the process of continuous improvement, which allows decisions to be made aimed at minimizing its impact on the environment” (Cámara de Comercio de España, 2023).

3. Methodology

The methodological approach of this research is based on a quasi-experimental design that is characterized by the management of non-randomized experimental variables in a controlled environment. This experimental approach involves the participation of students to foster research, creativity, and innovation, as well as promote awareness of important issues such as sustainability.

It is proposed to structure this research in three stages in the short, medium, and long term, to ensure the continuity of both the research work and the participation of the students throughout these periods. This phased approach will make it possible to progressively address the proposed objectives and will facilitate the collection of data over time for a more robust and conclusive analysis.

In addition, during the development of the study, relatively controlled conditions will be established to ensure the internal validity of the results obtained. This implies the implementation of measures to minimize possible confounding factors and ensure that the differences observed in the variables are attributable to the experimental treatment and not to other external influences.

The purpose of this research is to carry out a feasibility analysis of the module or construction component, which is based on an existing Lattice, incorporating Textile fibers and Epoxy Resin. To achieve this, various fundamental physical tests will be carried out to identify and demonstrate the physical properties of these elements. In addition, they will be compared with similar elements to detect possible advantages or deficiencies in the component. Likewise, new forms of construction will be explored to assess their potential in terms of efficiency, functionality, and sustainability, in line with lattice standards.

The study will focus on the evaluation of the physical properties resulting from the incorporation of Textile fibers and Epoxy Resin in the pre-existing Lattice. Scientific techniques and methods will be used to carry out the necessary tests and measurements. In addition, comparative analyzes will be applied between the modified module and similar elements to establish significant differences and determine their implications.

The focus of this research lies in the search for innovative and sustainable construction solutions, with the potential to improve the performance and functionality of trusses. It is expected that the results of this study will contribute to a better understanding of the properties and characteristics of the proposed module and allow the identification of opportunities for its practical application in the field of construction.

Within the research strategies, three phases have been outlined with specific objectives that will be carried out in the short, medium, and long term.

In the short-term phase:

- Documentary and field research will be carried out to collect relevant information, both bibliographic and obtained in situ.
- The nature of existing and/or commercial prototypes related to the subject of study will be analyzed and characterized.

In the medium-term phase:

- The textile materials that will be used in the investigation will be selected.
- The selection of the epoxy resin to be used in the project will also be carried out.
- The experimentation of the selected materials will be carried out, defining the samples and the appropriate proportions in the mixture of textiles and epoxy resin.
- The materials and the constructive element (prototype) will be subjected to non-specialized conventional tests.
- An exhaustive analysis of the results obtained in the tests will be carried out.

In the long-term phase:

- The construction processes necessary to produce the final element will be determined.
- Prototypes will be made on a real scale, following the guidelines established in the previous stages.
- The prototypes will undergo specialized laboratory tests, focusing on their strength and compression.
- A comparison will be made of the costs of the product in the current market with respect to other existing alternatives.
- A comprehensive analysis of the function, resistance and durability of the prototypes will be carried out.
- The benefits derived from the manufacture of ecological latticework, such as cost reduction and its functional advantages, will be identified, and quantified.
- The integration of the ecological Lattice in the construction market will be sought, with the aim of achieving national recognition of the product.
- With this methodological approach and planning for different terms, it is intended to obtain solid and well-founded results that allow a potential successful implementation of the ecological lattice in the construction sector, thus contributing to its sustainable development and its large-scale adoption.

- With this methodological approach and planning for different terms, it is intended to obtain solid and well-founded results that allow a potential successful implementation of the ecological lattice in the construction sector, thus contributing to its sustainable development and its large-scale adoption.
- As mentioned by Abdel & Abo (2023), it is also of utmost importance to consider the objective of savings in construction costs and affordability without leaving behind the main objective, which is structural performance and environmental benefits.

4. Results and discussion

Below are some of the research strategies that will be implemented in the medium-term stage, in the context of the prototyping process:

- Selection of Textile Materials and Epoxy Resin:

At this stage, a rigorous selection process will be carried out for the textile materials and the Epoxy Resin that will be used in the creation of the prototype. Different options available on the market will be evaluated and their physical, mechanical, and chemical properties will be considered to ensure that they are suitable for the prototype.

- Raw Material Elaboration Process:

Once the materials have been selected, the raw material will be prepared. This process may involve the preparation and conditioning of the textiles and the mixing of the epoxy resin with the appropriate components to obtain the desired characteristics in the prototype.

- Experimentation of Materials and Definition of Samples and Proportions:

At this stage, experiments and tests will be carried out to assess the properties of the selected materials and their behavior when combined in different proportions. The appropriate samples and mixtures will be defined to achieve the technical and functional specifications required in the prototype.

Materials

The prototype elaboration process will imply the use of textile materials and epoxy resin specifically selected for the project, scientific and technical criteria will be applied in the selection of these materials, considering their suitability for the prototype, and ensuring the quality and coherence of the results obtained.

It should be noted that this is only part of the research strategies, and it will be carried out in the medium-term phase. The research seeks to obtain substantiated and scientifically based results for the successful development of the prototype and its subsequent application in the corresponding field.

Recycled clothing

Reuse or reprocessing of used clothing, fibrous material, and clothing remains from the manufacturing process, this material is characterized according to its origin, whether natural or chemical, among the natural ones we have cotton, wool, silk, linen, leather, hemp, jute and chemicals rayon, cellophane, polyester, nylon, lycra (elastane), liocel, fleece, etc. (Hollen N. & Saddler, A. 2006).

Epoxy resin

It is a good thermal insulator, resists humidity, has adhesive properties, and resists high temperatures. Commercial brands of epoxy resin are made from a chemical reaction between two products: epichlorohydrin and bisphenol-a. The epoxy resin can react with catalytic homopolymerization (that is, with itself) or using co-reactives, such as acids, alcohols, phenols, thiols, and acid anhydrides. (Navarro, 2013)

Catalyst or peroxide

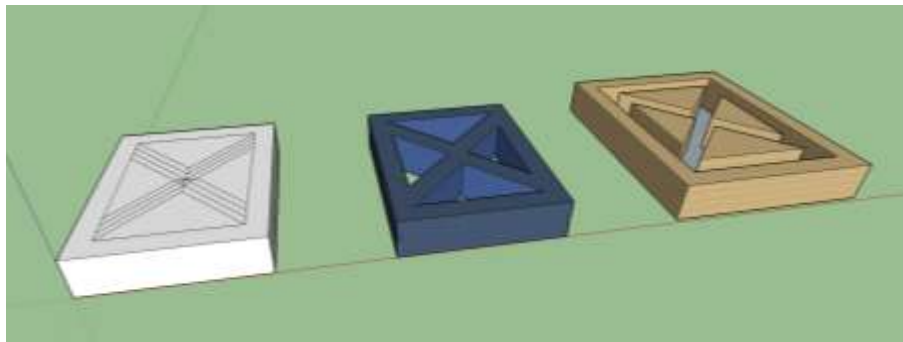
A resin catalyst is an organic peroxide in charge of making the reaction to harden the resin. (Navarro, 2013)

Experimental part

Mold for lattice

- a. Lattice design, dimensions 200 mm. x 250mm. x 50mm. A simple and conventional design was chosen for the element, so that it does not present problems when making the mold, but that it complies with the lattice concept, that partially protects the views from lighting and ventilation, hence the holes.

Figure 3 Lattice design



Reference Source: (Author's Own, 2023)

- b. Elaboration of the mold, based on waste Wood.

Figure 4 Wooden mold.



Reference Source: (Author's Own, 2023)

Process of elaboration of the raw material

- a. Collection of textile waste or used clothing, it must be sought that the material is free of impurities or dirt.

Figure 5 Collection of clothes



Reference Source: (Own Photo, 2023)

- b. Classification of Clothing or Textile Waste, the classification was carried out in denim, cotton, and synthetic clothing.

Figure 6 Clothing Classification



Reference Source: (Own Photo, 2023)

- c. Removal of buttons, zippers, or any metallic element to obtain a homogeneous material clean of dirt that may affect the preparation of the base material.

Figure 7 Removal of metal parts



Reference Source: (Own Photo, 2023)

- d. Reduction of the size of the material obtained by chopping or cutting through manual means where small pieces will be obtained, to improve its compaction.

Figure 8 Material size reduction



Reference Source: (Own Photo, 2023)

- e. Selection of epoxy resin

Epoxy resin floors ecopoxy epck11 transparent and catalyst

Figure 9 Bio-resina ecológica epck11



Reference Source: (Ecopoxy.com, 2023)

- f. The ecological Bio-Resin from EcoPoxy was chosen for its qualities such as transparency, non-yellowing, durability, and chemical resistance. low odor, low volatile organic compound content, non-toxic. 100% waterproof long term, excellent chemical resistance and toughness, high adhesion, self-priming on most surfaces, resists cracking, peeling, and chipping, dries in 48 hours, fills rough areas, low spots, and cracks, creates a uniform surface. (Ecopoxy.com, 2023)

Inside a container, the epoxy resin is prepared with the catalyst.

Figure 10 Resin preparation



Reference Source: (Own Photo, 2023)

- g. The mold is cleaned, and release agent (polyvinyl alcohol) is applied.
- h. Gradually add the pieces of fabric mixing vigorously so that the entire fabric is impregnated with the binder.
- i. Add the mixture into the mold.

Figure 11 Add the mixture to the mold



Reference Source: (Own by the author, 2023)

- j. It is applied under pressure inside the mold.

Figure 12 Pressure is applied to the entire mixture



Reference Source: (Own by the author, 2023)

- k. The mold is opened

Figure 13 Unmolded



Reference Source: (Own by the author, 2023)

- l. Air dried for the mixture to harden.

Figure 14 Weather drying



Reference Source: (Own by the author, 2023)

Preparation of mixtures

The experimentation of the first mixtures was carried out to analyze the behavior of the materials among themselves and a 250 x 200 x 50 mm mold built with plywood and strips of wood was taken as a base, for the casting of the mixtures.

Which were the following:

Table 1 Mixture dosages

Materiales	Unidades	Mezcla 1	Mezcla 2	Mezcla 3
textiles	grams	2000	2500	3000
epoxy resin	milliliters	500	500	500
catalyst	milliliters	100	125	250

(Own by the author, 2023)

Table 2 Drying time

Materiales	Mezcla 1	Mezcla 2	Mezcla 3
Hours	1080	720	552
Days	45	30	23

(Own by the author, 2023)

Mixture 1

A mix was made with 2000 grams of Textiles, 500 milliliters of epoxy resin, and 100 mm of catalyst. These materials were vigorously mixed in a single container and poured into the mold, according to the procedure described above. (See table1&2).

When carrying out this test, it was observed that the proportion of Textiles and epoxy resin was not adequate because the textiles absorb the resin quickly, the resin, when in contact with the textiles, begins to form a viscous mixture without achieving the proper accommodation of the material. Inside the mold, even applying pressure, the drying time is very slow during the process, and it takes 45 days for a semi-dry drying since the prototype, although it already has the hardness, to date still presents a sticky texture to the touch.

Mixture 2

A mixture of 2500 grams of Textiles, 500 milliliters of epoxy resin, and 125 milliliters of catalyst was made, this test showed that by increasing textile waste, epoxy resin is more manageable, although the mixture also took on a viscous consistency when mixed with the textiles however, it begins to have more stability achieving a better accommodation of the material inside the mold, the drying time outdoors took 30 days to have the pertinent hardness however the texture to the touch is still a bit sticky.

Mixture 3

A mix was made with 3000 grams of Textiles, 500 milliliters of epoxy resin, and 250 milliliters of catalyst. Analyzing this test, it was observed that by increasing the proportion of textile waste, and more catalyst to the resin, as the textiles were better, the resin was insufficient, leaving an uneven mixture also having more catalyst, the mixture began to harden more quickly inside the mixing container and wanting to incorporate it into the textiles is therefore the result of the little uniformity of the mix. The drying time outdoors took fewer days than the previous mixtures, which were 23 days though, an inhomogeneous prototype remained, and it continues to present that sticky consistency to the touch.

5. Thanks

To the Tecnológico de Estudios Superiores de Jocotitlán for the support received, for the realization of this investigation and experimentation of the prototype.

6. Conclusions

According to the test tests of the mixtures and the process of elaboration of the materials and methods, it is concluded that mixture 2 is the most viable for the elaboration of the prototype "lattice of recycled clothing and epoxy resin".

However, it was noted that the amount of resin and catalyst depends a lot on their proportions for the malleability of the mix and adhesion. The drying time is very susceptible to climate changes; however, a favorable result was obtained since the materials reacted adequately.

The lattice based on aggregates of textile waste and bio-resins can become a solution to current problems of contamination with textile waste, since it is considered, according to the UN, as the 4th most polluting worldwide and the environmental impact it causes is damage. irreversible to the lives of all living beings on the planet. The inclusion of the textile residue, with the bio-resin in the lattice was finally an alternative with viable results in the composition of the lattice as confirmed in the general objective.

It was verified that the project can be a sustainable construction element that can be an option to the existing lattices in the market to raise awareness about caring for the environment and reduce pollution from the construction industry.

The importance of this proposal lies in its sustainable approach, which seeks to reduce pollution and preserve the economic, social, and environmental values of the environment. By focusing on the recycling of materials and the reduction of the ecological footprint, this initiative represents a significant step towards a more conscious and responsible construction with the planet.

Knowing the properties of each material used will allow us to investigate more about the results that we could get, since each characteristic positively contributed to the lattice with benefits of stability, hardness, and aesthetics.

Because there are no specific standards for this type of material, such as construction elements based on textile waste, it will be based on the NMX-C-036-ONNCCE-2013 standard. This Mexican Standard establishes the test method for determining the compressive strength, which is applicable to blocks, partitions or bricks, partitions, lattices, and paving stones of national and imported manufacture, which are marketed in national territory.

Based on said standard, tests will be carried out to observe the behavior of the material during its process, it is important to mention that resistance, humidity, and fire tests will be carried out in accordance with the standards to specify the operation, test methods carried out for the lattice in which said samples will be tested according to the following standards:

NMX-C-441-ONNCCE-2005 Construction industry - Blocks, partitions or bricks and partitions for non-structural use - Specifications.

NMX-R-060-SCFI-2013.- "This Mexican standard establishes the properties of windows, doors and enclosures in order to guarantee users the quality and safety of these products in national territory."

"Applies to windows, enclosures, and doors in general, including roof windows, balcony doors and emergency pedestrian doors, which operate manually and/or motorized, with or without blinds, shutters and/or fixed and adjustable lattices, fixed and folding mosquito nets. or roll-up, regardless of the type of materials, including all the necessary fittings for its manufacture and installation".

This lattice is a product with radical innovation since there are only latticework made of conventional materials such as ceramic, plaster, wood, PVC, etc. without the use of textile waste or any other type of waste that allows recycling. The materials that were used in the lattice of this research make it a viable product, in addition to seeing the recycling of textile waste as the best alternative to reduce environmental impact.

It is important to mention that education plays a fundamental role in this task, since it is from the classrooms where environmental awareness can be formed and sensitize the new generations about the importance of adopting sustainable practices. By incorporating technological innovation proposals that involve constructive products from recycled clothing in the teaching-learning process, students are given the opportunity to understand how reuse can contribute to caring for the planet and building a more sustainable future.

Only through a coordinated and committed effort from all sectors of society, including education, will it be possible to face the challenge of textile pollution and move towards a more environmentally friendly fashion and construction industry. The adoption of these practices will not only contribute to reducing the environmental impact but will also foster a culture of responsible and sustainable consumption, thus benefiting present and future generations.

These research projects within educational institutions make it possible to generate new knowledge and propose solutions to problems that can be related to multiple aspects, which, in the medium and long term, can mean economic growth, improved productivity and the social development of a nation.

Architecture has direct effects on the living space, which is why it has taken this reality into account and is in constant search for innovation in other ways of building while adhering to sustainability.

7. References

Abdel Gelil Mohamed, N., & Abo Eldardaa Mahmoud, I. (2023). *Cost-effectiveness and affordability evaluation of a residential prototype built with compressed earth bricks, hybrid roofs and palm midribs*. *Frontiers in Built Environment*, 9, 1058782.

Caballero, J (2020) *Proyecto Artium: Diccionario visual de términos artísticos*, <https://es.scribd.com/doc/6222555/DICCIONARIO-VISUAL-DE-ARTE-1-A-K#>

Cámara de comercio de España, (2023), *Ecodiseño: Diseño de Productos-Servicios Sostenibles*, <https://www.camara.es/innovacion-y-competitividad/como-innovar/disenio-sostenible>

Ceramicaamanoalzada.com, (2023), *Celosia*, <https://ceramicaamanoalzada.com/celosia-diagonal-4-ejemplos-de-colocacion-en-fachada-e-interiorismo/>

Chowdhury, T. S., Mohsin, F. T., Tonni, M. M., Mita, M. N. H., & Ehsan, M. M. (2023). *A Critical Review on Gas Turbine Cooling Performance and Failure Analysis of Turbine Blades*. *International Journal of Thermofluids*, 100329

Consumer.es, (2023), *Celosía*, <https://www.consumer.es/bricolaje/celosias-utilidades-y-tipos.html>

Definición.com., (2023), *Resina epóxica*, <https://www.definicionabc.com/general/resina-epoxi.php>

Ecopoxy.com, (2023), *ecopoxy epclk11 transparente y catalizador*, <https://www.ecopoxy.com/>

Fletcher y Grose, (2012), *Gestionar la sostenibilidad en la moda*, E. Blume, Barcelona, I.S.B.N.:978-84-9801-594-1

Greenpeace, (2021), *Fast fashion: de tu armario al vertedero*, <https://www.greenpeace.org/mexico/blog/9514/fast-fashion/>

Hollen N. & Saddler, A. (2006), *Introducción a los textiles*, E. Limusa Noriega, Mexico, I.S.B.N.: 978-96-8181-898-2

Lajo, R. y Surroca, J. (1997), *Léxico de arte*, Editorial Akal, Ediciones, S.A. Madrid, España I.S.B.N.: 978-84-460-0924-5

Martell, C. (2022), *Industria textil de las más contaminantes y dañinas para el planeta*, <https://www.yoinfluyo.com/mexico/medio-ambiente/industria-textil-de-las-mas-contaminantes-y-daninas-para-el-planeta/>

Navarro, G. (2013), Desarrollo de un sistema fotocurable epoxi-amina/tiol-ene, E. Centro de aplicación de química avanzada, Saltillo, Coahuila, [Tesis], <https://ciqa.repositorioinstitucional.mx/jspui/handle/1025/26>

Neoma, (2023) Diccionario de neologismos del español actual, <https://www.um.es/neologismos/index.php/v/neologismo/4894/ecofriendly>

UN, (2023), *El costo ambiental de estar a la moda*, <https://news.un.org/es/story/2019/04/1454161>

SEMARNAT, (2023), *Residuos Sólidos Urbanos*, <https://www.gob.mx/semarnat/acciones-y-programas/clasificacion-reciclaje-y-valoracion-de-los-rsu>

Terrazacym.com, (2023), celosía, <https://terrazacym.com.mx/>

Warshaw, L., (2006), *Industrias textiles y de la confección, enciclopedia de salud y seguridad en el trabajo*, https://www.academia.edu/34766882/INDUSTRIA_DE_PRODUCTOS_TEXTILES

Chapter 2 Design and Implement of a Class E Source for possible sputtering application and dielectric barrier discharge

Capítulo 2 Diseño e Implementación de una Fuente Clase E con posible aplicación de pulverización catódica y descarga de barrera dieléctrica

DE LA CRUZ-ESCOBAR Jorge^{1,2,†*}, ALBERTO-SERRANO, Alejandro^{1,2}, MASTACHE-MASTACHE, Jorge Edmundo^{2,3} and NAMIGTLE-JIMENEZ, Jesús^{2,3}

¹*Estudiante TESJO, División de Ingeniería Mecatrónica*

²*TecNM/Tecnológico de Estudios Superiores de Jocotitlán*

³*Universidad de Ixtlahuaca, Facultad de Ingeniería*

ID 1st Author: *Jorge, De La Cruz-Escobar* / **ORC ID:** 0009-0004-7960-0080

ID 1st Co-author: *Alejandro, Alberto-Serrano* / **ORC ID:** 0009-0007-9952-1533

ID 2nd Co-author: *Jorge Edmundo, Mastache-Mastache* / **ORC ID:** 0000-0001-6104-6764, **CVU CONAHCYT ID:** 544943

ID 3rd Co-author: *Jesús, Namigtle-Jiménez* / **ORC ID:** 000-0002-0908-4592, **CVU CONAHCYT ID:** 624757

DOI: 10.35429/H.2023.5.18.28

J. De La Cruz, A. Alberto, J. Mastache and J. Namigtle

*jorge.mastache@tesjo.edu.mx

R. López (AA.) Engineering and Architecture in the Northern part of the State of Mexico. Handbooks-TI-©ECORFAN-Mexico, Estado de México, 2023

Abstract

In the following work, a class E voltage amplifier is presented, it can generate an electric arc, thus producing a dielectric barrier discharge (DBD). The design and assembly of this class E amplifier involves a proper selection of high-speed switching components, this amplifier topology was used due to its ability to maintain the transistors in an ideal switching state, thus reducing power losses during on and off transitions, as well as the losses that are due to dissipation. To be used to generate a dielectric barrier discharge, we rely on software model simulations and measurable experimental tests to get the most out of the amplifier's electrical characteristics, we implement a resonance technique thus improving the efficiency of the amplifier. To generate high power pulses between two electrodes and a dielectric thus manifesting dielectric barrier discharges for which we have designed an adjustable capacitive load, due to the numerous applications of a DBD such as plasma technology, surface treatment, modulation of power and ozone generation this research is relevant in industrial and scientific fields.

Amplifier, Discharges, Plasma, Resonance, Dielectric, Efficiency

Resumen

En el siguiente trabajo se presenta un amplificador de voltaje clase E, este es capaz de generar un arco eléctrico produciendo así una descarga de barrera dieléctrica (DBD). El diseño y armado de este amplificador clase E implica una selección adecuada de componentes de alta velocidad de conmutación, esta topología de amplificador fue usada debido a su capacidad para mantener los transistores en un estado de conmutación ideal reduciendo así las pérdidas de energía durante las transiciones de encendido y apagado, así como las pérdidas que son debido a la disipación. A fin de ser usado para generar una descarga de barrera dieléctrica, nos apoyamos de simulaciones del modelo por software y pruebas experimentales medibles para obtener el mayor provecho que las características eléctricas del amplificador puede otorgarnos, implementamos una técnica de resonancia mejorando así la eficiencia del amplificador para generar pulsos de alta potencia entre dos electrodos y un dieléctrico manifestando así descargas de barrera dieléctrica para lo cual hemos diseñado una carga capacitiva regulable, debido a las numerosas aplicaciones de una DBD como la tecnología de plasma, el tratamiento de superficies, la modulación de potencia y la generación de ozono de esta investigación resulta relevante en ámbitos industriales y científicos.

Amplificador, Descarga, Plasma, Resonancia, Dieléctrico, Eficiencia

1. Introduction

In a high-performance amplifier, it makes efficiency gains that at first glance seem minor, but can be very significant, for example, increasing efficiency from 80% to 90% halves losses (Laquidara , 2020). However, there is a fundamental trade-off between efficiency and linearity in power amplifiers (PAs). The classes of operation class A and AB offer in general very good linearity, but on the other hand they are very inefficient (Albulet, 2001). The basic amplification techniques are also known as classes of operation of power amplifiers and are classified as A, B, C, D, E (Lizárraga, 2009).

Class A amplifiers reach a maximum efficiency of 50%. Class A amplification is inherently linear; therefore, it is used in applications where low power, high linearity, high gain, broadband or high frequency operation are required (Kenington, 2000).

The maximum efficiency of the class B amplifier is 78.54%. For low signal levels, the class B AP (Power Amplifier) is more efficient than class A. This type of amplifier is generally used in a complementary configuration (push-pull) in such a way that the drain current adds to produce forms a sine wave with high linearity (Cripps, 2000).

In the class C amplifier, the conduction angle can be reduced to zero degrees to arbitrarily increase the efficiency up to 100%. Consequently, the output power is reduced to zero. A typical compromise between efficiency and power output is for a 150° conduction angle with an ideal efficiency of 85%, with very poor linearity (Krauss, 1980).

Class D amplifiers use two or more transistors which are toggled to generate a square waveform of drain voltage so that the amplifier acts as a switch mode voltage source and potentially reaches 90% efficiency. These APs are classified as high-efficiency amplifiers (Grennevikov 2012) y (Albulet, 2001). Class E amplifiers are a specialized type of amplifier designed to achieve high efficiency. Efficiency in this context refers to the ability to convert power from the power supply into useful output power while minimizing energy losses in the form of heat or other unwanted forms. Class E amplifier efficiency is achieved by careful design of the output signal waveform and operation of semiconductor devices.

This class of amplification uses a single MOSFET or transistor that operates as a switch and is classified as a high efficiency AP (Power Amplifier). The drain voltage waveform is the result of the sum of the DC current and the RF output current (Radio Frequency) charging and discharging the drain capacitor.

In optimal class E AP (Power Amplifier) operation, the drain voltage drops to zero and has zero slope just as the transistor is turned on, ideally there is no overlap of current and drain voltage, as a result the ideal efficiency is almost 100%, eliminating losses associated with charging and discharging parasitic drain capacitance as in the class D amplifier, reducing turn-on and turn-off losses and presenting good tolerance to component variation (Raab, 1978).

On the other hand, the same voltage ranges can be reached with different types of high voltage sources such as the Flyback topology which, when selected to generate the adequate AC signal, contemplates an approximation based on a natural commutation switch; This type of switching has the following advantages over forced switching:

1. The transformer has two windings (one primary and two secondary), which allow the voltages generated in auxiliary circuits to be used, taking advantage of a single magnetic core, reducing the use of passive components (Mammano, 2001).
2. The primary winding can be used as the main inductor of the resonant topology. This also makes it possible to set a natural frequency and a suitable capacitor.

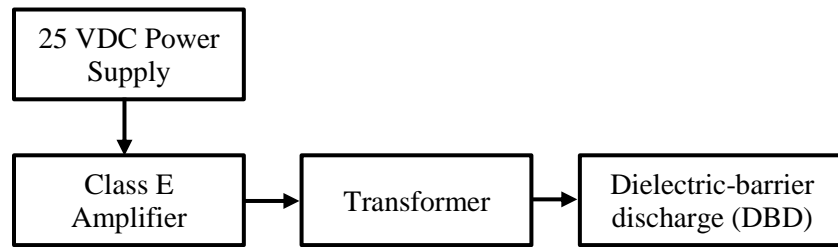
The isolated design of the source allows relating the powers consumed in both segments with Ohm's law. A design that uses sinusoidal signals considerably reduces the problem of high frequency overshoot that devices are subjected to in switched sources. Without these overshoots, the losses due to parasitic resistive components are also reduced (Pimentel Velázquez, 2022).

Due to the disadvantages of the flyback source such as power limitation, limited voltage regulation and even electromagnetic interference, it was decided for the design, calculation and manufacture of the class E voltage amplifier for its compact design, for the applications that They can be done with radio frequencies, but above all because of their high efficiency and even because of their ability to work at high frequencies before other types of power supplies capable of producing high voltages.

One of the main reasons for developing a Class E amplifier is the increasing demand for energy efficient devices and systems. Class E amplifiers offer remarkably high efficiency compared to other types of amplifiers. The purpose is to develop a system capable of generating a Dielectric Barrier Discharge to have a low-cost, highly efficient system that is stable under operating conditions.

2. Description of the method

Figure 1.1 shows a block diagram of the general project, which starts from a 25V DC voltage source which will provide the operating voltage of the Class E Amplifier, the voltage output provided by the amplifier is applied to a transformer which will raise the voltage that will later be applied to a capacitive charge, in which it seeks to generate a Dielectric Barrier discharge.

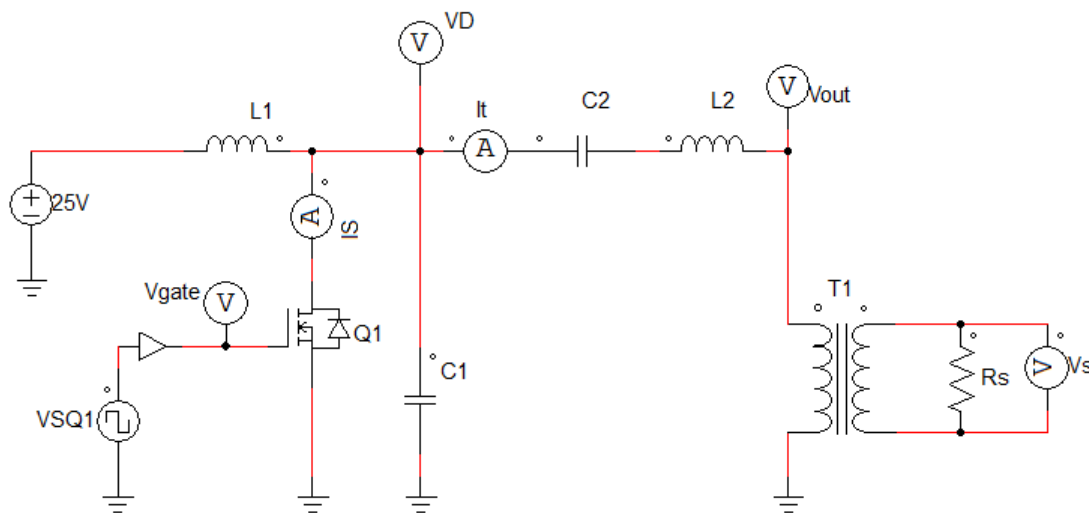
Figure 1.1 Block diagram of the proposed system

Consultation Source: Own Elaboration

3. Class E Amplifier Design

Figure 1.2 shows the blocks corresponding to the class E amplifier and the transformer, its construction is based on the switching of a Power semiconductor device (MOSFET Q1) operating as a switch acting in continuous conduction mode, which switches at the operating frequency. Determined by a PWM generator (VSQ1), a series LC resonant circuit (L2 and C2), a bypass capacitor (C1) and an inductor Lf (L1). In particular, the switch is turned on at zero voltage if the values of the resonant circuit components are chosen correctly. Since the switch current and voltage waveforms do not overlap during switching time intervals, switching losses are virtually zero, resulting in high efficiency.

The output voltage is then applied to a transformer (T1) with a ratio of 1:100 to raise the voltage in order to achieve the Dielectric Barrier Discharge.

Figure 1.2 Class E Amplifier Schematic Diagram

Consultation Source: Own Elaboration

4. Design Criteria

The parameters that must be considered for the design of the class E amplifier are explained in (Kazimierczuk, 2008). Table 1.1 shows the value of the necessary components taking the following specifications: $V_I = 25$ V, $D=0.5$, $P_{o\ max} = 50$ W, $Q_L = 14$ and $f = 125$ kHz.

Table 1.1 Class E Amplifier Component Values

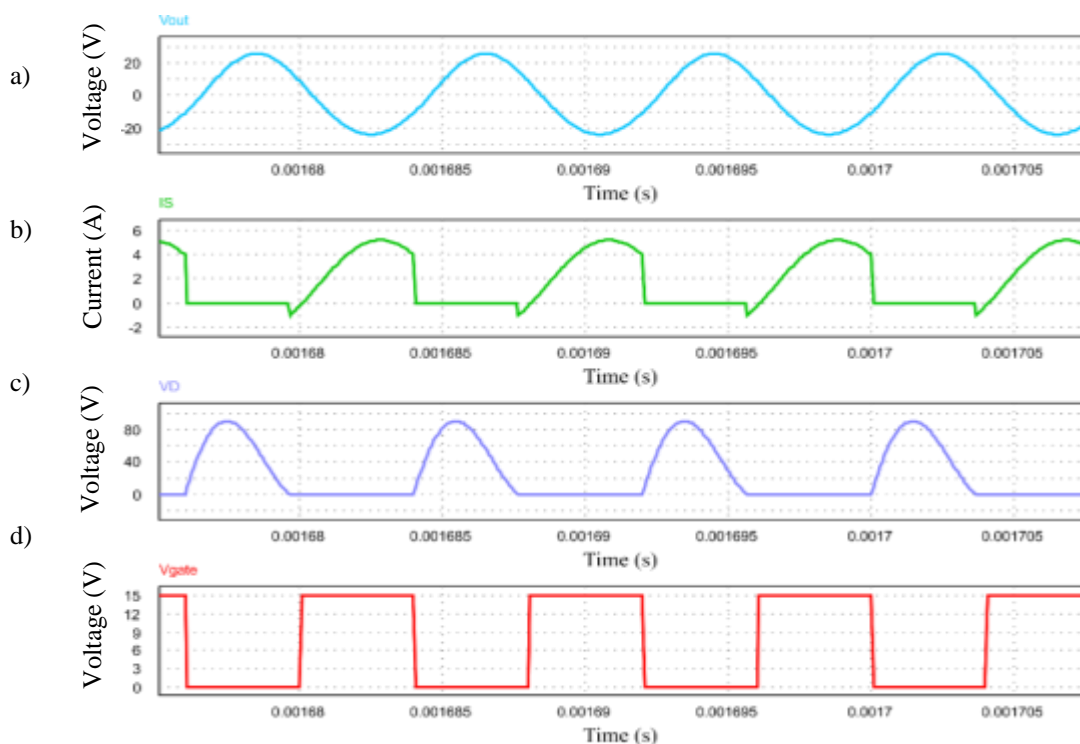
Variable	Description	Equation	Value
R	Load resistance	$\frac{8}{\pi^2+4} \frac{V_I^2}{P_o}$	7.21 Ω
V_{Rm}	Output voltage	$\frac{4}{\sqrt{\pi^2+4}} V_I$	26.8515 V
V_{SM}	Maximum voltage across the MOSFET	$3.562 V_I$	89.05 V
I_{SM}	Switching current	$\left(\frac{\sqrt{\pi^2+4}}{2} + 1\right) I_I$	5.724 A
$I_{S rms}$	MOSFET RMS Current	$\frac{I_I \sqrt{\pi^2+28}}{4}$	3.076 A
L	Resonant circuit load inductor	$\frac{Q_L R}{\omega}$	128.521 μH
C_1	shunt capacitor	$\frac{8}{\pi(\pi^2+4)\omega R}$	32.423 nF
C	Resonant circuit charge capacitor	$\frac{1}{\omega R \left[Q_L - \frac{\pi(\pi^2-4)}{16} \right]}$	13.745 nF
L_f	Choke inductance	$2 \left(\frac{\pi^2}{4} + 1 \right) \frac{R}{f}$	400.000 μH
R_s	Load resistance on the secondary of the transformer	$R n^2$	72100 Ω

Consultation Source: Own Elaboration

5. Simulation

The simulation software PSIM v 9.1 was used, to perform the simulation of the circuit in figure 1.2, the graphs shown in figure 1.3 are obtained, in which the waveforms at the voltage output of the class E amplifier are displayed (figure 1.3 a) with a voltage of 25.86Vp, the current flowing through the MOSFET (figure 1.3b) with a value of 5.1015Ap, as well as the voltage at the Drain terminal of the MOSFET (figure 1.3c) showing a value of 90.14 Vp, and its corresponding gate voltage (figure 1.3d), the operation of a ZVS occurs at the points where the MOSFET is cut off and likewise at the moment the MOSFET begins to conduct.

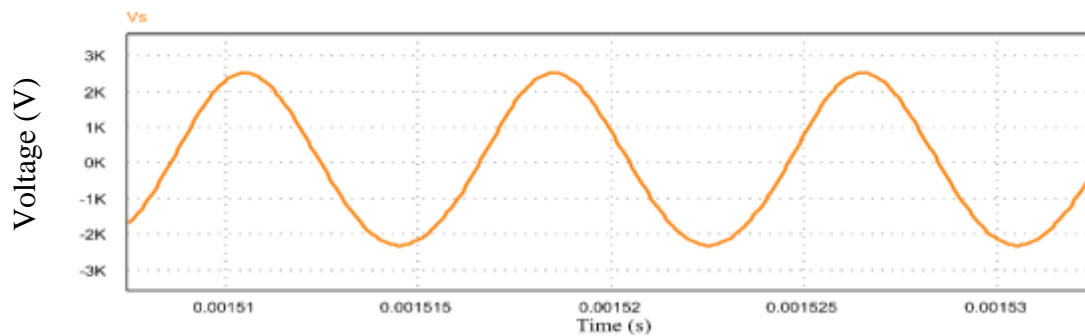
Figure 1.3 Voltage and current waveforms of the Class E Amplifier; a) Output voltage of the Class E Amplifier (V_{out}), b) Current through the MOSFET (I_S), c) Voltage at the DRAIN terminal (V_D), d) Voltage at the GATE terminal (V_{gate}).



Consultation Source: Own Elaboration

Graph 1.4 shows the voltage output of the transformer which gives a satisfactory voltage of 2.586kVp necessary to carry out the Dielectric Barrier Discharge, this considering a unitary coupling in the transformer.

Figure 1.4 Transformer Output

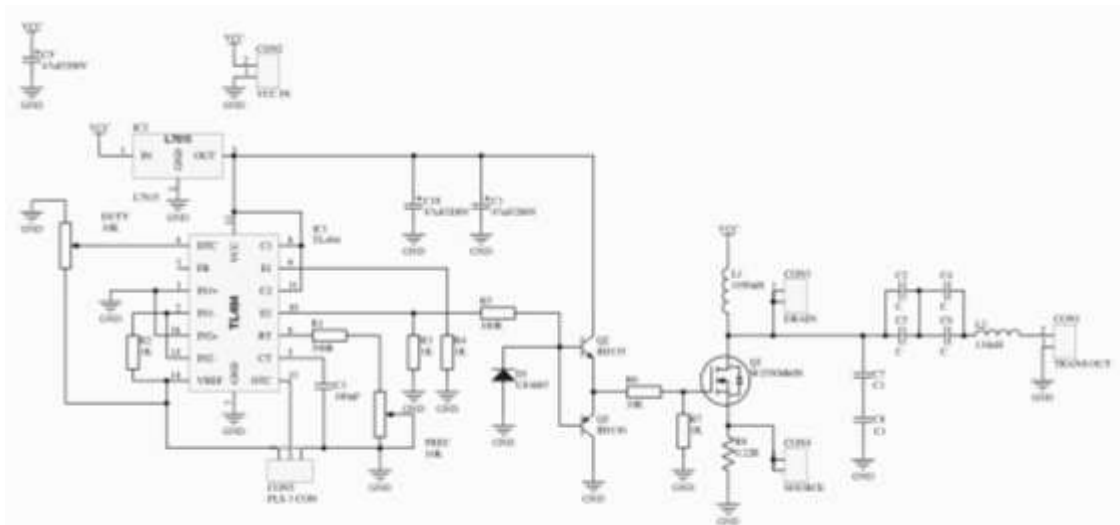


Consultation Source: Own Elaboration

7. Circuit Construction

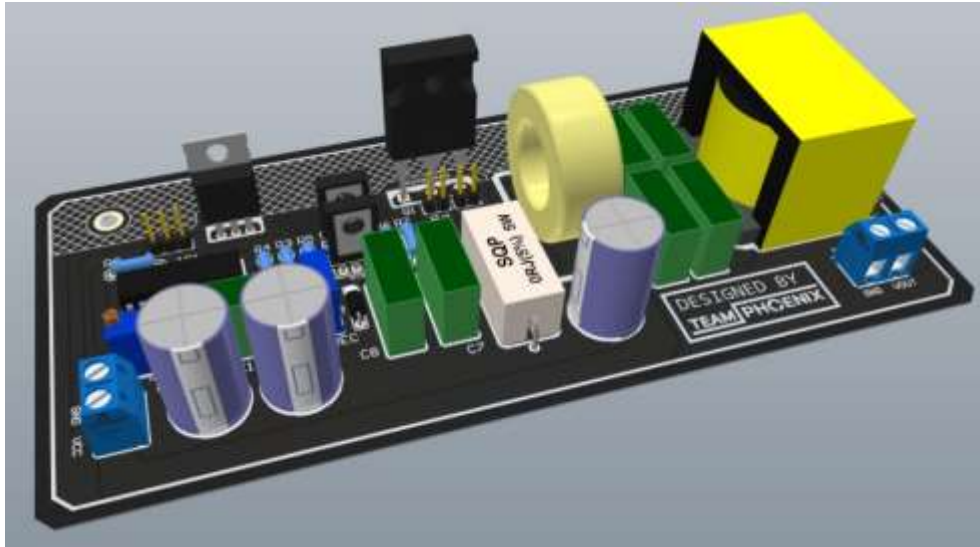
It was decided to use the design software Altium Designer for the realization of the circuit board (PCB, printed circuit board) of the Class E Amplifier, the complete circuit diagram is shown in figure 1.5.

Figure 1.5 Class E Amplifier Schematic



Consultation Source: Own Elaboration

The final design of the amplifier can be seen in figure 6 showing the (MOSFET) on the back, the TL494 located to the left of the board in charge of generating the PWM as well as the 2 transistors BD136 and BD135 that make up the driver for the MOSFET, the Choke inductance is made up of a T106-26 toroid, the inductance "L" and the capacitors that form "C" are observed on the right side of the plate.

Figure 1.6 3D Layout of Amplifier PCB

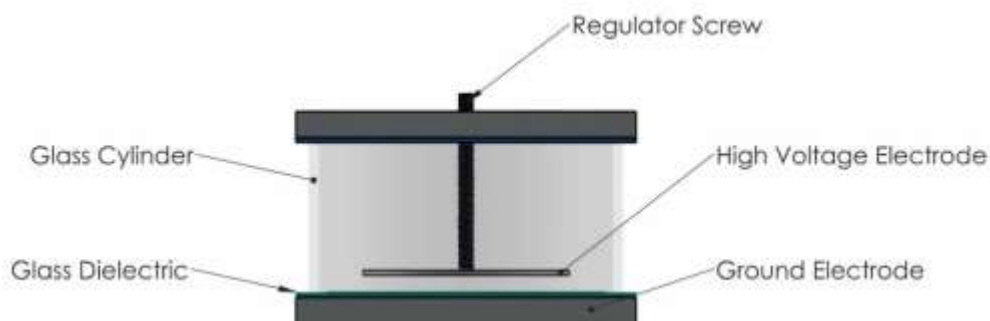
Consultation Source: Own Elaboration

8. Transformer Assembly

Figure 5 shows the transformer which was made based on a Ferroxcube EE55/28/21 ferrite core of 3C90 material, with the purpose of minimizing losses due to skin effect in the transformer conductors, the use of 280-wire litz cable for the primary winding of the transformer, 29-gauge enameled copper wire was used for the secondary winding. Special care was taken in the insulation between layers using polypropylene mica.

9. Dielectric Barrier Discharge

With the purpose of being able to vary the value of the impedance of the capacitive load, a design was chosen in which the separation of the plates can be adjusted, the load consists of a glass cylinder on which 2 aluminum covers are placed. , on one of them a glass dielectric is placed as an insulator to form the Dielectric Barrier Discharge, the second electrode is regulated from the adjustment of a screw that allows to vary the separation between plates as shown in the figure 1.7.

Figure 1. 7 Ozone generating cell design

Consultation Source: Own Elaboration

10. Experimental results

The final assembly of the prototype is shown in figure 1.8 where the class E amplifier, the transformer and the load are shown.

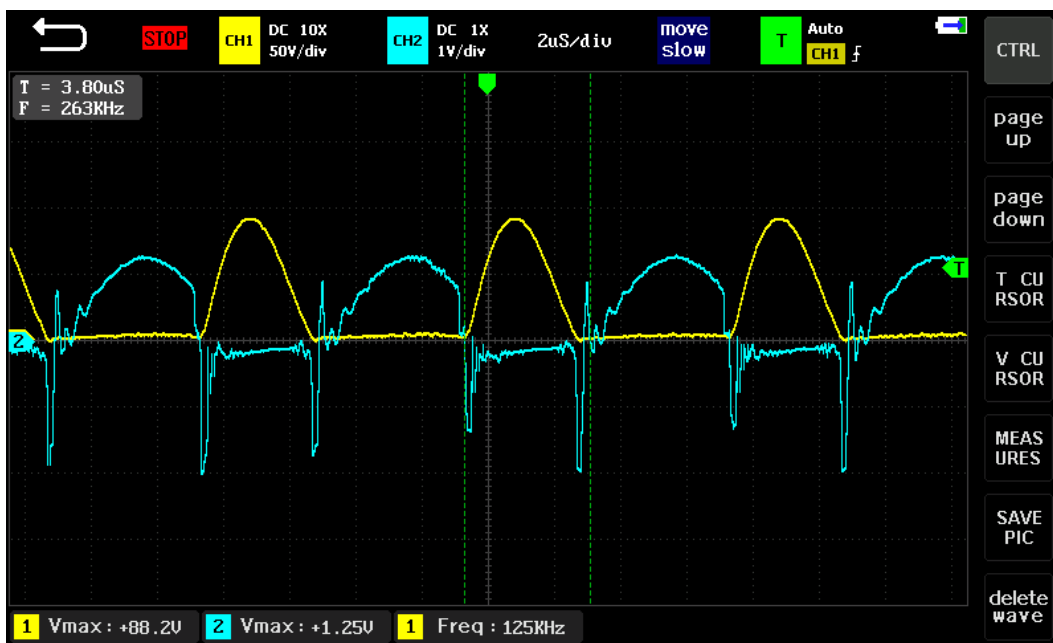
Figure 1.8 Assembly of the Prototype



Consultation Source: Own Elaboration

Figure 1.9 shows the waveform of the voltage at the Drain terminal of the MOSFET (yellow color) with a voltage of 88.2Vp, as well as the current flowing through the MOSFET (blue color) measured through a Shunt resistor with value of $0.22\ \Omega$ obtaining a current of 5.68Ap, due to the non-linearity of the real elements as well as parasitic elements not contemplated, small transients are observed in the current of up to 5.68Ap circulating through the MOSFET.

Figure 1.9 Voltage and Current on the MOSFET

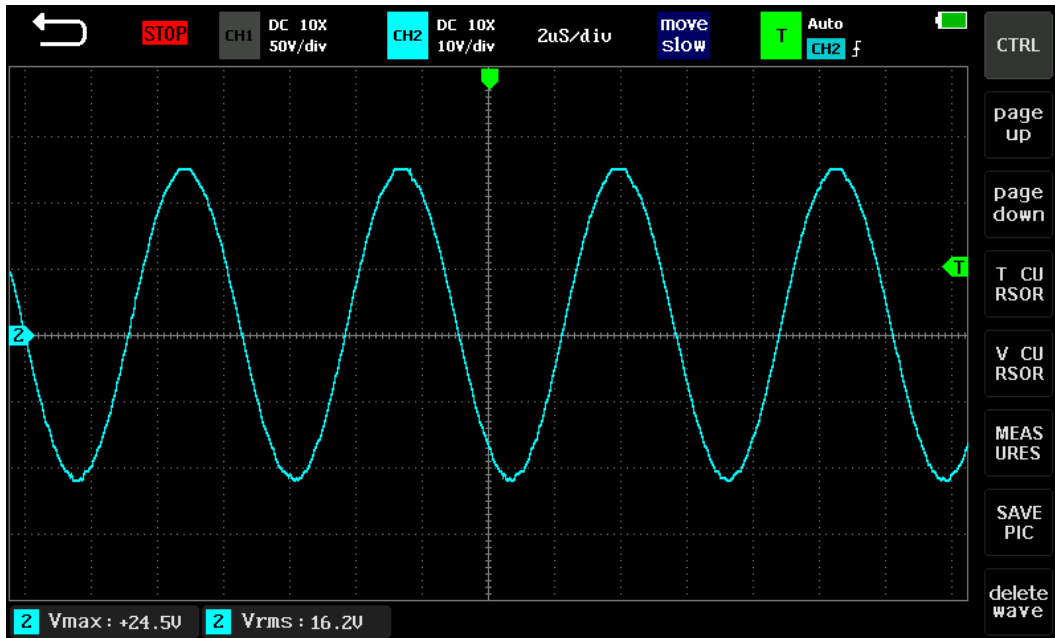


Consultation Source: Own Elaboration

To measure the output voltage of the transformer, a resistive divider formed by 2 resistors of $R_2=100k$ and $R_1=10M$ is made. Figure 1.10 shows the voltage waveform at the output of the resistive divider (blue color), noticing an in a sinusoidal waveform, an output with a voltage of 24.5Vp is observed, therefore the transformer voltage (V_s) is given by equation 2, obtaining a voltage of 2474.5 Vp.

$$V_{in} = \frac{V_{out}(R_2+R_1)}{R_2} \quad (2)$$

Figure 1.10 Output Voltage



Consultation Source: Own Elaboration

During the tests carried out, the separation distance between plates was varied until a separation distance of 0.8 mm was achieved, in which the formation of the Dielectric Barrier Discharge occurs, as shown in figure 1.11, the discharge was maintained during a time of 10 min during which a temperature increase was observed in the MOSFETs of the power block to a value of 32 degrees Celsius while the Transformer was kept at room temperature.

Figure 1.11 Dielectric Barrier Discharge



Consultation Source: Own Elaboration

Table 1.2 shows the results obtained for voltage, current and power (input and output) at the source, as well as the efficiency during the tests. RMS values are useful for determining the powers involved in AC signals.

Table 1.2 Experimental results of input and output voltage (V_{in} - V_{out}) in converter, power (P_{in} - P_{out}) and current (I_{in} - I_{out})

Variable	Description	Value
V_{in}	Input voltage	24.58 V_{RMS}
I_{in}	Input current	2.15 A_{RMS}
P_{in}	Input power	52.847 W
V_{out}	Output voltage	17.5 V_{RMS}
I_{out}	Output current	2.73 A_{RMS}
P_{out}	Output power	47.775 W
η	Efficiency	90.5035%

Consultation Source: Own Elaboration

11. Conclusions

The Class E amplifier generated a voltage of 2474.5 Vp for which the adequate calibration between the two internal electrodes of the chamber was approximately 0.8 mm, considering that the electrodes were heated to 53 °C, but it did not impede the generation of arcs. Having this configuration, the chamber, allowed us to take advantage of the non-linear properties of the dielectric to generate controlled discharges. In addition, the E-Class technology controlled the power output effectively, which was essential in the controlled production of the shocks.

In summary, the design and assembly of a Class E amplifier to generate dielectric barrier discharges implied the creation of a highly efficient and controlled circuit using commutation and resonance principles to generate high power pulses in a dielectric medium. This approach seeks to maximize the efficiency and precision in the generation of electrical discharges, which makes it relevant in a variety of industrial and scientific applications.

12. Acknowledgments

The authors of the work appreciate the support granted by the TECNM, the Tecnológico de Estudios Superiores de Jocotitlán and the University of Ixtlahuaca for the development of the tests and equipment, as well as being a product of the project with financing SYSTEM FOR OBTAINING SEMICONDUCTORS WITH POTENTIAL APPLICATION IN POWER CONVERTERS AND SOLAR CELLS of the call, SCIENTIFIC RESEARCH Project of the TECNM

13. References

- Albulet, M. (2001). RF Power Amplifiers. Institution of Engineering and Technology. <https://doi.org/10.1049/SBEW030E>
- Cripps, S. C. (2000). RF power amplifiers for wireless communications. IEEE Microwave Magazine, 1(1), 64-64. <https://doi.org/10.1109/MMW.2000.823830>
- Grebennikov, A., Sokal, N. O., & Franco, M. J. (2012). Class-d power amplifiers. En Switchmode RF and Microwave Power Amplifiers (pp. 83-128). Elsevier. <https://doi.org/10.1016/B978-0-12-415907-5.00002-X>
- Kazimierczuk, M. K. (2008). RF power amplifiers. Wiley. <https://doi.org/10.1109/MIE.2009.932575>
- Kenington, P. B. (2000). High-linearity RF amplifier design. Artech House.
- Laquidara, A. (2020). CIRCUITOS ELECTRONICOS, Amplificadores clase E. La plata, Buenos Aires, Argentina: Facultad de ingeniería. Retrieved from: <https://bit.ly/3EtKMNm>
- Lizárraga, R. A. (2009). ESTUDIO TEORICO Y EXPERIMENTAL DE LA CONFIGURACION DE TRANSMISOR DESFASADO PARA MEJORAR LA EFICIENCIA EMPLEANDO AMPLIFICADORES CLASE E. (C. CENTRO DE INVESTIGACIÓN CIENTÍFICA Y DE EDUCACIÓN SUPERIOR, Ed.) Ensenada, Baja California Norte, México.

Mammano, B. (2001). Resonant mode converter topologies. Texas instruments documentations on power technology. Retrieved from: <https://bit.ly/486u8kE>

Pimentel Velázquez, L. A., Suárez Aparicio, H., & Velázquez Machuca, M. A. (2022). Prototipo generador de ozono basado en fuente de alto voltaje y descarga de barrera dieléctrica. *Ingeniería Investigación y Tecnología*, 24(2), 1-11. <https://doi.org/10.22201/fi.25940732e.2023.24.2.013>

Raab, F. H. (1978). Effects of circuit variations on the class E tuned power amplifier. *IEEE Journal of Solid-State Circuits*, 13(2), 239-247. <https://doi.org/10.1109/JSSC.1978.1051026>

Scheibe, A., & Krauss, W. (1980). A two-transistor SIMOS EAROM cell. *IEEE Journal of Solid-State Circuits*, 15(3), 353-357. <https://doi.org/10.1109/JSSC.1980.1051398>

Chapter 3 Filtration as gray water treatment using conventional and unconventional adsorbent beds

Capítulo 3 La filtración como tratamiento del agua gris utilizando lechos adsorbentes convencionales y no convencionales

GARCIA-SANCHEZ, José Juan †* & GARCIA-GARCIA, Eduardo

Tecnológico Nacional de México, Tecnológico de Estudios Superiores de Jocotitlán, Carretera Toluca-Atacomulco Km 44.8, Ejido de San Juan y San Agustín Jocotitlán, 50700 Jocotitlán, México

ID 1st Author: *Jose Juan, García-Sanchez*

ID 1st Co-author: *Eduardo, García-García* / **ORC ID:** 0009-0002-5176-7845

DOI: 10.35429/H.2023.5.29.46

J. García & E. García

*jjuangs1@gmail.com

R. López (AA.) Engineering and Architecture in the Northern part of the State of Mexico. Handbooks-TI-©ECORFAN-Mexico, Estado de México, 2023

Abstract

Water pollution is a global problem that can be a threat to the environment and human health, which is why efficient technologies are required for the treatment and comprehensive management of residues from wastewater treatment. In this sense, the present study used different filtration media such as zeolite, pumicite, tezontle, dolomite, ground corn straw, coconut fiber and biocalcium to analyze the physical-chemical interaction of these materials and the components of graywater from laundry in a simple filtering process. Four filter columns with different bed layers, same graywater and a filtration rate established by each filter were installed and operated at laboratory scale and in parallel. The pollution reduction was from 70.2% - 98% for selected parameters (COD, TSS, TDS, PO₄ and NO₃) in filter columns. Thus, filters with different arrangement of unconventional filtration media are efficient in purifying greywater.

Wastewater, Adsorption, Unconventional adsorbents, Filtration

Resumen

La contaminación del agua es un problema global que puede constituir una amenaza para el medio ambiente y la salud humana, por lo que se requieren tecnologías eficientes para el tratamiento y manejo integral de los residuos del tratamiento de aguas residuales. En este sentido, el presente estudio utilizó diferentes medios de filtración como zeolita, pumicita, tezontle, dolomita, paja de maíz molida, fibra de coco y biocalcio para analizar la interacción físico-química de estos materiales y los componentes de las aguas grises de lavandería en un proceso de filtración simple. Se instalaron y operaron a escala de laboratorio y en paralelo cuatro columnas filtrantes con diferentes capas de lecho, las mismas aguas grises y una tasa de filtración establecida por cada filtro. La reducción de la contaminación fue del 70,2% - 98% para los parámetros seleccionados (DQO, SST, SDT, PO₄ y NO₃) en las columnas filtrantes. Así pues, los filtros con diferentes disposiciones de medios de filtración no convencionales son eficaces para depurar las aguas grises.

Aguas residuales, Adsorción, Adsorbentes no convencionales, Filtración

1 Introduction

Water is a highly vulnerable resource, so it is necessary to design a water management system from a circular economy perspective; optimizing use and consumption; reducing the amount of energy and chemicals used in treatment systems. The current management in the treatment of residual water is inefficient and contributes to the production of waste and contamination in other environmental vectors. The soil is a vector that has been affected by solid waste from treatment plants, due to its chemical composition and toxicity. The effects of the current models of wastewater treatment on the soil, mainly agricultural, make it necessary to generate technological and management alternatives.

The consumption of washing water is one of the most critical issues, where large amounts of water are used for washing every day (Manouchehri & Kargari, 2017). Laundromat effluents are categorized as graywater and their effluents contain detergents, degreasers, neutralizers, and softeners. Detergents are a source of phosphorus in wastewater, they inhibit biological activity and decrease oxygen solubility. Moreover, dyes contained in graywater persist in the environment, are difficult and expensive to remove. The usual characteristics of these effluents are pH: 7.5 - 11.5, alkalinity: 60 - 250 mg/L of Na₂CO₃, total solids 800 - 1200 mg/L, BOD 30 - 305 mg/L, COD 150 - 2054 mg/L and phosphates 5 - 7 mg/L (Eriksson *et al.*, 2002).

Some processes to treat these effluents are through membrane filtration or activated carbon and Advanced Oxidation Processes can be used to reduce dyes (López *et al.*, 2007). The filtration process is a treatment that removes; fecal coliforms, suspended, dissolved and total solids, BOD, Oils and Fats.

A filter is made up of a filter medium and a support with several layers of different materials and commonly has a last layer that provides support and aeration to the system, ensuring the permeability of the filter. The filters combine the filtration operation with adsorption, using filter materials that in turn act as adsorbents.

An ideal filtration medium is one, with a certain granulometry and grains of a certain specific weight, which is capable of removing the greatest possible number of suspended particles from an effluent. Hence, the materials of a filtration medium must have a high retention capacity (Molina, 2016). Materials such as zeolite, pumicite, tezontle, dolomite in a filtration process may serve as a support. While ground corn straw, coconut fiber and biocalcium can be used as organic filtration media.

The objective of this research was to analyze the filtration efficiency, the quality of the treated water and the properties of the generated bed to determine the efficiency of water purification. It is intended to find a solution for the integral management of wastewater from laundry.

1.1 Water

Water is one of the most important resources in the world. It constitutes most of living matter and helps in different biological processes, water is the second most essential material for human survival (S. Ahuja, 2009; Elehinafe *et al.*, 2022). It is also fundamentally important for human activity, it is needed and used for practically everything, from household domestic use to industrial and agricultural production (Oki & Quioco, 2020).

Around 70% of the Earth is covered by water, of which 97% of this is sea water (S. Ahuja, 2009; Grzegorzek *et al.*, 2023). Since seawater is rarely available for human consumption, the world population depends on only the 3% available freshwater. Out of the available freshwater, only 0.06% can be easily accessed as the rest comprises the frozen polar ice cap or glaciers, groundwater, and swam (Musie & Gonfa, 2023).

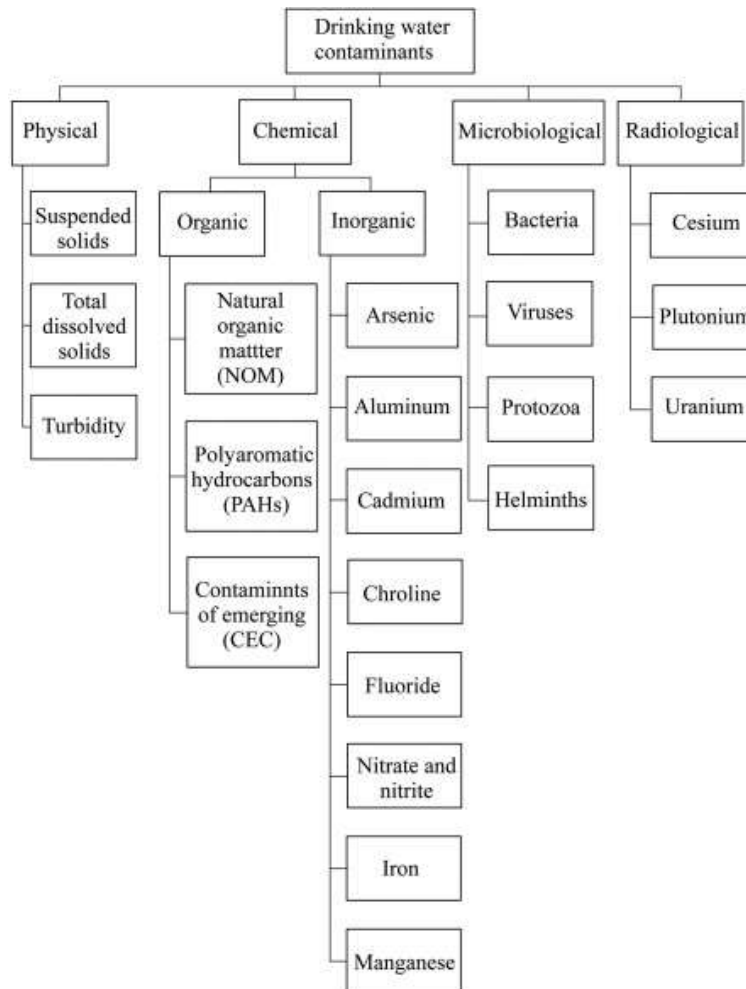
Due to the relevance of this resource and as the world's population increases, the demand for water is growing day by day and threatens to exacerbate water scarcity in many areas (Qu *et al.*, 2013). Additionally, climate change affects water scarcity by altering both water supply and demand (Sun *et al.*, 2023). The spatial and temporal distribution of water resources are affected by climate change, and the use of water in irrigation and other sectors (energy and food production) is also affected by changes in temperature (Orlowsky *et al.*, 2014; Sun *et al.*, 2023).

It is not only the water quantity that matters, the quality of water we use is also equally important (Musie & Gonfa, 2023). Most of the countries in the world suffer from a water deficit and approximately 1.2 billion people drink unclean water, resulting in a high number of deaths (S. Ahuja, 2009). That is why the search for alternatives sources so as the to cover the demand of this resource and its management is one of the greatest global challenges of this century.

1.2 Water contaminants

Water pollution, by definition, is the contamination of available water by pollutants or alien materials that lead to death and disease of livestock, aquatic life and humans (Elehinafe *et al.*, 2022). The common sources of water pollution can vary from wholly natural to man-made sources such as release of domestic and industrial wastewaters. Many industries, including textile, aquaculture, paper, agricultural production, energy production, pharmaceutical and so on, would produce a large amount of polluted wastewater (Xu *et al.*, 2023).

Depending on the origin, wastewaters could have various types of water pollutants in varying concentrations include, among others, organic, inorganic pollutants, suspended solids, pathogens, nutrients or even radioactive pollutants (Figure 1) (Singh *et al.*, 2020). Inorganic and organic pollutants are main contaminants in wastewater (Wasewar *et al.*, 2020).

Figure 1. Types of water pollutants

Source: Shah *et al.*, 2023

Organic pollutants are persistent in nature, they can travel far-off and remain deposited and contribute to the toxicity of water systems and the environment (Ghaffar *et al.*, 2023). They are emitted from sewage, urban wastewater, industrial wastewater and agricultural waste. Consequently, some of the common organic pollutants are organic dyes, polychlorinated biphenyls (PCBs), aromatic hydrocarbons (PAHs), pesticides, herbicides, petroleum, and organo-chlorine pesticides (OCPs). They are hydrophobic chemicals that survive in water systems for a long time and are associated with sediments (Masindi & Muedi, 2018; Touliabah *et al.*, 2022).

Furthermore, one group of organic pollutants called emerging pollutants (EPs) has gained attention in recent years. Emerging contaminants are primarily organic chemicals found in aquatic systems and the major sources of this pollutants are pharmaceuticals, personal care products, pesticides, and flame retardants (Dubey *et al.*, 2023). Dyes, pharmaceuticals, phenolic contaminants, and personal care products can be considered the most critical emerging organic pollutants, they can adversely affect the ecology and human health (Mohammadi *et al.*, 2022).

On the other hand, inorganic pollutants are usually substances of mineral origin, with metals, salts and minerals being examples (Masindi & Muedi, 2018). Commonly found inorganic contaminants of water include arsenic, fluoride, iron, nitrate, heavy metals, and their presence at more than permissible levels degrades water potability for living organisms (Srivastav & Ranjan, 2020). The high levels of inorganic nitrogen pollutants (nitrate, nitrite, ammonium) and inorganic phosphates in water lead to many health problems (Singh *et al.*, 2020). Moreover, the most studied heavy metals in the wastewater generated by various industries are arsenic, copper, chromium, lead, mercury, nickel, and zinc (Srivastav & Ranjan, 2020).

Other contaminants are biological pollutants (pathogens), they are described as pollutants which exist because of humanity's actions and impact on the quality of aquatic environment. This type of pollutants are small microbes that cause disease, including bacteria, viruses, pills, and certain parasites (Singh *et al.*, 2020). These pathogens can cause water-borne diseases like jaundice, diarrhea, cholera, typhoid, nosocomial infections, giardiasis, etc. (Chakraborty *et al.*, 2023).

All the three categories of contaminants mentioned above if left untreated or inadequately treated directly affect and impact the environment. The degree of impact depends on the type and concentration of the contaminants (Sharma *et al.*, 2019).

Besides the contaminants in water, esthetic water quality is also extremely important. Unpleasant odors, unpalatable taste (e.g., bitter, salty, and metallic), and unappealing appearance/color of water do not pose any serious public health threats but render the consumption of water difficult (Palansooriya *et al.*, 2020).

1.3 Water quality

Water quality problems, are rapidly emerging as a result of urbanization, increasing the variety and number of microbial pathogens, pollutants, and nutrients in receiving water bodies (Salerno *et al.*, 2018). The quality of water can be described in terms of physical, chemical and biological contaminants, and the evaluation of water quality is essential for water resource management (Yan *et al.*, 2022). Many indices for assessing surface water quality (e.g., water quality indices (WQIs), trophic status indices (TSIs), and heavy metal indices (HMIs)) have been designed to assess water quality (Yan *et al.*, 2022).

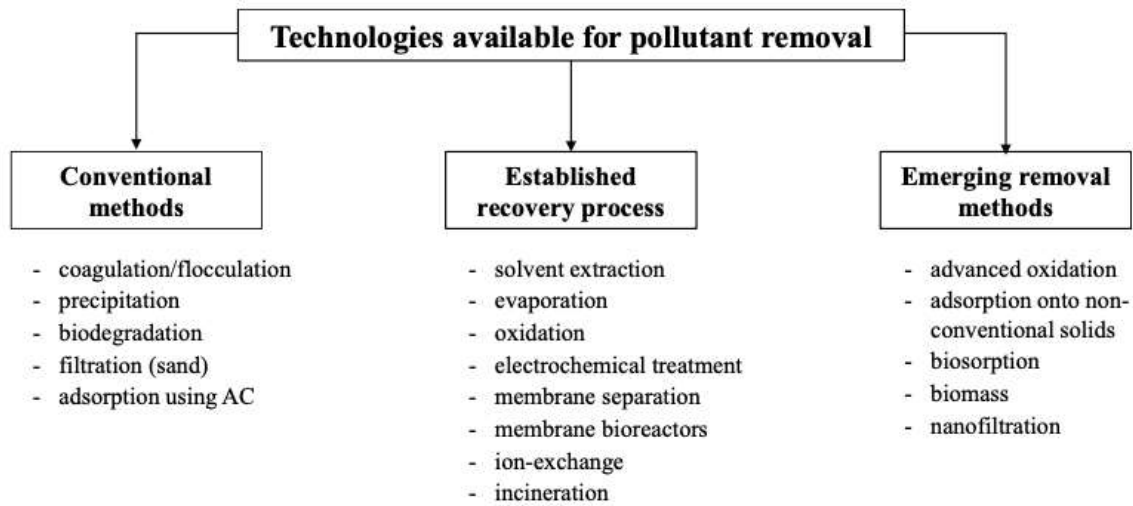
The WQI can be used effectively to represent water quality, it allows to estimate in general the degree of purity or contamination of a sample or an effluent (Valladares-Cisneros *et al.*, 2018). The general parameters used to calculate WQI are dissolved oxygen (DO), pH, temperature, coliforms, specific conductance, alkalinity and chloride. Nevertheless, based on the situation in specific areas many modifications have been considered for WQI, generating different WQIs (Tyagi *et al.*, 2020). For this reason, specific determinations must be made to distinguish the individual concentration of the compounds of interest according with the region.

Different water quality evaluation indices can be selected to assess the water quality levels based on the situation in a specific area. The trophic state index (TSI) and trophic level index (TLI) are commonly used methods for evaluating the eutrophication state of lakes and reservoirs (Ding *et al.*, 2021). For the other hand, in aquatic ecosystems where exist an excess number of heavy metals that can be a risk for human health, the analysis of dissolved metals in water is a useful tool for assessing the state of pollution (Alves *et al.*, 2014). The most widely used HMI for analyzing the exposure risk of heavy metals is the US Environmental Protection Agency (USEPA) guidance (Saha *et al.*, 2017; Yan *et al.*, 2022).

1.4 Wastewater treatment methods

Various methods are used to treat contaminated water, these techniques frequently incorporate physical, chemical, and biological procedures that successfully treat water in several ways (Nishat *et al.*, 2023). However, the type of treatment to be used depends on the environment where the wastewater would be discharged and the type of impact it would have on this environment.

A multitude of techniques classified in conventional methods, established recovery processes and emerging removal methods can be used (Figure 2). The main treatment methods are coagulation and flocculation, evaporation, adsorption, ion exchange, membrane-based purification, catalytic methods, and biological methods (biodegradation) (Mohammadi *et al.*, 2022). Additionally, individual treatments can have combined each other in treatment schemes categorized into three main classes: primary, secondary, and tertiary schemes.

Figure 2. Methods for water treatments

Source: Crini & Lichtfouse, 2019a.

Generally, primary treatments are design to remove organic and inorganic solids, only those pollutants which have the tendency to float or settle under the influence of gravity (Sharma *et al.*, 2019). Primary treatment consists of temporarily holding the sewage in a quiescent basin where heavy solids can settle to the bottom while oil, grease and lighter solids float to the surface (Rawat *et al.*, 2011).

On the other hand, secondary treatment consists in biological process where dissolved or suspended organic matter are remove by microorganisms. Secondary treatment is typically performed by indigenous, water-borne microorganisms in a managed habitat (Rawat *et al.*, 2011). The process carried out two major ways aerobic and anaerobic conditions with the action of microorganisms (Sathya *et al.*, 2023). Tertiary treatment scheme popularly known as effluent polishing is employed to remove plant nutrients like phosphorous and nitrogen which are responsible for eutrophication of water bodies (Sharma *et al.*, 2019). The tertiary treatment employs physical, chemical and biological procedures.

1.5 Filtration and adsorption

Filtration is the process of removing contaminants where the polluted water enters the top of the filter vessel, flows through the filter medium which retains solids and water passes through the lower section, the driving force in filtration can be pressure gradient, such as gravity (Saravanan *et al.*, 2021). This technology is a physical separation technique using a selectivity mechanism to eliminate particles and organics from wastewater which generates an effluent with great quality and low pollutants (Keyvan Hosseini *et al.*, 2023).

Particle and membrane filtrations are the two common filtration types, varying in removal contaminant size (Song *et al.*, 2023). The process of membrane filtration relies on the use of a semi-permeable membrane that allows only water to pass through it while withholding substances such as suspended and dissolved solids present in water (Al-Ghouti *et al.*, 2023). This type includes microfiltration (MF), ultrafiltration (UF) and nanofiltration (NF) membranes.

In granular filtration, water passes through a filter consisting of a packed bed of granular materials (Simate, 2015). Filters combine the filtration operation with adsorption, using filtration media that in turn act as adsorbents. Filtration media could be in the form of sand, gravel, fine mesh and many others (Oteng-Pepurah *et al.*, 2018). Moreover, the adsorption capacity of the filtration media towards pollutants ions is associated with the presence of a higher number of binding sites on the media surface.

Adsorption is a mass transfer process that involves the accumulation of molecules of liquid on a solid surface and becomes bound through physical or chemical connections (Mishra *et al.*, 2018; Nishat *et al.*, 2023). In physical adsorption, the particles of adsorbate (the substance which is adsorbed) attach to the surface of the adsorbent (the adsorbing material) by forces like van der Waals forces and hydrogen bonding. Conversely in chemisorption, the adsorbate-adsorbent attachment occurs by relatively stronger forces such as an ionic bond or a chemical bond (Al-Ghouti *et al.*, 2023).

The adsorbents include nano-sized metal oxides (NMOs), activated carbon, clay minerals, biomass, agricultural waste, and other substances (Nishat *et al.*, 2023). The capacity of adsorbent for the adsorption process depends on adsorbent dosage, concentration of pollutants, temperature, pH and contact time (Saravanan *et al.*, 2021). Thus, the combination of filtration with other unitary processes, such as adsorption that uses a filtration medium as an adsorbent, proposes a better performance in the removal of pollutants from residual waters.

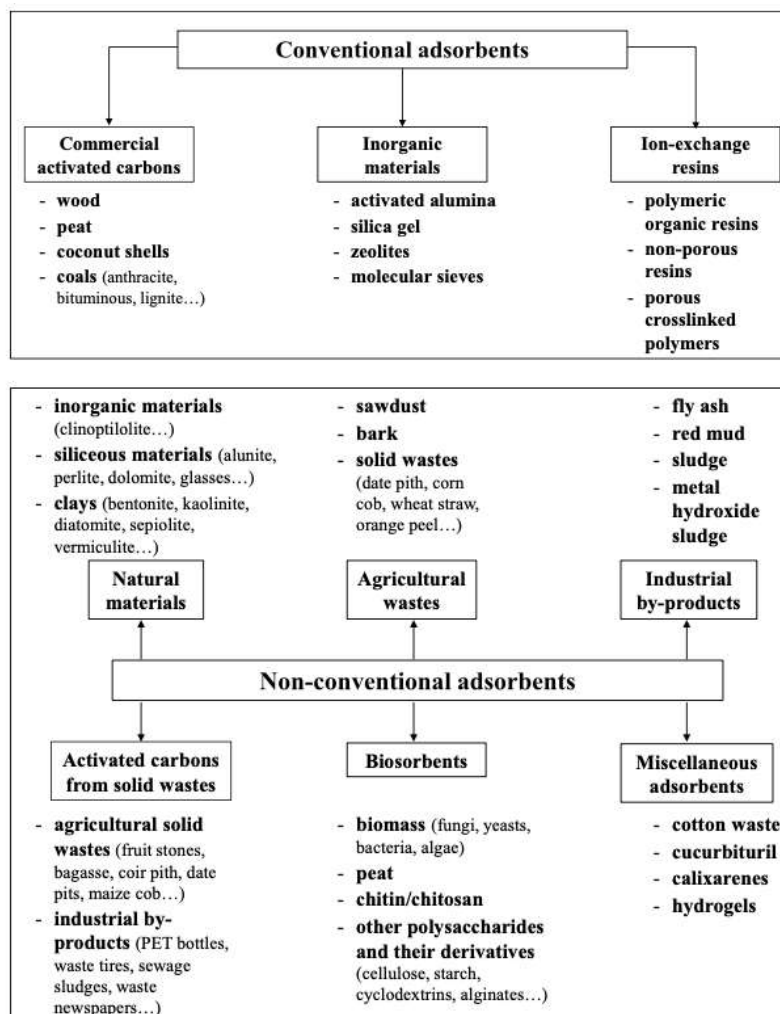
1.6 Adsorbents

Adsorbents are the solid materials that allows liquid or gaseous molecules to bind to its surface and are used for the removal of toxic pollutants from the wastewater or industrial effluents (Abegunde *et al.*, 2020; Saravanan *et al.*, 2021). Generally, adsorbent's performance depends on the physicochemical properties of the adsorbent surface, solution conditions, as well as that of the soluble substances (Mpatani *et al.*, 2021).

An ideal adsorbent should possess a wide surface area and a small volume. Furthermore, a good adsorbent material must include high mechanical strength, chemical and thermal stability, high porosity and low pore diameter leading to increase exposed surface area and hence suitable surface chemistry giving rise to high adsorption capacity (Abegunde *et al.*, 2020; Amalina *et al.*, 2022).

There are a variety of adsorbents existing in different nature which can either be utilized in different structures, adsorbents are generally utilized in the form of spherical pellets, rods, moldings, or monoliths, depending on the filter configuration (Amalina *et al.*, 2022; Chai *et al.*, 2021). Natural and synthetic adsorbents are the two types of adsorbents classified based on the source from which they obtained. However, another simplified classification, can be used as follows: conventional and non-conventional.

Figure 3. Conventional and non-conventional adsorbents



Source: Crini *et al.*, 2019b

1.6.1 Conventional adsorbents

Mainly comprise by activated carbons, ion-exchange resins, and inorganic compounds like activated aluminas, silica gel, and zeolites (Figure 3). They are readily available in the nature, easy to use and are widely applied for the treatment of wastewater and in aquaculture (Mangla *et al.*, 2022). In addition, these materials are previously treated and once used, they need to be regenerated to recover their properties (Valladares-Cisneros *et al.*, 2018).

Activated carbon (AC) is a porous, amorphous solid made up of microcrystallites with a graphite lattice. AC is produced from a carbon-rich precursor (coal, coconut shell and wood) by removing the vast bulk of volatile non-carbon components and a portion of the native carbon content via thermal or chemical processes (Amalina *et al.*, 2022; Chai *et al.*, 2021). High degree of micro porosity, well developed surface area, and high adsorption capacity are the key features of ACs (both granular and powdered) that make them suitable as adsorbent for the removal of organic contaminants (Ahmed *et al.*, 2015).

Ion-exchange resins are solid materials that provide path for the movement of ions from their surface to the solvent and vice versa (Ahmed *et al.*, 2015). The advantages of this materials include no loss of adsorbent on regeneration, reclamation of solvent after use and the removal of soluble contaminants at trace levels (Crini *et al.*, 2019b).

On the other hand, zeolites are crystalline aluminium, silicon and oxygen minerals. They have cavities and small chambers inside which small cations, water molecules and other species could be trapped and, in addition, act as cation exchangers (Mangla *et al.*, 2022). Therefore, minerals materials such as zeolites are considered highly effective adsorbents for trace element removal from aqueous solutions because of its characteristics (Al-Ghouti *et al.*, 2023).

Despite the availability, easy to use and high adsorption power of conventional materials, they hold some limitations such as high production costs and some adsorbents are not efficient for large-scale treatment process.

1.6.2 Unconventional adsorbents

Although conventional materials are the usual adsorbents for contamination removal, their high cost and regeneration restricts their application. As a result, alternate solutions for non-conventional adsorbents, mainly organic products and by-products, industrial and agricultural origin and from forest industries (green adsorbents), have been proposed, studied and implemented as economical and effective adsorbents (Rudi *et al.*, 2020).

The various non-traditional adsorbents include biochar, natural material such as clays, biomass, industrial by-products such as red mud, biopolymers (chitosan, cellulose, lignin, pectin, starch), and some other miscellaneous adsorbents (Figure 3). All these materials are interesting because they are available in nature in large quantities, inexpensive, and may have potential as complexing materials due to their physicochemical characteristics and particular structure (Crini *et al.*, 2019b). Some of them are described below.

Zeolite is a crystalline hydrated aluminosilicate with three-dimensional structures, made up of a grid of interconnected tunnels creating a large surface area for cation exchange and adsorption. Moreover, natural zeolites vary widely in their chemical composition, a product of their origin and deposition in nature. A common characteristic of their chemical compositions is the presence of O, Si, Al, as fundamental elements and Ca, Mg, Ba, Na and K as exchangeable cations (Jiménez-Cedillo, 2004).

Pumicite, also called pumice, is a porous volcanic rock, with a structure formed by multiple pores and closed voids. The porosity of pumicite allows it to function as an absorbent. Moreover, its chemical composition, 65.90% silicic anhydride, 11.20% aluminum oxide, 1.25% ferric oxide, 0.52% magnesium oxide, 2.10% sodium oxide and 3.20% potassium oxide prevail, so it has great chemical reactivity (Cornejo Soldevilla, 2015). The modified or activated pumice has good ionic exchange and adsorption capacity for chemical contaminants such as fluorides (Sepehr *et al.*, 2013) and dyes (Samarghandi *et al.*, 2012).

Tezontle is a porous, inert volcanic rock, neutral pH, low ionic exchange capacity (IEC) and moisture retention capacity. The elemental composition of the tezontle shows that it contains O, Si, Al, Ca, C, Fe, Mg and Na (Trejo-Téllez *et al.*, 2013). The presence of iron oxides gives it a red or black color, characteristic depending on the presence of hematite or magnetite (Otazo *et al.*, 2011). The natural red tezontle was used to evaluate the removal of cadmium ions (Cd²⁺) finding a total adsorption capacity of 6.62 mg/g (Ponce-Lira, 2018).

Dolomite is a sedimentary rock; a carbonate of calcium and magnesium that makes up about 2% of the earth's crust. Its chemical formula is (CaMg(CO₃)₂); it contains 30.41% CaO, 21.86% MgO and 47.73% CO₂, in its purest form (Dirección General de Desarrollo Minero, 2017). Studies where dolomite has been used as a metal ion adsorbent have demonstrated its excellent ionic exchange properties (Ivanets *et al.*, 2016).

Corn straw consists of the leaves, stalks, and corn cob (*Zea mays ssp. Mays L.*) left in a field after harvest. It is a fibrous material with a high lignification state, 95.8 % dry matter and with a mineral content of Cu, Fe, Mn, Zn (Arrieche & Mora, 2005; De Blas *et al.*, 2013; Fuentes *et al.*, 2001). Corn straw as biosorbent for plumb and cadmium in wastewater presented an adsorption capacity of 4.27 and 3.43 mg/g according to the Langmuir model (Astudillo *et al.*, 2020).

The fruit of the coconut tree *Cocos nucifera L.* is formed by a thick layer that makes up 35% of the coconut called mesocarp, lignocellulosic material, composed of hard multicellular fibers. Lignin, cellulose and hemicellulose give it good absorption and water retention capacity (Reyes, 2016). Therefore, the adsorption of Cr (VI) has been reported using the shell of the fruit of the *Cocos nucifera L.* plant as organic biomass, with removal values of 93.71 to 96.85 % (Pérez Silva *et al.*, 2014).

Biocalcium from eggshells is made up of calcium carbonate, calcium phosphate and magnesium carbonate. Additionally, contains minerals such as sodium, zinc, magnesium, manganese, iron, aluminum, boron and copper. The use of biocalcium as an adsorbent material in the elimination of contaminants present in wastewater has had excellent results. For example, the adsorption capacity of the eggshell membrane in textile dyes has been reported, achieving a sorption greater than 81.8 % in aqueous solution (Arami *et al.*, 2006).

2 Materials and methods

The materials that were used in the filtration system were zeolite, pumicite, tezontle, dolomite, ground corn straw (GCS), coconut fiber, biocalcium and olote. The materials that make up the beds of the filter bed were obtained locally; washed, dried and sieved. The characteristics of each material are shown in Table 1. The particle size was determined by sieving through US standard steel mesh sieves number 20 and 40, obtaining a size of 0.850-0.425 mm in all materials.

The graywater used in the different tests was obtained from a laundry, with a washing load capacity of 208 kg/d (Table 2). The inputs used are commercial detergents and fabric softeners. Hence, ten liters of graywater was collected daily for one week, stored refrigerated and continuous agitation. Four identical filter columns made of clear acrylic were used. The height of each column was 90 cm and the diameter 5 cm. A glass wool layer was attached to the bottom of each filter. The filters were fixed with a wooden support. A 50 L capacity feed tank was raised from the floor and connected to a distributor (pipe) with four outlets over the four filters.

Table 1. Characteristics of the bed material in the filtration system

Filter material	Apparent density (kg/m ³)	Porosity (%)	Filtration Velocity (mL/min cm ²)
<i>Zeolite</i>	0.689	64.39	3.99
<i>Pumicite</i>	0.507	63.79	3.44
<i>Tezontle</i>	0.857	64.31	20.41
<i>Dolomite</i>	1.253	53.70	3.48
<i>Ground corn straw</i>	0.451	68.74	1.55
<i>Coconut fiber</i>	0.077	60.75	17.38
<i>Biocalcium</i>	0.919	44.57	8.36
<i>Olote</i>	0.096	68.37	21.71

Source: Own elaboration

Table 2 Laundry greywater characteristics

Parameter (mg/L)	Greywater used as an influent		
	Maximum	Minimum	Average
DQO	365	312	330.8
SST	597	492	548
SDT	3042	2478	2885.4
Phosphates - (PO ₄)	6.5	3.2	9.04
Nitrates - (NO ₃)	6.2	2.6	4.3
pH	10.1	8.7	9.6

Source: Own Elaboration

2.1 Samples evaluation

Additionally, filtered samples from the four filters, as well as the feed wastewater sample, were analyzed for total solids (TS), suspended and dissolved solids (SS and DS), chemical oxygen demand (COD), nitrates (NO₃), phosphates (PO₄) and pH. Standard analytical methods and a HACH DR2800 spectrophotometer were used.

3 Filtration systems

A simple completely randomized design (CRD) was carried out (Minitab statistical program), it consisted of four treatments (Factor T: T1, T2, T3, T4), combining 4 support materials and 4 as filtration medium. The efficiency of the combination of said materials in the removal of contaminant load from graywater was evaluated. The study factor will be the filtration medium (organic and inorganic materials) in four different combinations as detailed in Table 3. When combining organic and inorganic materials in a water filter, it is recommended that the organic material be supported by inorganic material. Therefore, the random design was applied at the X-Y-Y-X level according to the indicated factors.

Table 3 Factorial arrangement in a completely randomized design

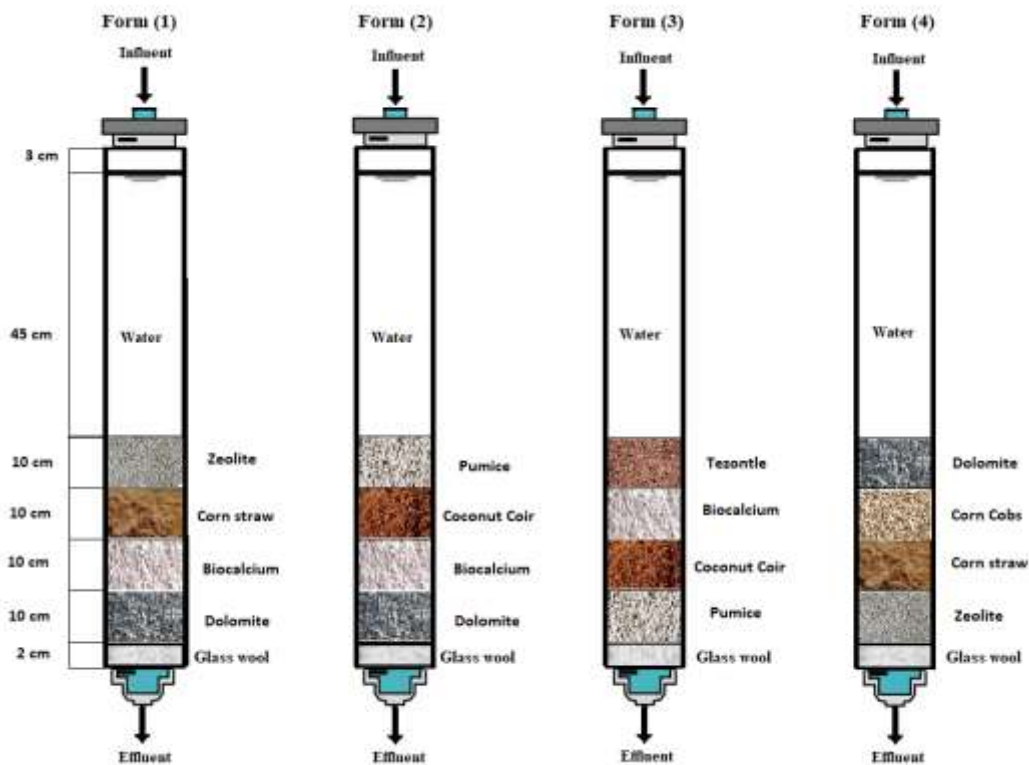
Study factors		
Factor X: Inorganic materials		Factor Y: Organic materials
<i>X₁: Zeolite</i>		<i>Y₁: GCS</i>
<i>X₂: Pumicite</i>		<i>Y₂: Coconut fiber</i>
<i>X₃: Tezontle</i>		<i>Y₃: Biocalcium</i>
<i>X₄: Dolomite</i>		<i>Y₄: Olote</i>
Treatment	Arrangement	Description
T ₁	X ₁	Zeolite
	Y ₁	GCS
	Y ₄	Biocalcium
	X ₄	Dolomite
T ₂	X ₂	Pumicite
	Y ₂	Coconut fiber
	Y ₃	Biocalcium
	X ₃	Dolomite
T ₃	X ₃	Tezontle
	Y ₃	Biocalcium
	Y ₂	Coconut fiber
	X ₂	Pumicite
T ₄	X ₄	Dolomite
	Y ₄	Olote
	Y ₁	GCS
	X ₁	Zeolite

Source: Own Elaboration

3.1 Filter evaluation

Four filter columns with different bed layers, same graywater and a filtration rate established by each filter were installed and operated at laboratory scale and in parallel. Figure 4 shows the media used in the filtration of graywater, whose particle size was 0.425 to 0.850 mm. During the experiment a constant influent was maintained in each filter and a sample was collected from each one at the end of the following times 0.5, 1.0, 2.0, 4.0, 6.0, 12.0 and 24.0 hours. Consequently, the liquid obtained was kept refrigerated for further characterization.

Figure 4. Different configurations of filter media



Source: Own Elaboration

4 Results and discussion

In order to verify the efficiency of the filter beds, physicochemical analyzes of the residual water were carried out after the filtration process. Table 4 shows the results of the greywater quality analysis before filtration (Residual water), after filtration at different times and the filtration velocity in each of the configurations of the materials used separately.

Table 4 Summary of physical-chemical analysis

Parameters (mg/L)	Residual water	Filter 1						
		0.5 h	1.0 h	2.0 h	4.0 h	6.0 h	12.0 h	24.0 h
COD	330.8	86.34	67.15	71.29	73.15	83.68	81.65	79.43
TSS	556	104	84	60	48	52	20	16
TDS	2861	591	492	489	466	447	451	416
Phosphates - (PO ₄)	9.04	1.84	1.52	1.45	1.36	1.32	1.25	1.14
Nitrates - (NO ₃)	4.3	0.87	0.72	0.69	0.65	0.63	0.59	0.54
pH	10	7.39	7.39	7.38	7.38	7.38	7.38	7.37
Filtration Velocity (mL/min cm ²)		0.97	0.93	0.92	0.91	0.85	0.79	0.73
		Filter 2						
COD	330.8	98.34	79.15	83.29	85.15	95.68	93.65	91.43
TSS	556	124	107.5	88	92	60	24	20
TDS	2861	767	711	671	630	499	463	436
Phosphates - (PO ₄)	9.04	1.89	1.627	1.536	1.446	1.356	1.356	1.536
Nitrates - (NO ₃)	4.3	1.55	1.4	1.37	1.33	1.31	1.27	1.28
pH	10	7.37	7.39	7.40	7.39	7.39	7.41	7.40
Filtration Velocity (mL/min cm ²)		0.80	0.83	0.85	0.78	0.76	0.61	0.60

Filter 3								
COD	330.8	108.34	89.15	93.29	95.15	105.68	103.65	101.43
TSS	556	56	60	44	32	28	20	20
TDS	2861	459	416	427	395	388	383	347
Phosphates - (PO ₄)	9.04	2.15	2.63	2.54	1.85	1.96	1.56	1.74
Nitrates - (NO ₃)	4.3	1.1	0.95	0.92	0.89	0.86	0.82	0.87
pH	10	7.33	7.34	7.37	7.36	7.35	7.38	7.36
Filtration Velocity (mL/min cm ²)		0.90	0.90	0.88	0.86	0.83	0.78	0.69
Filter 4								
COD	330.8	91.34	82.15	76.29	88.15	88.68	86.65	84.43
TSS	556	95	84	64	57	47	21	19
TDS	2861	613	563.5	549	512.5	443.5	423	391.5
Phosphates - (PO ₄)	9.04	1.80	2.28	2.19	1.50	1.61	1.21	1.39
Nitrates - (NO ₃)	4.3	0.73	0.58	0.55	0.51	0.49	0.45	0.47
pH	10	7.36	7.37	7.38	7.38	7.37	7.39	7.38
Filtration Velocity (mL/min cm ²)		0.87	0.87	0.86	0.83	0.79	0.70	0.65

Source: Own Elaboration

As is show above, COD before filtration was 330.8 mg/L which significantly decrease to 79.4, 91.4, 101.43 and 84.43 for filter 1,2,3 and 4 respectively. Therefore, the systems achieved removal efficiencies of 69% - 75% after 24 hours, highlighting the filter 1 with the highest percentage.

On the other hand, the pH of effluent ranged from 7.3 – 7.4 in each filter. The process reduced the pH by 26%, the decrease may be due to chemical reactions influenced by a functional group of any filtration medium. Additionally, during adsorption (Vader Waal forces of attraction) there is the possibility of cations and anions being released into the system, keeping pH in the range (Tusiime *et al.*, 2022). The values obtained are in agreement with results reported before, which adsorption occurs in pH range of 6.5-8 (Christova-Boal *et al.*, 1996; Fernando *et al.*, 2009; Finley *et al.*, 2009).

Other parameters such as TSS and TDS were also reduced by the filtration process. For TSS, the filter 1 presented the highest removal efficiency with 97.12% at 24 h. However, the highest TDS removal efficiency was achieved with the filter 3 with 87% at 24 h. (Finley *et al.*, 2009), obtained similar values of TDS in the treatment of a graywater from shower and washer machines.

Finally, initial values of nutrients were reduced to 84-87% and 87-89% for PO₄ and NO₃, respectively. Having a better and similar performance the filters 1 and 3. The study by (Samayamanthula *et al.*, 2019) reported similar minimum concentrations of PO₄ in greywater treated by a filter with different filtration media. Similarly, the study by (Parjane & Sane, 2011) reported comparable concentrations of NO₃ in greywater treatment.

The most efficient configuration was the filter 1, having a removal percentage of 75%, 97.1%, 87% and 87% for COD, TSS, PO₄ and NO₃, respectively. Filter 4 has a similar behavior, which has the peculiarity of sharing 3 of the 4 materials of filter 1, so it is possible to infer that these 3 materials have the best adsorption capacity. On the other hand, the one that did not have such high removal percentages is filter 2, which has different materials such as pumicite and coconut fiber. The materials and their conformation are an important point to consider for the development of filters capable of removing contaminants from graywater.

5 Conclusion

This study developed and evaluated a filtration system that uses different conformations of unconventional materials in order to obtain better filter performance in graywater treatment. According to the results obtained, the physicochemical parameters showed that the filter beds were effective in removing contaminants after 24 hours through filter media such as zeolite, pumicite, tezontle, dolomite, ground corn straw (GCS), coconut fiber, biocalcium and olote. The configuration with the highest removal percentage in most of the parameters studied was the filter 1, having a removal percentage of 75%, 97.1%, 87% and 87% for COD, TSS, PO₄ and NO₃, respectively. The results reinforce the potential of nonconventional adsorbents in the wastewater treatment and offers a full treatment of greywater with available materials.

6 Acknowledgments

To the Tecnológico de Estudios Superiores de Jocotitlán (TESJo) for the facilities for the use of laboratory equipment.

7 References

- Abegunde, S. M., Idowu, K. S., Adejuwon, O. M., & Adeyemi-Adejolu, T. (2020). A review on the influence of chemical modification on the performance of adsorbents. *Resources, Environment and Sustainability*, 1(July), 100001. <https://doi.org/10.1016/j.resenv.2020.100001>
- Ahmed, M. B., Zhou, J. L., Ngo, H. H., & Guo, W. (2015). Adsorptive removal of antibiotics from water and wastewater: Progress and challenges. *Science of the Total Environment*, 532, 112–126. <https://doi.org/10.1016/j.scitotenv.2015.05.130>
- Ahuja, S. (2009). *Handbook of water purity and quality* (S. B. T.-H. of W. P. and Q. Ahuja (ed.); pp. 1–16). Academic Press. <https://doi.org/10.1016/B978-0-12-374192-9.00001-7>
- Al-Ghouti, M. A., Ashfaq, M. Y., Khan, M., Al Disi, Z., Da'na, D. A., & Shoshaa, R. (2023). State-of-the-art adsorption and adsorptive filtration based technologies for the removal of trace elements: A critical review. *Science of The Total Environment*, 895(April), 164854. <https://doi.org/10.1016/j.scitotenv.2023.164854>
- Alves, R. I. S., Sampaio, C. F., Nadal, M., Schuhmacher, M., Domingo, J. L., & Segura-Muñoz, S. I. (2014). Metal concentrations in surface water and sediments from Pardo River, Brazil: Human health risks. *Environmental Research*, 133, 149–155. <https://doi.org/10.1016/j.envres.2014.05.012>
- Amalina, F., Razak, A. S. A., Krishnan, S., Zularisam, A. W., & Nasrullah, M. (2022). The effects of chemical modification on adsorbent performance on water and wastewater treatment - A review. *Bioresource Technology Reports*, 20(October), 101259. <https://doi.org/10.1016/j.biteb.2022.101259>
- Arami, M., Yousefi Limaee, N., & Mahmoodi, N. M. (2006). Investigation on the adsorption capability of egg shell membrane towards model textile dyes. *Chemosphere*, 65(11), 1999–2008. <https://doi.org/10.1016/j.chemosphere.2006.06.074>
- Arrieche, I., & Mora, O. (2005). Efecto de la aplicación de residuos orgánicos sobre el cultivo del maíz en suelos degradados del Estado Yaracuy, Venezuela. *Bioagro*, 17(3), 155–159. http://ve.scielo.org/scielo.php?script=sci_arttext&pid=S1316-33612005000300005&lng=es&tlng=es
- Astudillo, S., L., V., J., A., & C., C. (2020). Evaluación del poder biosorbente de la hoja de maíz en la remoción de metales pesados. Afinidad. *Journal of Chemical Engineering Theoretical and Applied Chemistry*, 77(591 SE-Articles). <https://raco.cat/index.php/afinidad/article/view/377165>
- Chai, W. S., Cheun, J. Y., Kumar, P. S., Mubashir, M., Majeed, Z., Banat, F., Ho, S. H., & Show, P. L. (2021). A review on conventional and novel materials towards heavy metal adsorption in wastewater treatment application. *Journal of Cleaner Production*, 296, 126589. <https://doi.org/10.1016/j.jclepro.2021.126589>
- Chakraborty, U., Kaur, G., Rubahn, H.-G., Kaushik, A., Ram Chaudhary, G., & Kumar Mishra, Y. (2023). Advanced Metal Oxides Nanostructures to Recognize and Eradicate Water Pollutants. *Progress in Materials Science*, 101169. <https://doi.org/10.1016/j.pmatsci.2023.101169>
- Christova-Boal, D., Eden, R. E., & McFarlane, S. (1996). An investigation into greywater reuse for urban residential properties. *Desalination*, 106(1), 391–397. [https://doi.org/10.1016/S0011-9164\(96\)00134-8](https://doi.org/10.1016/S0011-9164(96)00134-8)
- Cornejo Soldevilla, D. M. (2015). Determinación de la eficiencia de remoción de la dbo de agua residual doméstica mediante la utilización de un biofiltro de piedra pómez. <http://dspace.unitru.edu.pe/handle/UNITRU/3261>

- Crini, G., & Lichtfouse, E. (2019a). Advantages and disadvantages of techniques used for wastewater treatment. *Environmental Chemistry Letters*, 17(1), 145–155. <https://doi.org/10.1007/s10311-018-0785-9>
- Crini, G., Lichtfouse, E., Wilson, L. D., & Morin-Crini, N. (2019b). Conventional and non-conventional adsorbents for wastewater treatment. *Environmental Chemistry Letters*, 17(1), 195–213. <https://doi.org/10.1007/s10311-018-0786-8>
- De Blas, C., Mateos, G. G., & Rebollar, P. G. (2013). *Fundación Española para el desarrollo de la nutrición animal. Necesidades Nutricionales Para Ganado Porcino*. 2nd Ed. Madrid: FEDNA. https://www.fundacionfedna.org/sites/default/files/Normas PORCINO_2013rev2_0.pdf
- Ding, Y., Zhao, J., Peng, W., Zhang, J., Chen, Q., Fu, Y., & Duan, M. (2021). Stochastic trophic level index model: A new method for evaluating eutrophication state. *Journal of Environmental Management*, 280(December 2020), 111826. <https://doi.org/10.1016/j.jenvman.2020.111826>
- Dirección General de Desarrollo Minero. (2017). *Perfil de Mercado de la Dolomita*. Subsecretaria de Minería de Mexico, 53. https://www.gob.mx/cms/uploads/attachment/file/287798/Perfil_Dolomita_2017.pdf
- Dubey, S., Chen, C. W., Haldar, D., Tambat, V. S., Kumar, P., Tiwari, A., Singhania, R. R., Dong, C. Di, & Patel, A. K. (2023). Advancement in algal bioremediation for organic, inorganic, and emerging pollutants. *Environmental Pollution*, 317(December 2022), 120840. <https://doi.org/10.1016/j.envpol.2022.120840>
- Elehinafe, F. B., Agboola, O., Vershima, A. D., & Bamigboye, G. O. (2022). Insights on the advanced separation processes in water pollution analyses and wastewater treatment – A review. *South African Journal of Chemical Engineering*, 42(August), 188–200. <https://doi.org/10.1016/j.sajce.2022.08.004>
- Eriksson, E., Auffarth, K., Henze, M., & Ledin, A. (2002). Characteristics of grey wastewater. *Urban Water*, 4(1), 85–104. [https://doi.org/10.1016/S1462-0758\(01\)00064-4](https://doi.org/10.1016/S1462-0758(01)00064-4)
- Fernando, A., Monteiro, S., Pinto, F., & Mendes, B. (2009). Production of biosorbents from waste olive cake and its adsorption characteristics for Zn²⁺ ion. *Sustainability*, 1(2), 277–297. <https://doi.org/10.3390/su1020277>
- Finley, S., Barrington, S., & Lyew, D. (2009). Reuse of Domestic Greywater for the Irrigation of Food Crops. *Water, Air, and Soil Pollution*, 199(1), 235–245. <https://doi.org/10.1007/s11270-008-9874-x>
- Fuentes, J., Magaña, C., Suárez, L., Peña, R., Rodríguez-Herrera, S. A., & de la Rosa, B. O. (2001). Análisis químico y digestibilidad “in vitro” de rastrojo de maíz (*Zea mays* L.). *Agronomía Mesoamericana*, 12(2), 189–192. <https://www.redalyc.org/articulo.oa?id=43712209>
- Ghaffar, I., Hussain, A., Hasan, A., & Deepanraj, B. (2023). Microalgal-induced remediation of wastewaters loaded with organic and inorganic pollutants: An overview. *Chemosphere*, 320, 137921. <https://doi.org/10.1016/J.CHEMOSPHERE.2023.137921>
- Grzegorzec, M., Wartalska, K., & Kaźmierczak, B. (2023). Review of water treatment methods with a focus on energy consumption. *International Communications in Heat and Mass Transfer*, 143(December 2022). <https://doi.org/10.1016/j.icheatmasstransfer.2023.106674>
- Ivanets, A. I., Kitikova, N. V., Shashkova, I. L., Oleksienko, O. V., Levchuk, I., & Sillanpää, M. (2016). Using of phosphatized dolomite for treatment of real mine water from metal ions. *Journal of Water Process Engineering*, 9, 246–253. <https://doi.org/10.1016/j.jwpe.2016.01.005>
- Jiménez-Cedillo, M. J. (2004). *Caracterización de minerales zeolíticos mexicanos*. Toluca, Estado de México, México: Universidad Autónoma Del Estado De México, Facultad De Química. https://inis.iaea.org/collection/NCLCollectionStore/_Public/37/022/37022042.pdf

- Keyvan Hosseini, M., Liu, L., Keyvan Hosseini, P., Lee, K., & Miao, J. (2023). Performance evaluation of a pilot-scale membrane filtration system for oily wastewater treatment: CFD modeling and scale-up design. *Journal of Water Process Engineering*, 52(January), 103570. <https://doi.org/10.1016/j.jwpe.2023.103570>
- López, C., Moreira, M. T., Feijoo, G., & Lema, J. M. (2007). Tecnologías para el tratamiento de efluentes de industrias textiles. *Afinidad*, 64(531), 561–573. https://www.researchgate.net/publication/229058887_Tecnologias_para_el_tratamiento_de_efluentes_de_industrias_textiles
- Mangla, D., Annu, Sharma, A., & Ikram, S. (2022). Critical review on adsorptive removal of antibiotics: Present situation, challenges and future perspective. *Journal of Hazardous Materials*, 425(November 2021), 127946. <https://doi.org/10.1016/j.jhazmat.2021.127946>
- Manouchehri, M., & Kargari, A. (2017). Water recovery from laundry wastewater by the cross flow microfiltration process: A strategy for water recycling in residential buildings. *Journal of Cleaner Production*, 168, 227–238. <https://doi.org/10.1016/j.jclepro.2017.08.211>
- Masindi, V., & Muedi, K. L. (2018). Environmental contamination by heavy metals. *Heavy Metals*, 10, 115–132. <https://doi.org/10.5772/intechopen.76082>
- Mishra, S., Chowdhary, P., & Bharagava, R. N. (2018). Conventional methods for the removal of industrial pollutants, their merits and demerits. In *Emerging and Eco-Friendly Approaches for Waste Management*. https://doi.org/10.1007/978-981-10-8669-4_1
- Mohammadi, S. A., Najafi, H., Zolgharnian, S., Sharifian, S., & Asasian-Kolur, N. (2022). Biological oxidation methods for the removal of organic and inorganic contaminants from wastewater: A comprehensive review. *Science of the Total Environment*, 843(April). <https://doi.org/10.1016/j.scitotenv.2022.157026>
- Molina García, M. E. (2016). Elaboración de un filtro artesanal de agua utilizando materiales no convencionales, evaluando su eficiencia para la disminución de los niveles de contaminación de aguas residuales generada por una lavadora de autos. Universidad Técnica de Ambato. Facultad de Ingeniería Civil y Mecánica. <http://repositorio.uta.edu.ec/jspui/handle/123456789/24606>
- Mpatani, F. M., Han, R., Aryee, A. A., Kani, A. N., Li, Z., & Qu, L. (2021). Adsorption performance of modified agricultural waste materials for removal of emerging micro-contaminant bisphenol A: A comprehensive review. *Science of the Total Environment*, 780, 146629. <https://doi.org/10.1016/j.scitotenv.2021.146629>
- Musie, W., & Gonfa, G. (2023). Fresh water resource, scarcity, water salinity challenges and possible remedies: A review. *Heliyon*, e18685. <https://doi.org/10.1016/j.heliyon.2023.e18685>
- Nishat, A., Yusuf, M., Qadir, A., Ezaier, Y., Vambol, V., Ijaz Khan, M., Ben Moussa, S., Kamyab, H., Sehgal, S. S., Prakash, C., Yang, H. H., Ibrahim, H., & Eldin, S. M. (2023). Wastewater treatment: A short assessment on available techniques. *Alexandria Engineering Journal*, 76, 505–516. <https://doi.org/10.1016/j.aej.2023.06.054>
- Oki, T., & Quioco, R. E. (2020). Economically challenged and water scarce: identification of global populations most vulnerable to water crises. *International Journal of Water Resources Development*, 36(2–3), 416–428. <https://doi.org/10.1080/07900627.2019.1698413>
- Orlowsky, B., Hoekstra, A. Y., Gudmundsson, L., & Seneviratne, S. I. (2014). Today's virtual water consumption and trade under future water scarcity. *Environmental Research Letters*, 9(7), 74007. <https://doi.org/10.1088/1748-9326/9/7/074007>
- Otazo, E., Ortíz, A., Richards, R., & Ponce, B. (2011). Materiales Funcionales para la Remoción de Iones Metálicos contaminantes del agua. *Avances de Impacto, Tecnología y Toxicología Ambiental*, 85–118. <https://repository.uaeh.edu.mx/bitstream/handle/123456789/11453>

- Oteng-Peprah, M., Acheampong, M. A., & deVries, N. K. (2018). Greywater Characteristics, Treatment Systems, Reuse Strategies and User Perception—a Review. *Water, Air, & Soil Pollution*, 229(8), 255. <https://doi.org/10.1007/s11270-018-3909-8>
- Palansooriya, K. N., Yang, Y., Tsang, Y. F., Sarkar, B., Hou, D., Cao, X., Meers, E., Rinklebe, J., Kim, K. H., & Ok, Y. S. (2020). Occurrence of contaminants in drinking water sources and the potential of biochar for water quality improvement: A review. *Critical Reviews in Environmental Science and Technology*, 50(6), 549–611. <https://doi.org/10.1080/10643389.2019.1629803>
- Parjane, S. B., & Sane, M. G. (2011). Performance of grey water treatment plant by economical way for Indian rural development. *International Journal of ChemTech Research*, 3(4), 1808–1815. [https://sphinxsai.com/Vol.3No.4/chem/pdf/CT=13\(1808-1815\)OD11.pdf](https://sphinxsai.com/Vol.3No.4/chem/pdf/CT=13(1808-1815)OD11.pdf)
- Pérez Silva, R. M., Calzado Lamela, O., Cascaret Carmenaty, D. A., & Tur Naranjo, E. (2014). Adsorción de Cr (VI) por Cocos nucifera L. en aguas residuales de Fibrocemento en Santiago de Cuba. *Revista Colombiana de Biotecnología*, 16(1), 9–18. <https://doi.org/10.15446/rev.colomb.biote.v16n1.44183>
- Ponce-Lira, B. (2018). Remoción De Cadmio Mediante Adsorbentes Cerámicos Empacados En Columnas De Lecho Fijo. *Agro Productividad*, 11(4). <https://doi.org/10.32854/agrop.v11i4.282>
- Qu, X., Brame, J., Li, Q., & Alvarez, P. J. J. (2013). Nanotechnology for a Safe and Sustainable Water Supply: Enabling Integrated Water Treatment and Reuse. *Accounts of Chemical Research*, 46(3), 834–843. <https://doi.org/10.1021/ar300029v>
- Rawat, I., Ranjith Kumar, R., Mutanda, T., & Bux, F. (2011). Dual role of microalgae: Phycoremediation of domestic wastewater and biomass production for sustainable biofuels production. *Applied Energy*, 88(10), 3411–3424. <https://doi.org/10.1016/J.APENERGY.2010.11.025>
- Reyes, J. V. (2016). Determination of the efficiency of sawdust and coco fiber used as Biofilter for pollutant removal for the treatment of wastewater. *Enfoque UTE*, 7(3), 41–56. <https://doi.org/10.29019/enfoqueute.v7n3.104>
- Rudi, N. N., Muhamad, M. S., Te Chuan, L., Alipal, J., Omar, S., Hamidon, N., Abdul Hamid, N. H., Mohamed Sunar, N., Ali, R., & Harun, H. (2020). Evolution of adsorption process for manganese removal in water via agricultural waste adsorbents. *Heliyon*, 6(9), e05049. <https://doi.org/10.1016/j.heliyon.2020.e05049>
- Saha, N., Rahman, M. S., Ahmed, M. B., Zhou, J. L., Ngo, H. H., & Guo, W. (2017). Industrial metal pollution in water and probabilistic assessment of human health risk. *Journal of Environmental Management*, 185, 70–78. <https://doi.org/10.1016/j.jenvman.2016.10.023>
- Salerno, F., Gaetano, V., & Gianni, T. (2018). Urbanization and climate change impacts on surface water quality: Enhancing the resilience by reducing impervious surfaces. *Water Research*, 144, 491–502. <https://doi.org/10.1016/j.watres.2018.07.058>
- Samarghandi, M. R., Zarrabi, M., Noori Sepehr, M., Panahi, R., & Foroghi, M. (2012). Removal of Acid Red 14 by Pumice Stone as a Low Cost Adsorbent: Kinetic and Equilibrium Study. *Iranian Journal of Chemistry and Chemical Engineering*, 31(3), 19–27. <https://doi.org/10.30492/ijcce.2012.5947>
- Samayamanthula, D. R., Sabarathinam, C., & Bhandary, H. (2019). Treatment and effective utilization of greywater. *Applied Water Science*, 9, 1–12. <https://doi.org/10.1007/s13201-019-0966-0>
- Saravanan, A., Senthil Kumar, P., Jeevanantham, S., Karishma, S., Tajsabreen, B., Yaashikaa, P. R., & Reshma, B. (2021). Effective water/wastewater treatment methodologies for toxic pollutants removal: Processes and applications towards sustainable development. *Chemosphere*, 280, 130595. <https://doi.org/10.1016/j.chemosphere.2021.130595>

- Sathya, R., Arasu, M. V., Al-Dhabi, N. A., Vijayaraghavan, P., Ilavenil, S., & Rejiniemon, T. S. (2023). Towards sustainable wastewater treatment by biological methods – A challenges and advantages of recent technologies. *Urban Climate*, 47(October 2022), 101378. <https://doi.org/10.1016/j.uclim.2022.101378>
- Sepehr, M. N., Sivasankar, V., Zarrabi, M., & Senthil Kumar, M. (2013). Surface modification of pumice enhancing its fluoride adsorption capacity: An insight into kinetic and thermodynamic studies. *Chemical Engineering Journal*, 228, 192–204. <https://doi.org/10.1016/j.cej.2013.04.089>
- Shah, A., Arjunan, A., Baroutaji, A., & Zakharova, J. (2023). A review of physicochemical and biological contaminants in drinking water and their impacts on human health. *Water Science and Engineering*, xxx. <https://doi.org/10.1016/j.wse.2023.04.003>
- Sharma, N., Singh, A., & Batra, N. (2019). *Modern and Emerging Methods of Wastewater Treatment*. Springer Singapore. https://doi.org/10.1007/978-981-13-0149-0_13
- Simate, G. S. (2015). The treatment of brewery wastewater for reuse by integration of coagulation/flocculation and sedimentation with carbon nanotubes “sandwiched” in a granular filter bed. *Journal of Industrial and Engineering Chemistry*, 21, 1277–1285. <https://doi.org/10.1016/j.jiec.2014.06.001>
- Singh, J., Yadav, P., Pal, A. K., & Mishra, V. (2020). Water Pollutants: Origin and Status BT - Sensors in Water Pollutants Monitoring: Role of Material (D. Pooja, P. Kumar, P. Singh, & S. Patil (eds.)); pp. 5–20). Springer Singapore. https://doi.org/10.1007/978-981-15-0671-0_2
- Song, S., Le-Clech, P., & Shen, Y. (2023). Microscale fluid and particle dynamics in filtration processes in water treatment: A review. *Water Research*, 233(September 2022), 119746. <https://doi.org/10.1016/j.watres.2023.119746>
- Srivastav, A. L., & Ranjan, M. (2020). Chapter 1 - Inorganic water pollutants (P. Devi, P. Singh, & S. K. B. T.-I. P. in W. Kansal (eds.)); pp. 1–15). Elsevier. <https://doi.org/10.1016/B978-0-12-818965-8.00001-9>
- Sun, Y., Nan, Z., Yang, W., & Li, L. (2023). Projecting China’s future water footprints and water scarcity under socioeconomic and climate change pathways using an integrated simulation approach. *Climate Services*, 30(1), 100385. <https://doi.org/10.1016/j.cliser.2023.100385>
- Touliabah, H. E., El-Sheekh, M. M., Ismail, M. M., & El-Kassas, H. (2022). A Review of Microalgae- and Cyanobacteria-Based Biodegradation of Organic Pollutants. In *Molecules* (Vol. 27, Issue 3). <https://doi.org/10.3390/molecules27031141>
- Trejo-Téllez, L. I., Ramírez-Martínez, M., Gómez-Merino, F. C., García-Albarado, J. C., Baca-Castillo, G. A., & Tejeda-Sartorius, O. (2013). Evaluación física y química de tezontle y su uso en la producción de tulipán. *Revista Mexicana de Ciencias Agrícolas*, 4(SPE5), 863–876. <https://www.redalyc.org/articulo.oa?id=263128352001>
- Tusiime, A., Solihu, H., Sekasi, J., & Mutanda, H. E. (2022). Performance of lab-scale filtration system for grey water treatment and reuse. *Environmental Challenges*, 9(August), 100641. <https://doi.org/10.1016/j.envc.2022.100641>
- Tyagi, S., Sharma, B., Singh, P., & Dobhal, R. (2020). Water Quality Assessment in Terms of Water Quality Index. *American Journal of Water Resources*, 1(3), 34–38. <https://doi.org/10.12691/ajwr-1-3-3>
- Valladares-Cisneros, M. G., Cárdenas, C. V., Burelo, P. de la C., & Alemán, R. M. M. (2018). Non-conventional absorbers: sustainable alternatives for wastewater treatment. *Revista Ingenierías Universidad de Medellín*, 16(31 SE-Articles). <https://doi.org/10.22395/rium.v16n31a3>
- Wasewar, K. L., Singh, S., & Kansal, S. K. (2020). Process intensification of treatment of inorganic water pollutants. In *Inorganic Pollutants in Water*. INC. <https://doi.org/10.1016/B978-0-12-818965-8.00013-5>

Xu, Y., Zhang, X., Zhao, Y., Wu, Y., Liu, Y., Wang, R., Yang, Y., & Chen, J. (2023). Research status and progress in degradation of organic pollutants via hydrogen evolution reaction and oxygen evolution reaction in wastewater electrochemical treatment. *International Journal of Hydrogen Energy*, xxxx. <https://doi.org/10.1016/j.ijhydene.2023.05.167>

Yan, T., Shen, S. L., & Zhou, A. (2022). Indices and models of surface water quality assessment: Review and perspectives. *Environmental Pollution*, 308(March), 119611. <https://doi.org/10.1016/j.envpol.2022.119611>

Chapter 4 Theoretical-numerical analysis of the stress concentration factor in a stepped bar in tension

Capítulo 4 Análisis teórico-numérico del factor de concentración de esfuerzos en una barra escalonada sometida a tracción

SOTO-MENDOZA, Gilberto*, MARTÍNEZ-GARCÍA, José and COUTIÑO-MORENO, Elvis

Tecnológico Nacional de México. Tecnológico de Estudios Superiores de Jocotitlán. Departamento de Ingeniería Mecatrónica. Carretera Toluca-Atlacomulco KM 44.8, Ejido de San Juan y San Agustín, Jocotitlán, 50700 México.

ID 1st Author: *Gilberto, Soto-Mendoza* / **ORC ID:** 0000-0001-7357-9445, **CVU CONAHCYT ID:** 635154

ID 1st Co-author: *José, Martínez-García* / **ORC ID:** 0000-0002-7797-1062, **CVU CONAHCYT ID:** 612069

ID 2nd Co-author: *Elvis, Coutiño-Moreno* / **ORC ID:** 0000-0003-2455-2574, **CVU CONAHCYT ID:** 550285

DOI: 10.35429/H.2023.5.47.60

G. Soto, J. Martínez and E. Coutiño

*gilberto.soto@tesjo.edu.mx

R. López (AA.) Engineering and Architecture in the Northern part of the State of Mexico. Handbooks-TI-©ECORFAN-Mexico, Estado de México, 2023

Abstract

The stress concentration factor of different structural elements has been obtained analytical, experimental, and numerically. For the analytical part, there are several formulas established according to the element and the load condition to which the component is subjected. In the case of the numerical simulation results, they are approximations that depend on the refinement of the mesh. In this work, a comparative analysis was carried out between the analytical results and those obtained numerically from the stress concentration factor of a flat stepped bar subjected to tension, considering convergence criteria of 5%, 2% and 1%. An automatic mesh refinement tool was used, and several studies were run using design points. It was found that the average percentage variation between the analytical and the numerical approach according to the convergence criterion was 2.5%, 0.9% and 0.6%, respectively. Also, some points were found where the variation was notable.

Stress concentration, FEM, Simulation, ANSYS

Resumen

El factor de concentración de tensiones de diferentes elementos estructurales se ha obtenido analítica, experimental y numéricamente. Para la parte analítica, existen diversas fórmulas establecidas en función del elemento y de la condición de carga a la que está sometido el componente. En el caso de los resultados de simulación numérica, son aproximaciones que dependen del refinamiento de la malla. En este trabajo se realizó un análisis comparativo entre los resultados analíticos y los obtenidos numéricamente del factor de concentración de tensiones de una barra plana escalonada sometida a tracción, considerando criterios de convergencia del 5%, 2% y 1%. Se utilizó una herramienta de refinamiento automático de la malla y se realizaron varios estudios utilizando puntos de diseño. Se comprobó que la variación porcentual media entre el enfoque analítico y el numérico según el criterio de convergencia era del 2,5%, 0,9% y 0,6%, respectivamente. Además, se encontraron algunos puntos en los que la variación era notable.

Concentración de tensiones, MEF, Simulación, ANSYS

1. Introduction

In the field of engineering, when designing components such as shafts, supports, gears, among others, factors such as the concentration of efforts must be considered. Three different approaches can be used to determine these factors. The first is theoretical analysis. This is limited when dealing with complex geometries for which there are no established formulas or are very complex that it is not practical to use. The second is the experimental analysis, which is expensive to implement and the time to perform it is considerable. The third approach is simulation. The latter solves the governing equations of the physical phenomenon to be treated and has been implemented for the solution of structural, thermal, fluid mechanics problems, among others.

A reference author who has developed a series of formulas to obtain the concentration of stresses of several structural elements subject to different load conditions is Roark (Budynas & Sadegh, 2020). In his publication he presents a summary of formulas, facts and principles related to mechanics of materials. It contains a series of tables to obtain the stress concentration factor.

On the other hand, in the experimental approach, stress concentration studies using photoelasticity are reported. Among these studies Weibel (Studies in Photoelastic Stress Determination | J. Fluids Eng. | ASME Digital Collection, 1934) reports three laboratory studies to determine the concentration of efforts. Wilson and White (Wilson & White, 1973) use the method to analyze concentration of stresses generated by fillets and grooves in plates subjected to tension and bending. Other studies report the combination of the approaches mentioned for obtaining the stress concentration factor, for example, Ronald and Bastida (Roldan & Bastidas, 2002) report a study of the stress concentrator factor produced by a hole in a flat plate.

Regarding numerical simulation, this provides approximate solutions and is based on the Finite Element Method. In this methodology, geometry is divided into parts as if they were the pieces of a LEGO® (Chen & Liu, 2018). To represent the curves, smaller elements are required to define them better. The use of this approach has been potentiated due to the improvement in computer equipment and that compared to experimental studies represents a lower cost. Comparative studies have been carried out between analytical and numerical results. For example, Chmelko *et al* (Chmelko *et al.*, 2021) report a theoretical-numerical study focused on the analysis of the concentration of effort that are presented in notches considering different mesh sizes.

This paper aims to analyze the variation of the stress concentration factor in a tension step bar obtained with theoretical calculation and numerical analysis using automatic mesh refinement tools, to find the percentage variation under different convergence criteria.

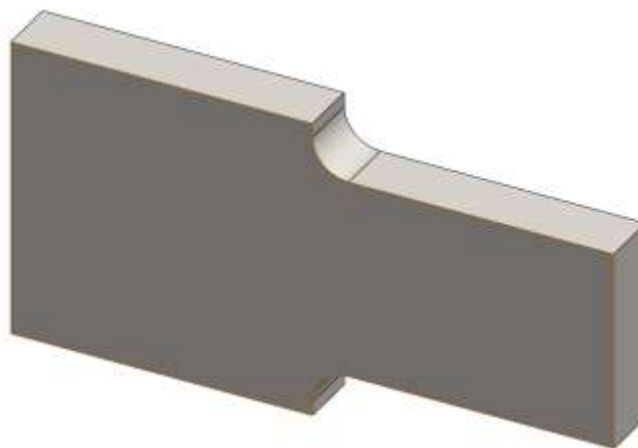
2. Description of the problem

The concentrations of stresses that occur in structural components of machines, land vehicles, aircraft, etc. cause that in the area where they are located, the stress resisted by the material when applying load is quickly reached. For this reason, it is important to have your values well defined. This can be carried out theoretical, experimentally, or numerically. The results obtained by the different approaches should be the same or very similar.

Currently, numerical simulation has become a very powerful tool in engineering. However, certain principles must be followed to validate that the result obtained is correct. In the case of structural static analysis, a mesh sensitivity analysis must be carried out, that is, a refinement of the mesh and that the desired result is the same regardless of the mesh size used.

It can be said that the theoretical solution is the exact or ideal solution and the numerical result is an approximate solution that will depend on the discretization of the component. There is a convergence tool that automatically performs the mesh refinement process considering a convergence criterion. In this paper, to find the percentage variation between theoretical analysis and numerical simulation considering different convergence criteria of a stepped flat bar (see Figure 1).

Figure 1 Stepped flat bar



3. Methodology

Once the type of element to be studied (stepped flat bar) was defined, to obtain the percentage of variation between the results of the theoretical and numerical approach, the following stages were followed:

1. Creation of geometry respecting the principle of Saint-Venant.
2. Theoretical calculation of the effort concentrator according to Roark.
3. Numerical simulation using a program CAE (Computer Aided Engineering).
4. Comparative analysis of results obtained theoretically with those obtained numerically.

The next section begins with the theoretical basis of the case study.

4. Theoretical basis

4.1. Stress Concentrations

Stress concentrations occur in regions of the components where fillets, grooves, holes, or some other change in geometry are found. To determine the maximum stress that is presented, the Equation 1 is used. For more information it is recommended to consult the references (Ferdinand *et al.*, 2020; Goodno & Gere, 2018; R. C. Hibbeler, 2018).

$$\sigma_{m\acute{a}x} = K\sigma_{nom} \quad (1)$$

Where:

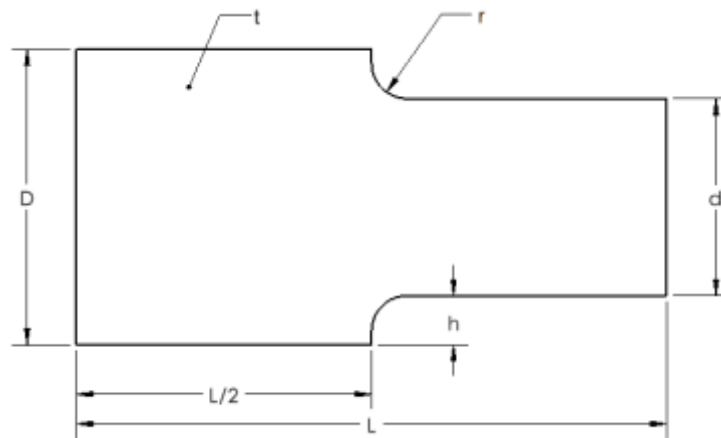
$\sigma_{m\acute{a}x}$ = Maximum stress

K = Stress Concentration Factor

σ_{nom} = Nominal stress

For a stepped flat bar (see Figure 2), it was found that the stress concentration factor is determined with Equation 2, according to Roark (Budynas & Sadegh, 2020):

Figure 2 Stepped flat bar with dimensions



$$K = C_1 + C_2 \left(\frac{2h}{D}\right) + C_3 \left(\frac{2h}{D}\right)^2 + C_4 \left(\frac{2h}{D}\right)^3 \quad (2)$$

To get the constants you must:

If $0.1 \leq h/r \leq 2.0$

$$C_1 = 1.007 + 1.000 \sqrt{\frac{h}{r}} - 0.0031 \frac{h}{r} \quad (3)$$

$$C_2 = -0.114 - 0.585 \sqrt{\frac{h}{r}} + 0.314 \frac{h}{r} \quad (4)$$

$$C_3 = 0.241 - 0.992 \sqrt{\frac{h}{r}} - 0.271 \frac{h}{r} \quad (5)$$

$$C_4 = -0.134 + 0.577 \sqrt{\frac{h}{r}} - 0.012 \frac{h}{r} \quad (6)$$

If $2.0 \leq h/r \leq 20.0$

$$C_1 = 1.007 + 1.000 \sqrt{\frac{h}{r}} - 0.0031 \frac{h}{r} \quad (7)$$

$$C_2 = -0.114 - 0.585 \sqrt{\frac{h}{r}} + 0.314 \frac{h}{r} \quad (8)$$

$$C_3 = 0.241 - 0.992\sqrt{\frac{h}{r}} - 0.271\frac{h}{r} \quad (9)$$

$$C_4 = -0.134 + 0.577\sqrt{\frac{h}{r}} - 0.012\frac{h}{r} \quad (10)$$

4.2. Numerical analysis

In general, the steps to perform a static structural numerical analysis are:

- Definition of the mechanical properties of the material.
- Mesh generation.
- Application of border conditions.
- Study solution.
- Obtaining the desired results such as deformation, efforts, etc. (Postprocessing).

Equation 11 corresponds to the governing equation for a linear structural static study.

$$[\mathbf{K}]\{\mathbf{D}\} = \{\mathbf{F}\} \quad (11)$$

Where:

$\{\mathbf{D}\}$ = Displacement vector

$\{\mathbf{F}\}$ = Force vector

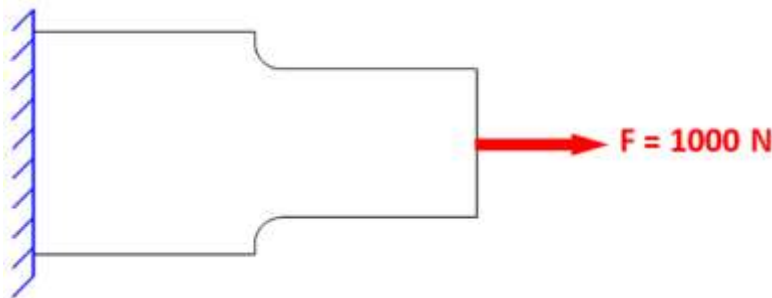
$[\mathbf{K}]$ = The stiffness matrix

5. Theoretical-numerical analysis

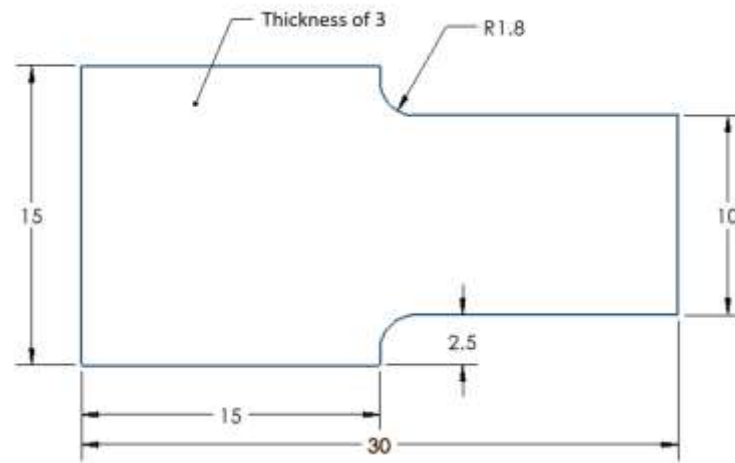
5.1. Theoretical analysis

This section shows the theoretical calculation of the maximum stress produced by the stress concentration of the flat step bar and the different stress concentration factors if the dimensions of the part are varied. Figure 3 shows a flat stepped bar recessed at its left end and a force of 1000 N is applied on its right side.

Figure 3 Support and load applied to the flat stepped bar



The dimensions of the part are illustrated in Figure 4. The dimensions are given in millimeters. For the construction of the geometry was considered the principle of Saint-Venant which says that the equation $\sigma = F/A$ defines axial stresses on a cross section of the bar only when the section is at least one distance B away from any concentrated load or discontinuity in its shape, where B is the largest lateral dimension of the bar (Goodno & Gere, 2018).

Figure 4 Dimensions of the flat step bar

To obtain the stress concentrator the equation 2 is used. It contains four constants: C_1 , C_2 , C_3 y C_4 . Which are calculated with equations 3 to 10. To define the equations to be used, the h/r ratio is calculated. From Figure 4 we have that $h = 2.5$ mm and $r = 1.8$ mm, therefore, $h/r = 2.5 \text{ mm}/1.8 \text{ mm} = 1.389$. This indicates that the equations to be used to obtain the constants are from 3 to 6. Substituting the numerical values into the equation yields:

If $0.1 \leq 1.667 \leq 2.0$

$$C_1 = 1.007 + 1.000 \sqrt{\frac{2.5}{1.8}} - 0.0031 \frac{2.5}{1.8} = 2.143$$

$$C_2 = -0.114 - 0.585 \sqrt{\frac{2.5}{1.8}} + 0.314 \frac{2.5}{1.8} = -0.3673$$

$$C_3 = 0.241 - 0.992 \sqrt{\frac{2.5}{1.8}} - 0.271 \frac{2.5}{1.8} = -1.3045$$

$$C_4 = -0.134 + 0.577 \sqrt{\frac{2.5}{1.8}} - 0.012 \frac{2.5}{1.8} = 0.5293$$

Substituting the values into equation 2 gives:

$$K = 2.143 + (-0.3673) \left[\frac{(2)(2.5)}{15} \right] + (-1.3045) \left[\frac{(2)(2.5)}{15} \right]^2 + (0.5293) \left[\frac{(2)(2.5)}{15} \right]^3 = 1.895$$

The maximum stress is now calculated. The force applied to the part is 1000 N. The nominal effort corresponds to the section on the right side (see Figure 4). The cross section is rectangular. Using Equation 2 we have:

$$\sigma_{nom} = \frac{1000 \text{ N}}{(10 \text{ mm})(3 \text{ mm})} = 33.33 \text{ MPa}$$

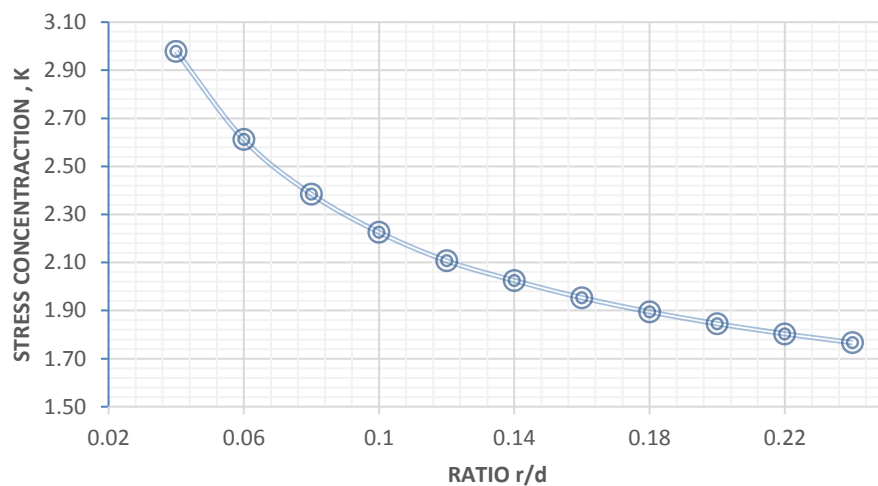
$$\sigma_{m\acute{a}x} = (1.895)[33.33 \text{ MPa}] = 63.2 \text{ MPa}$$

The above procedure is applied to obtain the stress concentrator when the radius of Figure 4 is modified. The other dimensions remain constant. A spreadsheet was created for efficiency. Table 1 shows the results of the stress concentrator and the maximum stress of the flat step bar for different radius dimensions.

Table 2 Maximum stress and stress concentrator for different radius

No.	Radio, r (mm)	Ratio r/d	Stress concentrator, K	Maximum stress, σ_{\max} (MPa)
1	0.4	0.04	2.98	99.3
2	0.6	0.06	2.61	87.1
3	0.8	0.08	2.38	79.5
4	1	0.1	2.23	74.2
5	1.2	0.12	2.11	70.2
6	1.4	0.14	2.02	67.5
7	1.6	0.16	1.953	65.1
8	1.8	0.18	1.895	63.2
9	2	0.2	1.845	61.5
10	2.2	0.22	1.803	60.1
11	2.4	0.24	1.767	58.9

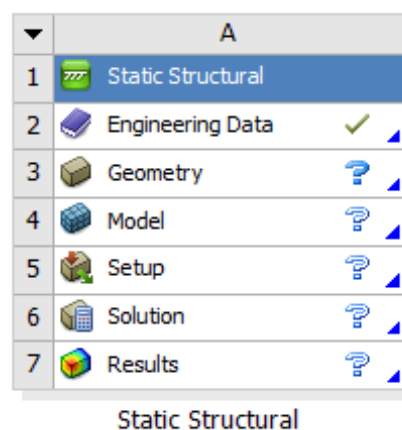
Derived from Table 1, Figure 5 is obtained. This shows on the vertical axis the effort concentrator and on the horizontal axis the ratio r/d, for a ratio $D/d = 15 \text{ mm}/10 \text{ mm} = 1.5$.

Figure 5 Stress concentration K vs ratio r/d for $D/d = 1.5$.

5.2. Numerical analysis

The numerical study was conducted in the ANSYS Student program, version 2023/R1. This is a free academic license. Which is limited to the number of elements or nodes that can solve, in particular, for structural analyses the limit is 128,000 nodes or elements, whichever is reached first. To download this package, consult the installation procedure, system requirements, license duration, among others, see the reference (ANSYS, 2023).

Below are each of the stages required for a Static-Structural study in the package. ANSYS (see Figure 6). The first cell A1, indicates the type of study “Static Structural”.

Figure 6 Structural Static Module in ANSYS Workbench

5.2.1 Material properties

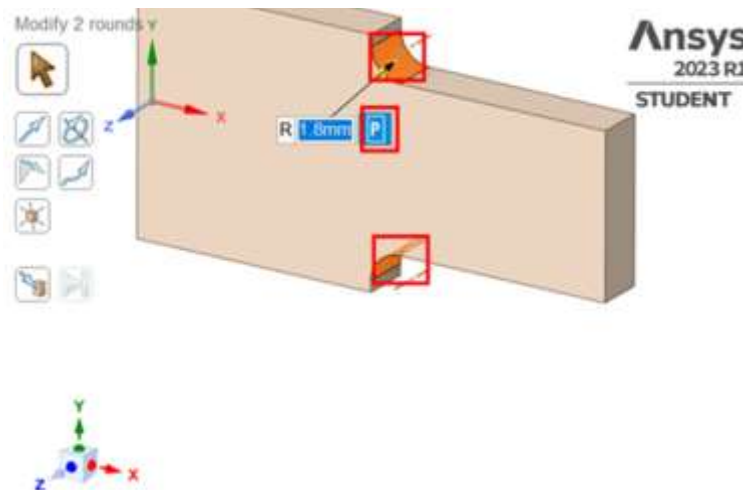
The second cell A2 of the workflow for the Static-Structural simulation corresponds to the materials “Engineering Data”. In this section you can select from the library the material or materials to be used. If they do not exist, they can be created according to the properties of the material to be used. For the case study, a structural steel is used that has the following properties:

- Young’s modulus = 200 GPa
- Poisson’s ratio = 0.3
- Yield Strength = 250 MPa

5.2.2 Geometry

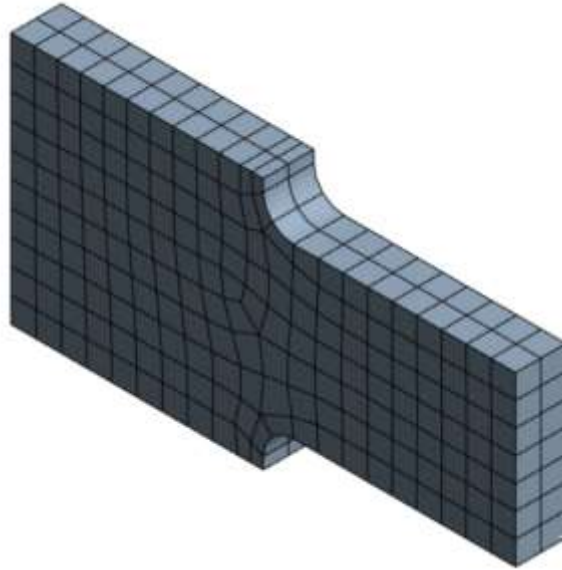
The geometry (cell A3) can be imported or created in the Computer Aided Design (CAD) programs of the same package. The available options integrated into the program are: SpaceClaim, DesingModeler and Discovery. In the present work, the SpaceClaim program was used to create the piece. In addition to this, the radius was parameterized, which allows several case studies to be carried out at a later stage. Figure 6 shows the part created. A red rectangle shows the radii to be parameterized and activating the box with a letter P activates the parameterization. When parameterizing either the geometry or some result, a box is created with the name of “Parameter Set”.

Figure 7 Geometry created in SpaceClaim



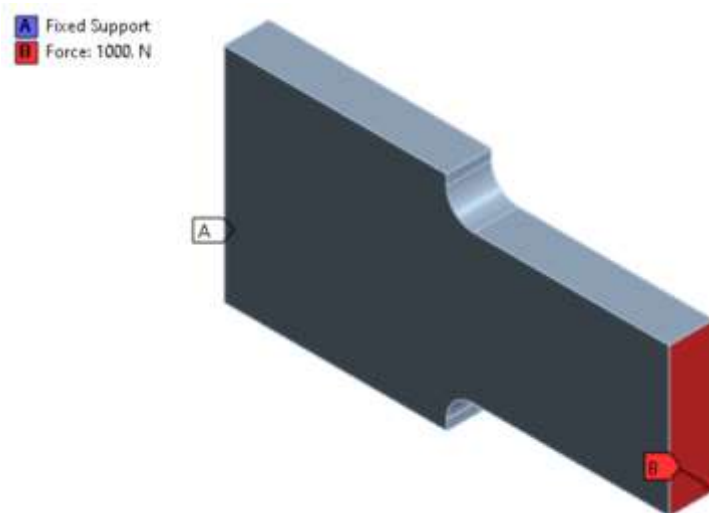
5.2.3 Mesh generation

The generation of the mesh was carried out in the program ANSYS Meshing. This is integrated into the cell module A4 Model. Related, to have 2 elements in the thickness of the piece in the global parameters of the mesh handles a mesh size of 1.5 mm. With an adaptive mesh and all other parameters are left by default. Obtaining a mesh with 2230 nodes, 353 elements and a minimum Element Quality of 0.66. Figure 8 shows the mesh created. This is an initial mesh for the study, since subsequently, a mesh sensitivity analysis is performed.

Figure 8 Mesh

5.2.4 Boundary conditions

Boundary conditions are a fixed support on the far-left side and a force of 1000 N on the right side. Figure 9 shows the boundary conditions of the part envelope. The blue color with the label "A" corresponds to the fixed support. The red color corresponds to the face where the force is applied and labeled with the letter "B".

Figure 9 Boundary conditions

5.2.5 Postprocesamiento

Once the material has been selected and the boundary conditions established, the study is sent for solution. As results, displacement and normal stress in the X direction were considered. Once the simulation was executed, the results illustrated in Figure 10 and Figure 11 were obtained. Figure 10 shows the displacement in the X direction, its maximum magnitude is represented in red with a value of 0.00425 mm. Figure 11 illustrates that the stress is concentrated in the radius (red zone) with a magnitude of 56.69 MPa.

Figure 10 Displacement in the X direction.

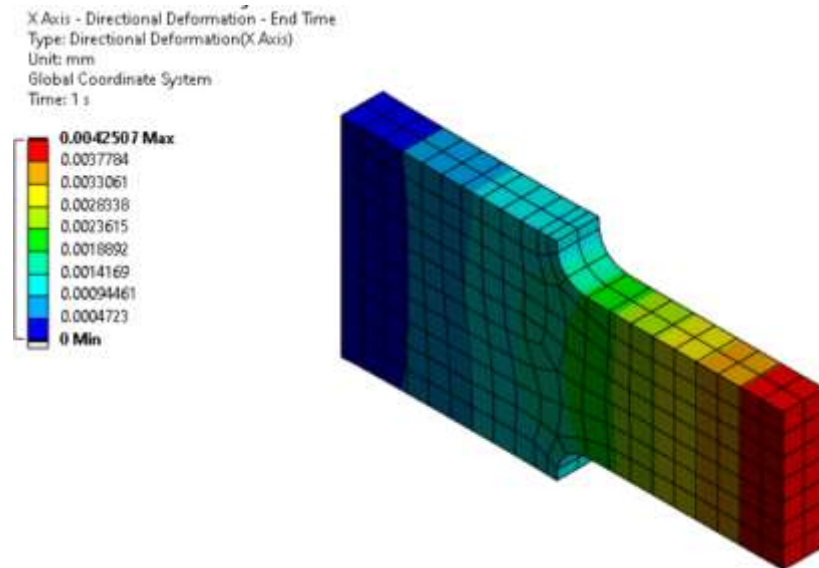
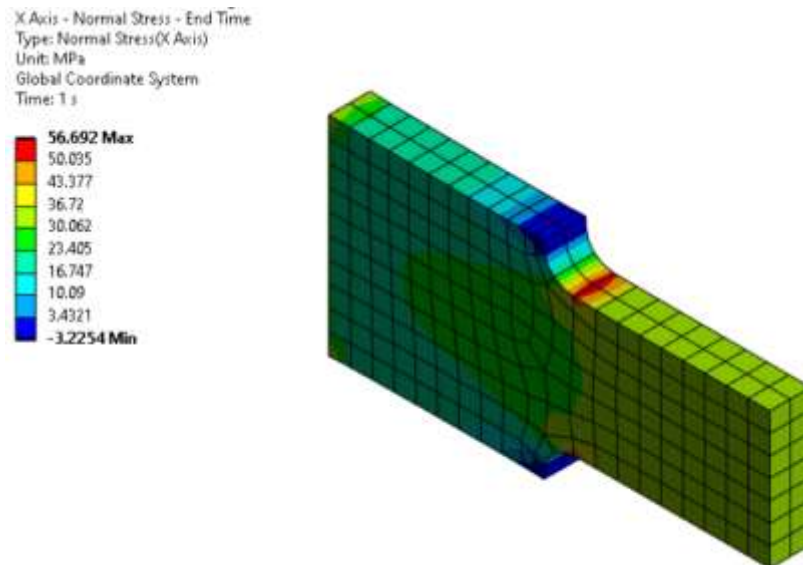


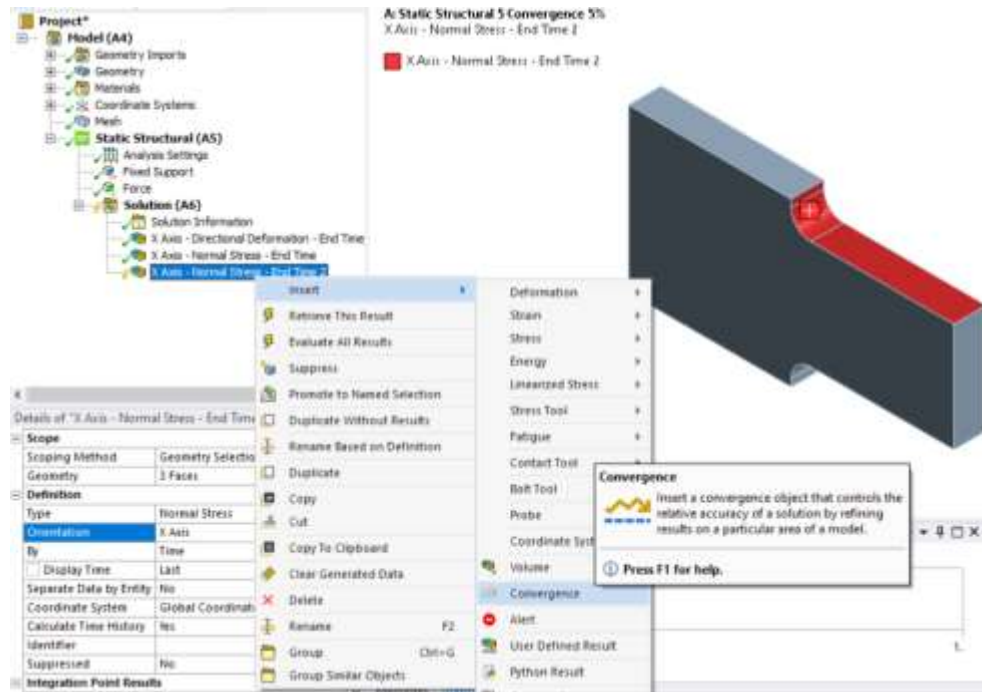
Figure 11 Normal stress in the X direction



5.2.6 Mesh sensitivity analysis

Since the results, in particular the efforts, vary with the size of the elements of the mesh, it is necessary to consider what is the acceptable percentage that indicates that convergence is achieved. Three are considered in this paper. The first when convergence is reached at 5%, the second when convergence is reached at 2% and the third when convergence is reached at 1%. One way to refine the mesh is to do it manually or use a tool “Convergence” (see Figure 12). In addition, the area of interest is where the radius is located, for this reason the face of the radius and the adjacent faces (red area) are selected.

Figure 12 Tool “Convergence”



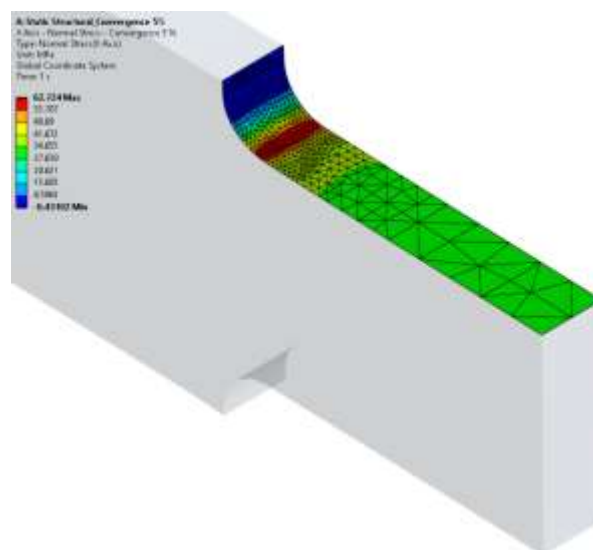
Considering a convergence criterion of 5% and executing the solution, the results shown in Table 2 are obtained. The first result obtained was 56.69 MPa with 2230 nodes and 358 elements. The convergence was reached in the third run obtaining an Stress of 62.72 MPa with 29787 nodes and 20012 elements. Between runs 2 and 3 the change in the result was -0.47%, so it meets the convergence criterion that indicates that the variation must be less than 5%.

Table 3 Mesh sensitivity analysis

Run	Normal Stress in the X direction (MPa)	Change (%)	Nodes	Elements
1	56.69		2230	358
2	63.02	8.838	13480	8374
3	62.72	-0.4702	29787	20012

Figure 13 shows the stress results in the area of interest. Also, the change in the size of the mesh elements can be observed.

Figure 13 Stress in the area of interest



5.2.7 Design Points

To obtain the stress for different radii considering a convergence of the results of 5%, 2% and 1%, at least 20 more runs have to be made. For this purpose, design points were used. Figure 14 shows in column B the different radii considered. Columns C, D and E show the Stress obtained considering a convergence of 5%, 2% and 1% respectively. It is important to note that in the case of cell E3 the result was not obtained because the refinement of the mesh reached the number of nodes that allows solving the academic license.

Figure 14 Design points

Table of Design Points				
	B	C	D	E
1	P6 - Radio (r)	P7 - X Axis - Normal Stress - Convergence 5 %	P9 - X Axis - Normal Stress - Convergence 2 %	P10 - X Axis - Normal Stress - Convergence 1 %
2	mm	MPa	MPa	MPa
3	0.4	94.785	99.725	✘ 99.725
4	0.6	86.316	86.992	86.992
5	0.8	79.75	79.75	79.75
6	1	74.512	74.512	74.512
7	1.2	71.15	71.15	70.85
8	1.4	60.468	67.291	67.541
9	1.6	64.535	64.965	62.724
10	1.8	62.724	57.686	62.724
11	2	60.449	60.97	60.97
12	2.2	59.857	59.437	59.437
13	2.4	57.893	58.009	58.009
*				

Table 3 shows the numerically obtained stresses and the stress concentration factor. To obtain the stress concentration factor, the numerical stress is divided by the nominal stress that for the case study is 33.33 MPa.

Table 4 Stress concentration factor derived from numerical simulation

No.	Radio, r (mm)	Convergence 5%		Convergence 2%		Convergence 1%	
		Maximum Stress, σ_{\max} (MPa)	Stress concentration, K	Maximum Stress, σ_{\max} (MPa)	Stress concentration, K	Maximum Stress, σ_{\max} (MPa)	Stress concentration, K
1	0.4	94.79	2.84	99.73	2.99	-	-
2	0.6	86.32	2.59	86.99	2.61	86.99	2.61
3	0.8	79.75	2.39	79.75	2.39	79.75	2.39
4	1	74.51	2.24	74.51	2.24	74.51	2.24
5	1.2	71.15	2.13	71.15	2.13	70.85	2.13
6	1.4	60.47	1.81	67.29	2.02	67.54	2.03
7	1.6	64.54	1.94	64.97	1.95	62.72	1.88
8	1.8	62.72	1.88	57.69	1.73	62.72	1.88
9	2	60.45	1.81	60.97	1.83	60.97	1.83
10	2.2	59.86	1.80	59.44	1.78	59.44	1.78
11	2.4	57.89	1.74	58.01	1.74	58.01	1.74

6. Analysis of results

In this section, a comparative analysis is carried out between the theoretical result of the stress concentration factor of a stepped flat bar and this same using numerical simulation with three different convergence ranges (5%, 2% and 1%). From Table 1 the results of the stress concentration factor obtained theoretically are extracted and from Table 3 the numerical values. Table 4 summarizes the values of concentration of stress and their percentage variation with respect to the theoretical value.

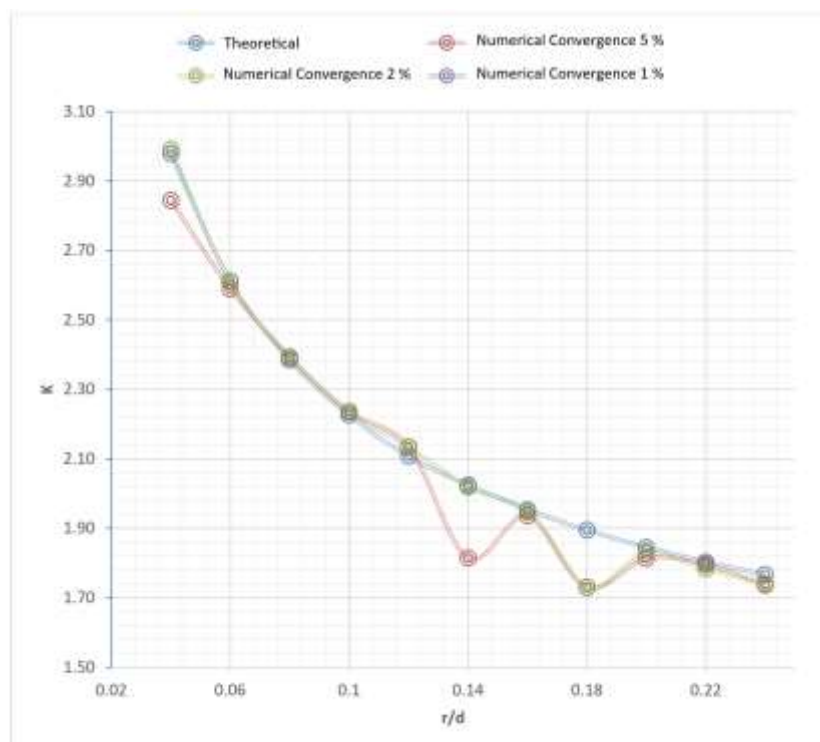
Table 5 Percentage variation of theoretical-numerical stress concentrations factors

No.	Radio, r (mm)	Theoretical stress concentration factor, K	Convergence 5%		Convergence 2%		Convergence 1%	
			Stress concentration factor, K	Variation (%)	Stress concentration factor, K	Variation (%)	Stress concentration factor, K	Variation (%)
1	0.4	2.98	2.84	4.5	2.99	-0.4	-	-
2	0.6	2.61	2.59	0.8	2.61	0.1	2.61	0.1
3	0.8	2.38	2.39	-0.3	2.39	-0.3	2.39	-0.3
4	1	2.23	2.24	-0.4	2.24	-0.4	2.24	-0.4
5	1.2	2.11	2.13	-1.3	2.13	-1.3	2.13	-0.9
6	1.4	2.02	1.81	10.4	2.02	0.3	2.03	-0.1
7	1.6	1.95	1.94	0.9	1.95	0.2	1.88	3.7
8	1.8	1.89	1.73	8.7	1.73	8.7	1.88	0.7
9	2	1.85	1.81	1.7	1.83	0.9	1.83	0.9
10	2.2	1.80	1.80	0.4	1.78	1.1	1.78	1.1
11	2.4	1.77	1.74	1.7	1.74	1.5	1.74	1.5

From Table 4 we must:

- The average of the percentage of fluctuation considering a convergence range of 5% is 2.5% and the maximum variation is 10.4%.
- The average of the percentage fluctuation considering a convergence range of 2% is 0.9% and the maximum variation is 8.7%.
- The average of the percentage of fluctuation considering a convergence range of 1% is 0.6% and the maximum variation is 3.7%.

As the magnitude of the convergence criterion is reduced, that is, the percentage of variation of the effort due to mesh refinement is lower, the numerical and theoretical results are closer. However, the number of nodes and elements increases, and this is reflected in a greater demand for computational resources. In the case of the academic license, it is limited to the permitted limit of nodes or elements mentioned in point 5.2. Figure 15 graphically illustrates the behavior of the analyses. When the ratio r/d is 0.14 and 0.18 with convergence criteria of 5% and 2% presented the greatest difference. On the other hand, in these same points considering a convergence criterion of 1% the variation presented was 0.7% and -0.1%.

Figure 15 Stress concentration factor K with respect to the ratio r/d.

7. Conclusions

Based on the analysis of comparative results between a theoretical and numerical study carried out on a flat stepped plate, the average stress concentration factor varied 2.5%, 0.9% and 0.6% with a convergence criterion of 5%, 2% and 1%, respectively. This using the tool “Convergence”. Also, points were found where the difference of the variation is maximum, being for a convergence criterion of 5% a variation of 10.4%; for a convergence criterion of 2% a variation of 8.7%; and for a convergence criterion of 1% a variation of 3.7%.

The results of numerical studies are approximations that depend on the discretizing process. As a more rigorous convergence criterion is applied, the theoretical and numerical results are closer. Further refinement impacts the study execution time and computational resource capacity required. In the case of academic leave used, at one of the design points the permissible limit was reached.

8. Referencias

- ANSYS. (2023). *Download Ansys Student | Workbench-based Simulation Tools*. <https://www.ansys.com/academic/students/ansys-student>
- Budynas, R. G., & Sadegh, A. M. (2020). *Roark's Formulas for Stress and Strain* (9th Edition). McGraw-Hill Education. <https://www.accessengineeringlibrary.com/content/book/9781260453751>
- Chen, X., & Liu, Y. (2018). *Finite Element Modeling and Simulation with ANSYS Workbench* (2nd ed.). CRC Press. <https://www.routledge.com/Finite-Element-Modeling-and-Simulation-with-ANSYS-Workbench-Second-Edition/Chen-Liu/p/book/9781138486294>
- Chmelko, V., Harakal', M., Žlábek, P., Margetin, M., & Ďurka, R. (2021). Simulation of Stress Concentrations in Notches. *Metals* 2022, Vol. 12, Page 43, 12(1), 43. <https://doi.org/10.3390/MET12010043>, <https://www.mdpi.com/2075-4701/12/1/43>.
- Ferdinand, P. B., Johnston, E. R., DeWolf, J. T., & Mazurek, D. F. (2020). *Mechanics of Materials* (8th ed.). McGraw-Hill Education.
- Goodno, B. J., & Gere, J. M. (2018). *Mechanics of Materials* (9th ed.). Cengage Learning.
- R. C. Hibbeler. (2018). *Mechanics of Materials* (10th ed.). Pearson Education.
- Roldan, F., & Bastidas, U. (2002). Estudio Experimental y por Análisis de Elementos Finitos del Factor de Concentrador de Esfuerzo Producido por un Agujero en una Placa Plana. *Dyna*, 69(137), 1–8. <https://www.redalyc.org/articulo.oa?id=49613701>
- Studies in Photoelastic Stress Determination | J. Fluids Eng. | ASME Digital Collection*. (1934). <https://asmedigitalcollection.asme.org/fluidsengineering/article-abstract/56/7/637/1157771/Studies-in-Photoelastic-Stress-Determination?redirectedFrom=fulltext>
- Wilson, I. H., & White, D. J. (1973). Stress-concentration factors for shoulder fillets and grooves in plates. *Journal of Strain Analysis*, 8(1), 43–51. <https://doi.org/10.1243/03093247V081043>, <https://journals.sagepub.com/doi/10.1243/03093247V081043>

Chapter 5 Study of electrically conductive adhesives in the manufacture of photovoltaic modules

Capítulo 5 Estudio de adhesivos conductores de electricidad en la manufactura de módulos fotovoltaicos

SORIANO-VARGAS, Orlando†*, MENDOZA-HERNÁNDEZ, Raúl, LOPEZ, Roberto and GARCIA-SANCHEZ, José Juan

TecNM/Tecnológico de Estudios Superiores de Jocotitlán, Carretera Toluca Atlacomulco km 44.8, Ejido de San Juan y San Agustín, Jocotitlán, México

ID 1st Author: *Orlando, Soriano-Vargas* / **ORC ID:** 0000-0002-9331-7909

ID 1st Co-author: *Raúl, Mendoza-Hernández* / **ORC ID:** 0009-0003-7169-6551

ID 2nd Co-author: *Roberto, López-Ramírez* / **ORC ID:** 0000-0001-8341-3684

ID 3rd Co-author: *Jose Juan, García-Sánchez* / **ORC ID:** 0000-0002-6415-7854

DOI: 10.35429/H.2023.5.61.85

O. Soriano, R. Mendoza, R. López and J. García

*orlando.soriano@tesjo.edu.mx

R. López (AA.) Engineering and Architecture in the Northern part of the State of Mexico. Handbooks-TI-©ECORFAN-Mexico, Estado de México, 2023

Abstract

In this work, the behavior of an electrically conductive adhesive (ECAs) was selected and studied, using shingled technology is a development in the connection of solar cells by means of superimposition with electrically conductive adhesives, thus obtaining higher powers than the previous welding process, also offers several advantages compared to standard photovoltaic modules, improving: efficiency, reduction of microcracks, better use of the surface, lower processing temperature, higher energy yield, and better aesthetics.

The objective of this study was to analyze electrically conductive adhesives for use in the manufacture of photovoltaic modules to propose a technological development to obtain greater efficiency in energy capture. Polycrystalline cells and monocrystalline cells were studied. The photovoltaic module manufacturing set was made using the conventional fixing method to join solar cells, based on the union by welding with Sn-Cu connection tapes. Loctite Ablestik ICP 8282 adhesive was selected for use in the manufacture of the overlay prototype and the substitution of the welding process in the manufacture of standardized photovoltaic modules. The adhesive curing consisted of depositing the joined cells, in the Stringer equipment, for 30 seconds at a temperature of 150°C.

The Shingled prototype went through the lamination process where the temperature was raised to 150 °C for 15 minutes for polycrystalline cells and monocrystalline cells. 5 modules were studied by the electroluminescence test showing defects such as cracks in the manually manufactured modules. Modulo 5 was acceptable because a homogeneous image is shown in each of its cells on the union by dosage, thus giving a figure free of microcracks and any other defect. The photovoltage test was a notable difference in module 5 its high efficiency of 20.90% that other. The shadow moment testing in modules 1 and 5 connected with electrically conductive adhesives are better because they have lower percentages in the presence of a clogged cell.

However, when we change the 20% shadow angle on each module, we will have a total loss in power and efficiency in modules 2 and 3. Thermographic performance shown the module 5 is a reference of the objective to be achieved with the use of the electrically conductive adhesive, but it did not obtain any loss of power or efficiency.

Electrically conductive adhesive, shingled technology, polycrystalline cells, monocrystalline cells

Resumen

En este trabajo se seleccionó y estudió el comportamiento de un adhesivo eléctricamente conductor (ECAs), utilizando la tecnología shingled es un desarrollo en la conexión de células solares mediante la superposición con adhesivos eléctricamente conductores, obteniendo así potencias superiores al proceso de soldadura anterior. También ofrece varias ventajas respecto a los módulos fotovoltaicos estándar, mejorando: eficiencia, reducción de microfisuras, mejor aprovechamiento de la superficie, menor temperatura de procesamiento, mayor rendimiento energético y mejor estética.

El objetivo de este estudio fue analizar adhesivos eléctricamente conductores para su uso en la fabricación de módulos fotovoltaicos para proponer un desarrollo tecnológico para obtener una mayor eficiencia en la captura de energía. Se estudiaron células policristalinas y células monocristalinas. El conjunto de fabricación del módulo fotovoltaico se realizó mediante el método de fijación convencional para unir células solares, basado en la unión mediante soldadura con cintas de conexión de Sn-Cu. Se seleccionó el adhesivo Loctite Ablestik ICP 8282 para su uso en la fabricación del prototipo de superposición y la sustitución del proceso de soldadura en la fabricación de módulos fotovoltaicos estandarizados. El curado del adhesivo consistió en depositar las células unidas, en el equipo Stringer, durante 30 segundos a una temperatura de 150°C.

El prototipo Shingled pasó por el proceso de laminación donde la temperatura se elevó a 150 °C durante 15 minutos para células policristalinas y células monocristalinas. Se estudiaron 5 módulos mediante la prueba de electroluminiscencia mostrando defectos como grietas en los módulos fabricados manualmente. El módulo 5 fue aceptable porque se muestra una imagen homogénea en cada una de sus celdas sobre la unión por dosificación, dando así una figura libre de microfisuras y cualquier otro defecto.

En la prueba de fotovoltaaje se observó una diferencia notable en el módulo 5 por su alta eficiencia del 20,90% respecto a los demás. Las pruebas de momento de sombra en los módulos 1 y 5 conectados con adhesivos eléctricamente conductores son mejores porque tienen porcentajes más bajos en presencia de una celda obstruida. Sin embargo, cuando cambiamos el ángulo de sombra del 20% en cada módulo, tendremos una pérdida total de potencia y eficiencia en los módulos 2 y 3. El rendimiento termográfico mostrado en el módulo 5 es una referencia del objetivo a conseguir con el uso del adhesivo eléctricamente conductor, pero no obtuvo ninguna pérdida de potencia o eficiencia.

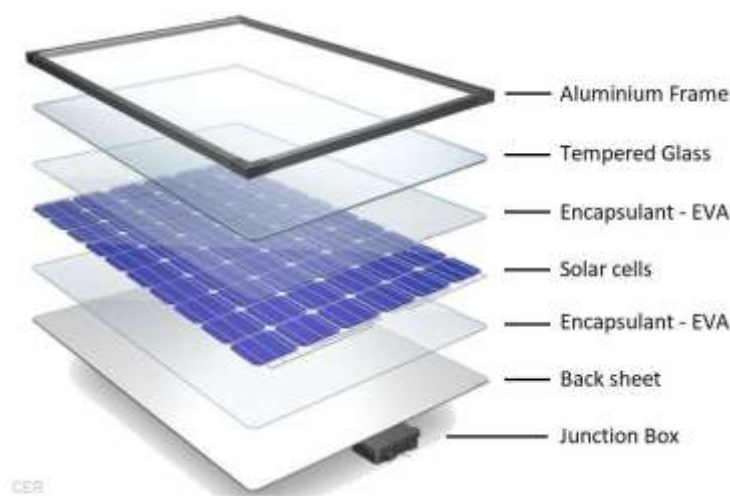
Adhesivo eléctricamente conductor, Tecnología shingled, Células policristalinas, Células monocristalinas

1. Introduction

1.1 Photovoltaic module

The photovoltaic module can be defined as a set of elements represented in figure 1, which convert solar energy into electrical energy through solar cells.

Figure 1 Structure of the components that make up a photovoltaic module



Source ([Svarc 2020](#))

1.1.1 Cell types

Monocrystalline: Cells cut from a single crystal of Silicon, are more efficient.

Polycrystalline: Cells cut from a block of silicon composed of many crystals.

1.2 Electrically Conductive Adhesives (ACE)

Electrically Conductive Adhesives (ACE) are prepared from an insulating polymeric matrix that provides adhesion and resistance, while a metallic filler is responsible for conducting electricity. To become a hybrid, different methods are used, such as doping with other components. Being connection materials that can be used to facilitate a mechanical coupling and an electrical connection (Springer and Bosco 2020).

1.2.1 Bonding material

The bonding material used are polymers of different compositions and reactive groups, epoxy is the most used material as an adhesive, being a thermosetting polymer (Springer and Bosco 2020).

1.2.2 Backfill material

The filler material is metallic elements on a nanometric scale, such as: silver, gold, and copper where you can find two types of conductive adhesives divided by their morphology and percentage of metallic filling (Springer *et al.* 2020). There are three different fill geometries in the form of spheres, lamellae, and holes.

1.3 Types of Electrically Conductive Adhesives (ACE)

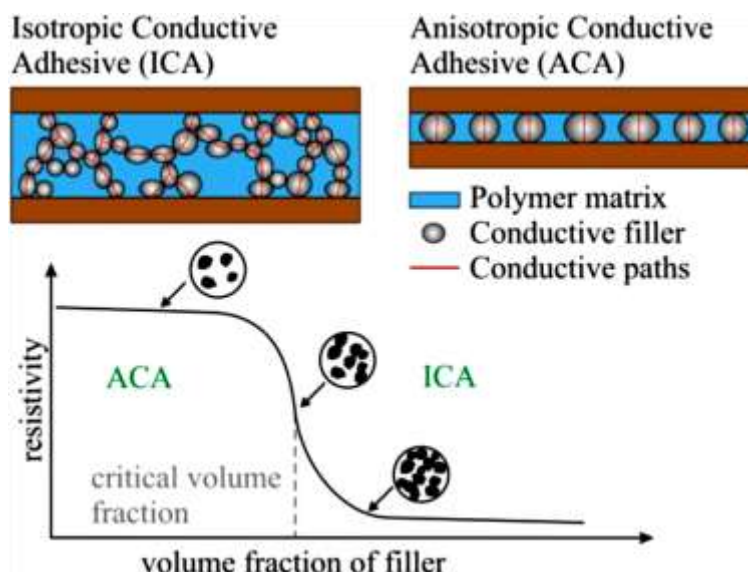
1.3.1 Isotropic Conductive Adhesives (ACI)

Isotropic adhesives consist of approximately 70-80% metal particles, when the adhesive cures the particles are evenly distributed and form a network within the polymer structure, allowing current flow in three directions (X, Y and Z) (Sharma *et al.* 2021).

1.3.2 Anisotropic Conductive Adhesives (ACA)

They are electrical conductors in only one direction, this directionality of the electrical property is called anisotropy. Anisotropy occurs when the polymer chains are oriented in the direction of flow. This directional conductivity is achieved by using a relatively low volume of metal filler well below the percolation point (5-10% volume) (Malik *et al.* 2021) Next, in figure 2 the structure of the two types of electrically conductive adhesives is shown.

Figure 2 Structural comparison of rates ACE

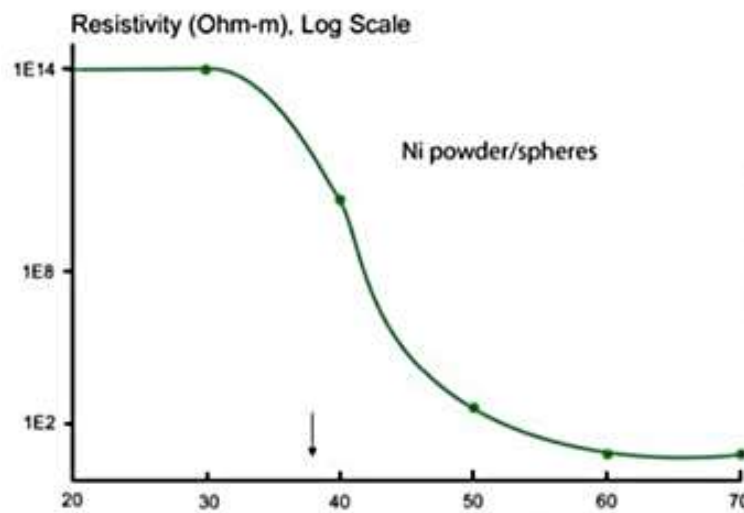


Source (Pander *et al.* 2014)

1.4 Percolation Theory

Percolation theory dictates a "critical" concentration on the metal filler at which a three-dimensional lattice and conductivity is established. Thereafter, the conductivity slowly changes with increasing metal filler concentration as can be seen in figure 3. The percolation point is reached when enough metal filler has been loaded into the polymer to transform the compound from an insulator to a conductor. In Anisotropic Conductive Adhesives, they have low volume metal fillers (typically 5-10% by volume). This is as opposed to Isotropic Adhesives (ACI), they typically have a higher amount of filler than is needed to reach the set point, approximately 70-80% (Pander *et al.* 2014).

Figura 3 Teoría de la percolación, % concentración

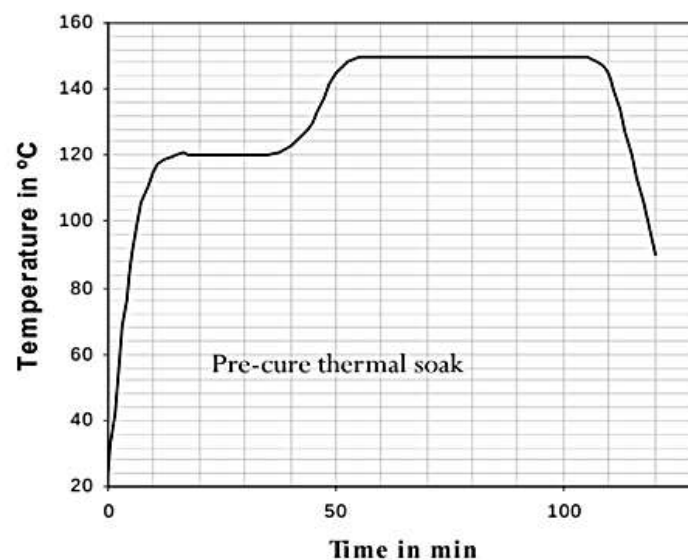


Source (Pander *et al.* 2014)

1.5 Curing Process

Figure 4 shows the schematic of the curing process, include exothermic reactions that convert monomers or pre-polymers in a liquid state into a three-dimensional network. Incomplete curing will result in weak adhesion, while over-curing can cause bond degradation (Elsayed *et al.* 2020).

Figure 4 Step of curing process



Source (Anderson *et al.* 2021)

1.6 Classification of electrically conductive adhesives (ECA)

1.6.1 Epoxy

Most epoxy adhesives contain Diglycidyl Ether of Bisphenol A (DGEBA) as the main epoxy resin base. Epoxy resins are very versatile structural adhesives because they can react together with many different resins and low molecular weight compounds (Saedi *et al.* 2022). Silver-filled epoxy adhesives provide a high-strength conductive bond. Its properties are: (such as cohesive strength, hardness, toughness, flexibility, chemical, electrical, and mechanical resistance) (Guo *et al.* 2023).

1.6.2 Silicones

Silicones are hybrid compounds that combine the function of a reactive organic group with the inorganic characteristic of an alkyl silicate, in one. The high flexibility of the silicone chain is due to the low rotational energy barrier of the Si-O bond. Electrically conductive silicone adhesives with graphite fillers are often used for antistatic systems. These materials are generally very high in viscosity and thick in consistency, making them suitable for large area bonding. An important feature to keep at a temperature (-20 °C) (Guo *et al.* 2023).

1.6.3 Polyurethane

Polyurethane adhesives have properties such as: rigid, hard, flexible, and soft. Silver-filled polyurethane adhesives are two-part adhesives, so they require mixing or are supplied pre-mixed like epoxies. They offer high peel strength and flexibility. Since they are filled with silver, high levels of conductivity can be achieved (around 0.0001 Ω/cm to 0.0004 Ω/cm) (Guo *et al.* 2023).

1.6.4 Acrylates

Acrylic adhesives are thermosetting systems, also called reactive acrylics. They are liquids with low viscosity that reach polymerization faster with less time before exposure to temperature, forming resistant bonds. Most thermosetting acrylic adhesives are two-part systems that provide shear strength (Guo *et al.* 2023).

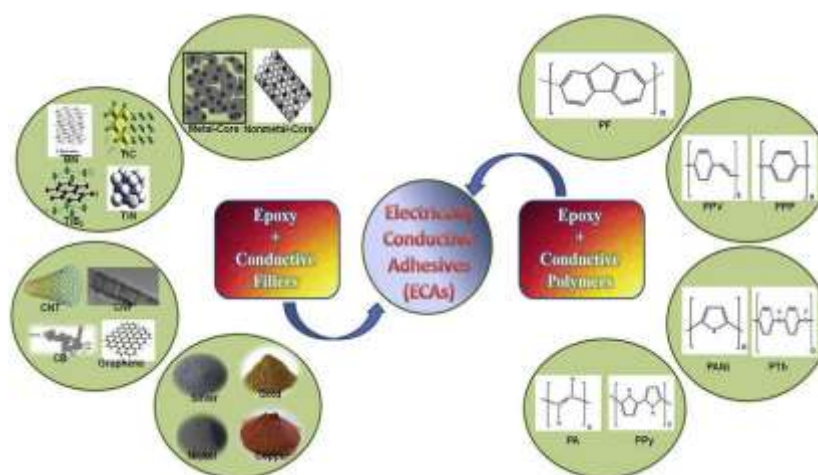
1.6.5 Bismaleimide

Bismaleimide (BMI) adhesives are used in the manufacture of printed electronic flexible circuits and other electronic devices, as well as in applications where resistance to high temperatures is required. As one of the most important mechanical properties is traction. Being suitable for long-term exposure to temperatures up to 200 °C and for short-term exposure up to 230 °C (Malik *et al.* 2021).

1.6.6 Hybrids

Adhesives composed of two or more types of electrically conductive adhesives. Next, in figure 5 the classification of ECAs is represented.

Figure 5 Classification of electrically conductive adhesives



Source (Aradhana *et al.* 2020)

1.7 Properties of electrically conductive adhesives

Electrical conductivity and bond strength are electrical properties of electrically conductive adhesives.

1.7.1 Electrical conductivity

Electrical conductivity is a transport phenomenon in which electrical charge (in the form of electrons or ions) moves through a system. Electrically conductive adhesives have a low conductivity before the curing process. This conductivity increases after the contraction of the adhesive, increasing the contact between the particles of the metallic filler. However, although thermosetting materials shrink slightly upon curing, excessive shrinkage can cause bond failure (Springer and Bosco 2020).

1.7.2 Strength of joints

The resistance of the joints is a characteristic property that will depend on the connection and the metallic elements in the bases that are assembled.

1.7.3 Cohesive force

The cohesive strength of an ECAs refers to the internal strength of the adhesive, which depends on the type of polymer used and the amount of metal filler present. It can be shown that a large amount of metal filler within the adhesive reduces the bond strength. Conversely, a reduction in metal filler will improve cohesive strength, but reduce electrical conductivity.

1.7.4 Bond adhesion strength

The adhesion force of a conductive adhesive refers to the adhesion force between the bases. Thermosetting materials, such as epoxy, have a higher bond strength than thermoplastics. Thermosetting polymers can produce both strong covalent and secondary bonds, whereas thermoplastics can only form secondary bonds (Springer and Bosco 2020).

1.8 Other factors that increase joint strength include.

1.8.1 Corrosion

Corrosion is a process that occurs under humid conditions in the presence of an electrolyte and is most prominent in high moisture absorption adhesives. The material with the highest electrochemical potential is ACE epoxy, which acts as the cathode and the base of the cell acts as the anode. During the electrochemical process, the anode corrodes (Springer and Bosco 2020).

1.9 Use of conductive adhesives as a replacement for solder

It is necessary to define the electrical and mechanical properties of electrically conductive adhesives (ACE), for substitution (Springer and Bosco 2020).

1.9.1 Electrical requirements.

Volume resistivity is the electrical resistance of a body whose length and area uniform cross section (Springer and Bosco 2020):

- Volumetric resistivity less than 0.001 Ohm/cm³.
- Displacement of joint movement less than 20%.

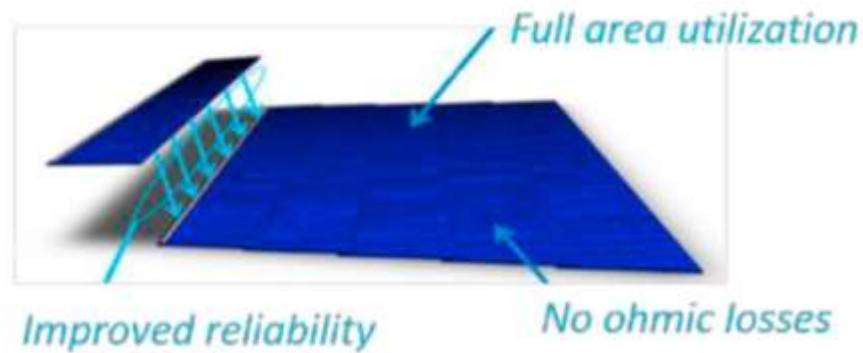
1.10 Overlay Technology

Overlay technology is a technological advance used to obtain a power increase, this technique eliminates the need for Sn-Cu connection tapes by 90% and therefore reduces resistance losses. The main difference with other techniques is the efficiency, aesthetics, and performance of the overlay photovoltaic modules.

The development of superimposition technology, implies the superposition of the cells, increasing the ratio between the limit of the cell and the area thereof, one on top of the other with an electrically conductive adhesive, the main advantage of which is an increase in the energy production, due to more efficient packing between the cells (Tonini *et al.* 2018).

For correct operation, the screen printing of each cell must follow the scheme, where there is a correct connection with the adhesive in the overlap, figure 6 shows how the screen printing of a cell should be.

Figure 6 Shingling interconnection scheme

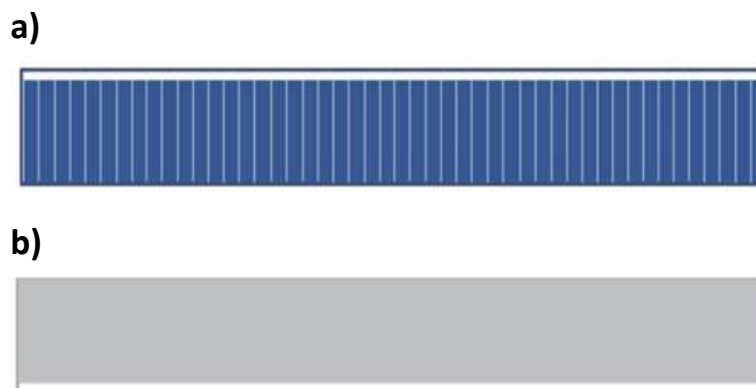


Source (Tonini et al. 2018)

1.10.1 Design of the cells

The cells must have a BUS-BAR (energy collector bar) along the edge, one at the front and one at the back as shown in figure 7, with cell dimensions $(156 \text{ mm} \times 31 \text{ mm}) \pm 0.1 \text{ mm}$ (Oh et al. 2020)

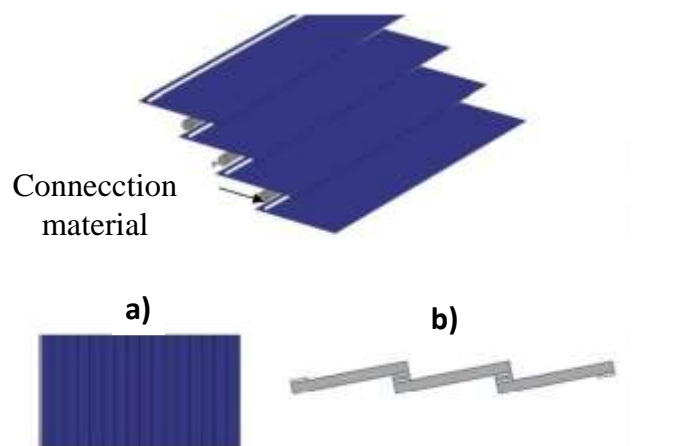
Figure 7 Design of a cell (a) Top View (b) Bottom View



Source (Beaucarne 2016)

To form a string (set of cells placed one on top of the other), the electrically conductive adhesive (ACE) dosing process is carried out, connecting the rear BUS-BAR with the next front cell as shown in the following figure. 8.

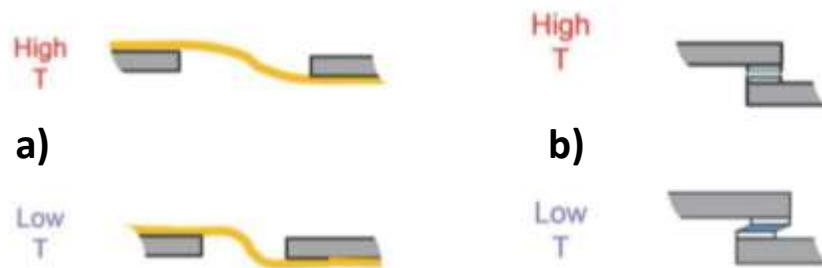
Figure 8 Design of a string (a) Top view of a string (b) Cross sectional view.



Source (Beaucarne 2016)

To verify its effectiveness absorbing tensions, a thermo-mechanical situation of two cells that are stimulated towards each other is assumed, section A was through the Sn-Cu welding process and simultaneously applying an increase in temperature where they will deform slightly allowing movement. Item B was carried out with the overlapping connection of the electrically conductive adhesives, the movement of the cell is much more limited and the joints between the cells tend to allow movement due to deformation while supporting mechanical stress as shown in the figure. 9.

Figure 9 Thermo-mechanical representation of the different connections (a) Deformation of the Sn-Cu welding process; (b) Deformation of the overlap joint

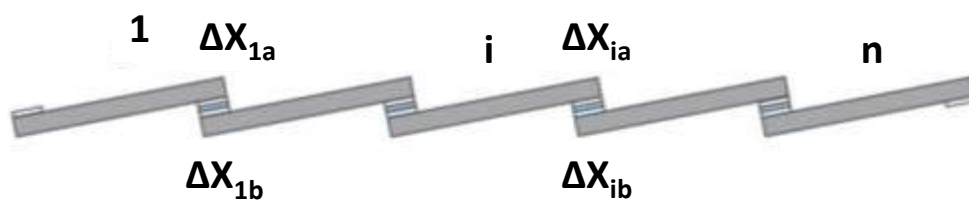


Source (Beaucarne 2016)

1.10.2 Structure

Figure 10 shows the structure of the string in the form of an overlap in a cross-sectional section. There are n cells and therefore $n-1$ junctions.

Figure 10 Structure of the overlay model, cross-sectional cut



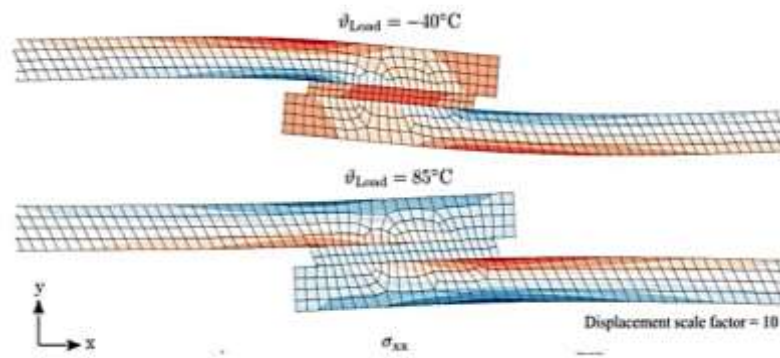
Source (Beaucarne 2016)

The junctions will form at 150 °C, it should be noted that if the string is cooled to -40 °C the silicon cells contract slightly. Because it is uncontrollable, the movement will not be opposed and there will be no mechanical stress.

1.10.3 Structural deformation of a connection by using ACE.

Complementing with the previous analysis of the effectiveness absorbing tensions, a simulation of deformation was carried out in the joints of two substrates with the application of an adhesive conductor of electricity, the first test was at a temperature of -40 °C where the deformation tends to contract, in the second test the application temperature was 85 °C, in which the stresses remain stable providing a favorable point of view to the photovoltaic modules as can be seen in figure 11, when they are exposed to different temperatures so as not to cause defects in the joints (Springer and Bosco 2020).

Figure 11 Structural deformation of a connection between an electrically conductive adhesive and two adjacent silicon cells for two different charging temperatures



Source (Springer and Bosco 2020)

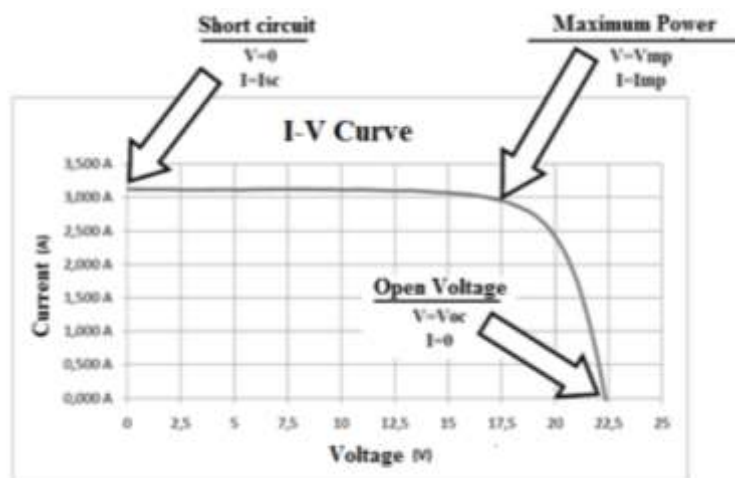
1.11 Electroluminescence

Electroluminescence (EL) solar cell imaging relies on the same principle as a light emitting diode (LED), where a source of current is provided into a solar cell and radiative recombination of emitted carriers causes a light emission. As an indirect bandgap semiconductor material, the peak of carrier recombination in silicon occurs through defected locations (Dhimish and Holmes 2019).

1.12 I-V curve

In the I-V curve (figure 12) can extract the electrical characteristics of the photovoltaic cell in standard conditions of measurement (SCM): ISC (short circuit current) is maximum intensity that can generate a photovoltaic cell or module when measuring the current if performing a short circuit (output voltage of 0 volts), VOC (open circuit voltage) is maximum voltage that can generate a photovoltaic cell or module when measuring the voltage if not flowing current (current of 0 amps), P_{MAX} (Maximum power) is maximum power that can generate a photovoltaic cell or module and it's the product of maximum voltage and current, V_{MAX} (Maximum Voltage) is the voltage at maximum power (around 80% of open circuit voltage) and I_{MAX} (Maximum Current) is the current at maximum power (Aparicio *et al.*, 2013)

Figure 12 Representation of an I-V Curve



Source (Aparicio *et al.*, 2013)

2. Methodology

2.1 Materials

Table 1 compares the 10 conductive adhesives. The adhesive "Loctite Ablestik ICP 8282" was selected for use in the manufacture of the overlay prototype and the substitution of the welding process in the manufacture of standardized photovoltaic modules. This adhesive has a resistance of 0.0037 Ohm/cm³, its time and temperature in the curing process it is 30 s at 150 °C. Being a single-component acrylate type adhesive, it does not need to be mixed with other additives. Too, the adhesive was based on commercial availability and in-stock at the company.

2.2 Overlay prototype

The overlay prototype was made by joining together 44 monocrystalline silicon cells with dimensions (156mm x 39mm). Obtaining these half cells was carried out by cutting an entire cell in two, by means of a laser cut. It should be noted that the process of cutting the half cells is a fragile process because it can generate fissures or microcracks.

2.3 Preparation of the Henkel Loctite 98666.




The dispensing equipment was connected to a compressor. adjusting the pressure to 500 kPa for the dosing of the adhesive, which was applied manually (figure 13). To obtain the volume of each application we will use the following equation1 of the cylinder, where we take as reference the internal radius of the dispensing needle (0.010") times the length of the cell and the calculated volume is 0.31 mL. The nozzle is cleaned each time it is used to avoid contamination and material buildup. The conservation of the material must be at a temperature of (-20 °C) this to avoid any possible polymerization.







Figura 3 Dosification process



Source (Own Elaboration)

Table 1 Comparison of the properties of ACE electrically conductive adhesives

Imagen	Type	ACE	Resistance Ohm/cm ³	Force shear N/mm ²	Cured °C	Thermal Conductivity W/(m·K)	Stock temperatura °C	Supplier
	8282	Acrylate	0.0037	9.1	0.5 min a 150 °C	-	-20 °C	Henkel
	SC10	Epoxi	0.0040	6	0.5 min a 180 °C	-	-20 °C	Heraeus
	8311	Acrylic	0.00039	11.4	0.16 a 0.25min a 150 °C	-	-20 °C	Henkel

	9410	Epoxi	0.0018	26	7 min a 120 °C	1.1	22 °C	Mg Chemicals
	QMI 529HT- LV	BMI	0.00005	20	30 min a 175 °C	8	-40 °C	Henkel
	3888	Epoxi two	< 0.001	12	60 min a 150 °C	1.5	-	Henkel
	56C	Epoxi two	0.0004	6	120 min a 50 °C	3	-	Henkel
	EC- 6601	Silicona	0.0027	1.61	30 min a 60 °C	2.12	-	Dowsil
	8331S	Epoxi two	0.006	65	40 min a 100 °C	1.3	-	Mg Chemicals

Source (Own Elaboration)

2.4 Preparation of the curing process

Considerations that must be considered to carry out the curing process, the aluminum base where the strings will be made, had a preheating of 25 °C to avoid a thermal shock when passing through the Stringer device "SOMOT" illustrated in figure 14. The Adhesive curing consists of depositing the joined cells, in the Stringer equipment, for 30 seconds at a temperature of 150 °C. This ensures the solidification of the adhesive, checking the temperature with an infrared thermometer.

Figure 14 "SOMOT" Stringer equipment and an Infrared thermometer



Source (Own Elaboration)

In each application of each cell on the string, an inspection of the surface was carried out looking for visible defects in the superimposition of the cells, for example: broken cells, narrow spaces in the strings. Subsequently, the curing process in each cell exposed to a constant temperature of 150 °C for 30 seconds.

Each string consisted of 10 dosages, the superimposition was made taking care of the integrity of the half cells, in total 4 strings with 11 monocrystalline half cells were obtained, as can be seen in figure 15.

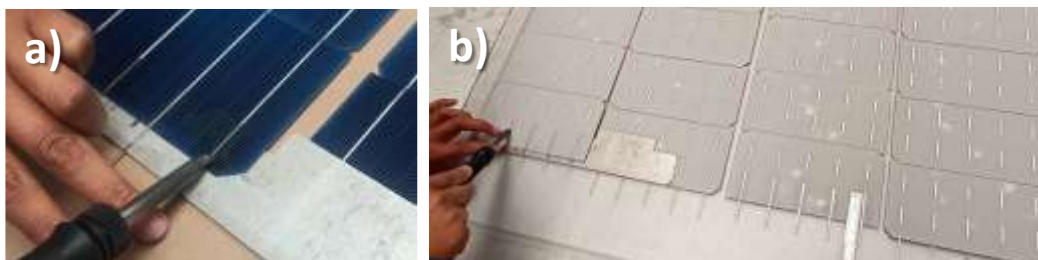
Figure 15 Formation of 4 strings

Source (Own Elaboration)

2.5 Assembly

The assembly procedure began by cutting transparent EVA back sheets and EVA encapsulants of (980 x 660) mm each, then the extra clear tempered glass of (970 x 654) mm is placed, later an EVA encapsulant sheet aligning all the components. The strings are then incorporated, maintaining a 2 mm separation between each string. For the Shingled prototype, 4 strings of 11 cells were needed, joining the connections to close the series circuit. For this step, Sn-Cu interconnection tapes with dimensions of 1 x 50 mm were cut, each string has a geometry of 5 Bus-Bar by end, we begin with the union of the Sn-Cu interconnection tapes by means of the union by the welding process in each Bus-Bar, Flux solution was applied to each weld at a height of 25 mm, with in order to eliminate oxides present in the component and have a better handling in the soldering station, at a temperature of 370 ± 5 °C. The connection in series begins on the negative side, the next string will begin the connection on the positive side of the cell, see figure 16. In the welding process, the components of the prototype are protected with a "Mecanitec" non-stick tape, this tape insulates the temperature so as not to melt transparent EVA back sheets.

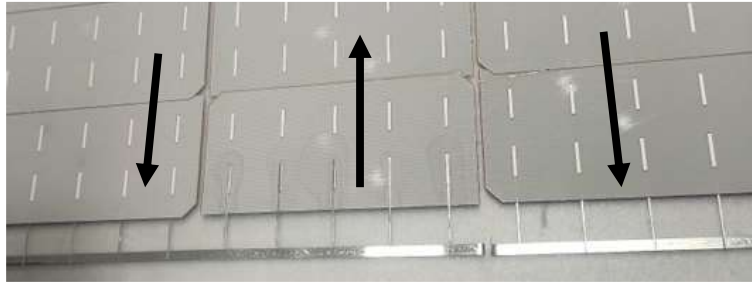
Figure 16 a) Use of "Mecanitec" anti-adherent tapes in each joint by welding, and b) join of the Sn-Cu interconnection tapes at the end of each string



Source (Own Elaboration)

Figure 17 shows Sn-Cu connection tapes, (6x350) mm, and (6x290) mm, were used to close the circuit of the photovoltaic module with positive and negative terminals. We placed another EVA encapsulating sheet and a white EVA back sheet.

Figure 17 Orientation of the strings and closure of the photovoltaic module circuit



Source (Own Elaboration)

2.6 Lamination process

The Shingled prototype went through the lamination process where the temperature was raised to 150 °C for 15 minutes, melting sheets of EVA (Ethyl-Venil-Acetate), thus encapsulating the components, later the prototype advanced to the area where 4 fans are located to cool the module for 10 minutes. Immediately transported the module on a table to remove the excess of the fused EVA back sheets with isopropyl alcohol removing traces of the molten polymer, the finished prototype can be seen in figure 18.

Figure 18 Shingled prototype assembled



Source (Own Elaboration)

2.7 Monocrystalline photovoltaic module (welding).

A photovoltaic module was made with the same monocrystalline cells, but with the standard process in the manufacture of conventional photovoltaic modules, production began by placing tempered glass (1050 x 670) mm, later an EVA encapsulating sheet was placed as illustrated in the figure 19.

Figure 19 Placement of a transparent EVA backsheet



Source (Own Elaboration)

For this test photovoltaic module, 4 strings of 12 half cells were needed, joining the half cells by the welding process, cutting Sn-Cu interconnection tapes with dimensions 1 x 50 mm for the length of each Bus-Bar, in each string has a geometry of 5 Bus-Bar per end, it begins with the union of the Sn-Cu interconnection tapes applying the Flux solution in each union by the welding process at a height of 25 mm, in order to eliminate oxides present and have a better handling in the soldering station, at a temperature of $370\text{ }^{\circ}\text{C} \pm 5\text{ }^{\circ}\text{C}$ (see figure 20). For the series circuit, the union began on the negative side, later for the next string the union will be on the positive part of the cell. In the soldering station, the components of the prototype are protected with a “Mecanitec” non-stick tape, it is isolated from the temperature so as not to melt the encapsulant EVA. Figure 25 Sn-Cu connection tapes, (6x350) mm and (6x290) mm, were used to close the circuit of the photovoltaic module.

Figure 20 Joining process of monocrystalline cells by means of the soldering station



Source (Own Elaboration)

2.8 Monocrystalline Lamination process

The Shingled prototype went through the lamination equipment, where the temperature was raised to $150\text{ }^{\circ}\text{C}$ for 15 minutes until the EVA (Ethyl-Venyl-Acetate) encapsulants melted to fix the components. Afterwards, the photovoltaic module is cooling for 10 minutes. The photovoltaic module was immediately cleaned with isopropyl alcohol, removing traces of the molten polymer (see figure 21).

Figure 21 Assembled monocrystalline photovoltaic module (by welding)

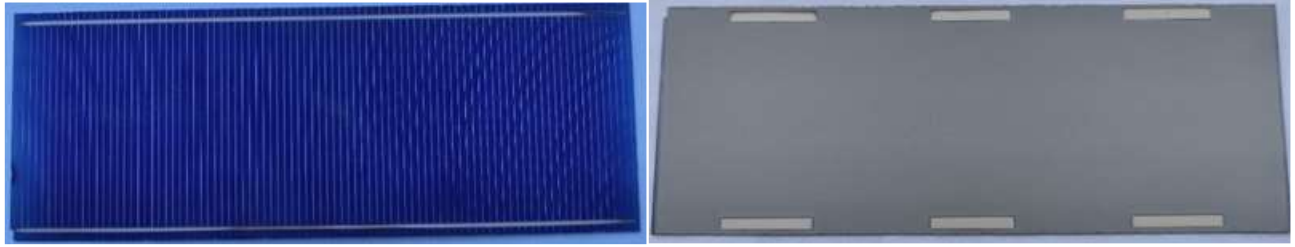


Source (Own Elaboration)

2.9 Polycrystalline shingled photovoltaic module

The preparation of this photovoltaic module was carried out with polycrystalline cells cut with dimensions (28x150) mm, see figure 22. The system is made up of 80 cells distributed in 4 strings.

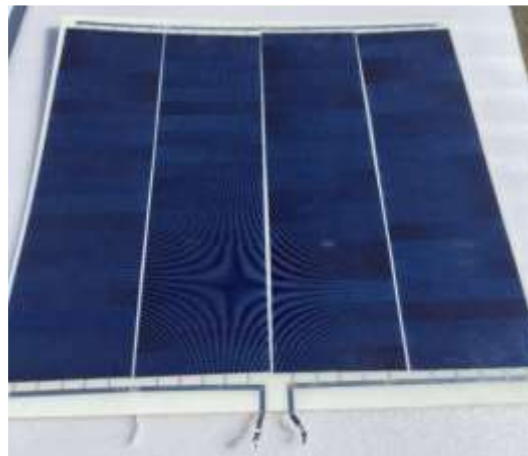
Figure 22 Polycrystalline cell (28x150) mm



Source (Own Elaboration)

The same assembly process of the Shingled prototype was used in this photovoltaic module, see figure 23. The union of the polycrystalline cells was with different dimensions, and a transparent EVA sheet was used. The photovoltaic module has a dimension (650x630) mm.

Figure 23 Shingled polycrystalline photovoltaic module

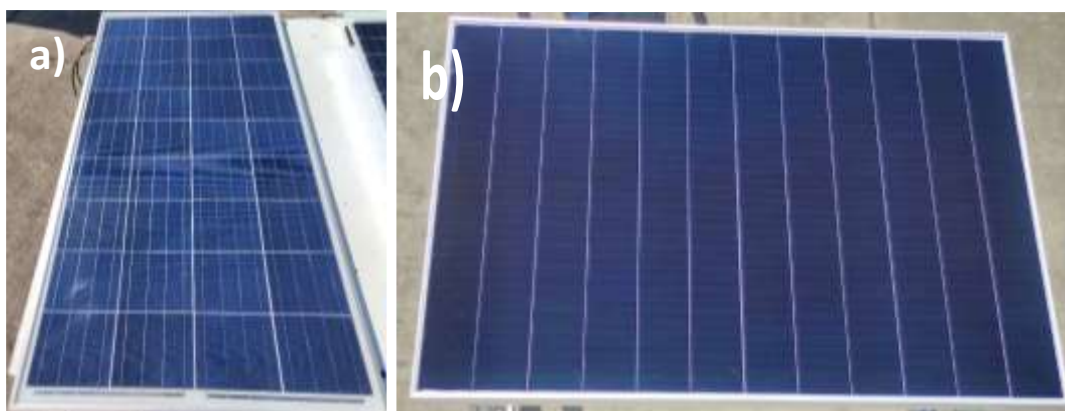


Source (Own Elaboration)

2.10 Polycrystalline photovoltaic module 120 W and monocrystalline shingled 375 W

Through the management, it was possible to obtain two photovoltaic modules by donation: a polycrystalline 120 W and a monocrystalline shingled 375 W (figure 24). The photovoltaic modules were manufactured in an automated system with the highest quality control.

Figure 24 Photovoltaic module a) 120W polycrystalline, and b) shingled 375W monocrystalline



Source (Own Elaboration)

2.11 Electroluminescence testing

The experimental modules were tested by electroluminescence and IV (under STC condition). Then, the module was put into the steady-state box, with the irradiance of $1000\pm 50\text{W/m}^2$, the temperature of $60\pm 5^\circ\text{C}$.

2.12 I-V Testing

Using a Solmetric PV analyzer I-V, the current density-voltage (J-V) curves of the PSCs were recorded from a solar simulator (AM1.5G, 1000mW/cm^2 , K). By means of the equipment "PV Analyzer I-V Curve Tracer" shown in figure 39, data on yields were obtained. The equipment allows knowing the effective power of each photovoltaic module under different climatic conditions at the different irradiation points of the day. This calculation can have significant variations, especially when the module is dirty, damaged or in unfavorable weather.

2.13 Thermographic testing

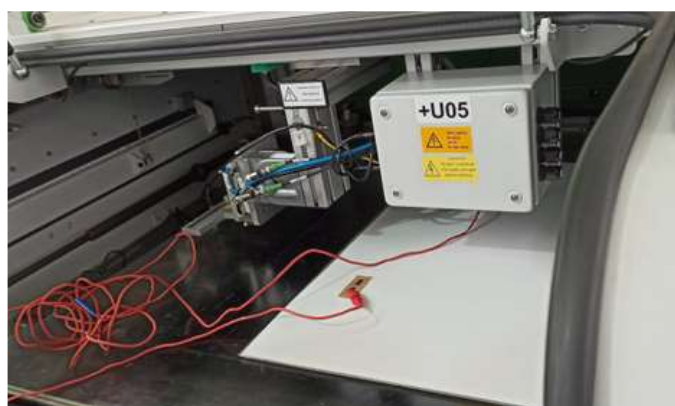
The thermographic inspection allows us to detect points of overheating, and existing broken cells in the photovoltaic modules. The camera provides a resolution of 384×288 pixels with a wide scale measurement over temperature, plus a spectral range parameter. Photovoltaic modules work in a temperature range not greater than 80°C . High temperatures directly impact photovoltaic modules presenting overheating, causing a drop in each aspect to be evaluated. Some additional parameters in this analysis are having a minimum distance of one meter in each inspection, its field of vision must have an inclination of 25° , and the working temperature in the photovoltaic modules must not exceed 80°C .

3. Results and Discussion

3.1. Electroluminescence test

In this test, the inspection of the photovoltaic modules was carried out in the cabin, in which the terminals were connected, see figure 25, inducing an electric current of 4.5 A to expose the defects (microcracks) in each module. The non-visible spectral response has a great variety between the polycrystalline and monocrystalline cell. The spectral response for polycrystalline PV modules is needed from 600-800 nm, however, for monocrystalline PV modules it is required from 1000-1200 nm.

Figure 25 Electroluminescence inspection system



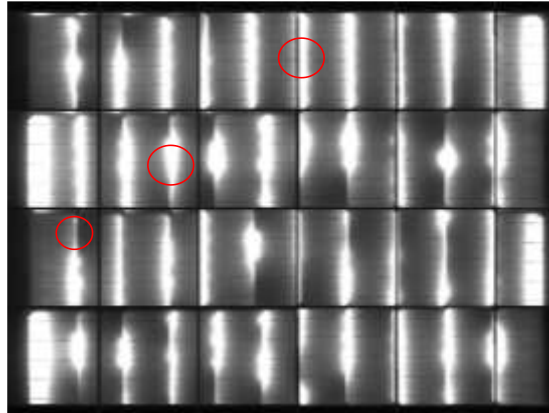
Source (Own Elaboration)

The results between each photovoltaic module are notorious, the first inspected module 1 presents luminous areas, (see figure 26), this is mainly due to the manufacturing procedure. Two main inconsistencies were deduced:

- The cut of the cells must conform to the structure of the Bus-Bar (see figure 7).
- In the dosage it presents uniformity of the adhesive.

It should be noted that the connection was not correct, however, there were no cracks or broken cells due to the dosing process.

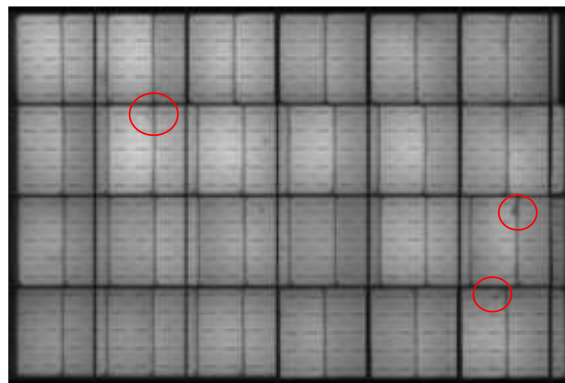
Figure 26 Electroluminescence testing: Module 1



Source (Own Elaboration)

In figure 27, the module 2 shows a homogeneous image, without change, but in the areas marked in red there are cracks and broken cells due to the welding process.

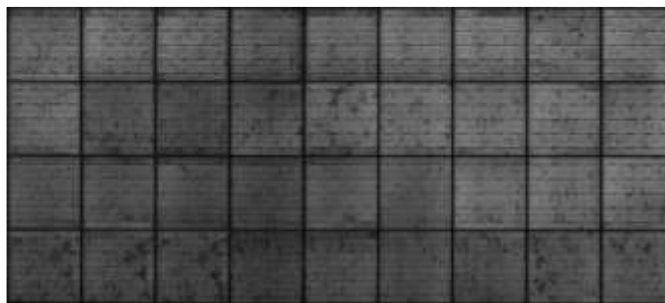
Figure 27 Electroluminescence testing: Module 2



Source (Own Elaboration)

Figure 28 shows a darker appearance with variations in the luminosity intensities, this is due to its composition of the polycrystalline cell, which is made up of small crystals, with an efficiency of approximately 25% compared to monocrystalline cells.

Figure 28 Electroluminescence testing: Module 3



Source (Own Elaboration)

Module 4 was made with polycrystalline cells using Shingled technology. No image was obtained in the electroluminescence test due to its low current caused in the laser cutting process, fracturing a large part of the cell as can be seen in figure 29. Module 4 was manufactured with great care, but without tempered glass it was replaced by a transparent EVA sheet instead.

Figure 29 Polycrystalline cell damaged by the laser cutting process



Source (Own Elaboration)

The last figure of this test is from module 5, which was acquired for analysis in the production area. The results were acceptable because a homogeneous image is shown in each of its cells on the union by dosage, thus giving a figure free of microcracks and any other defect (see figure 30).

Figure 30 Electroluminescence testing: Module 5

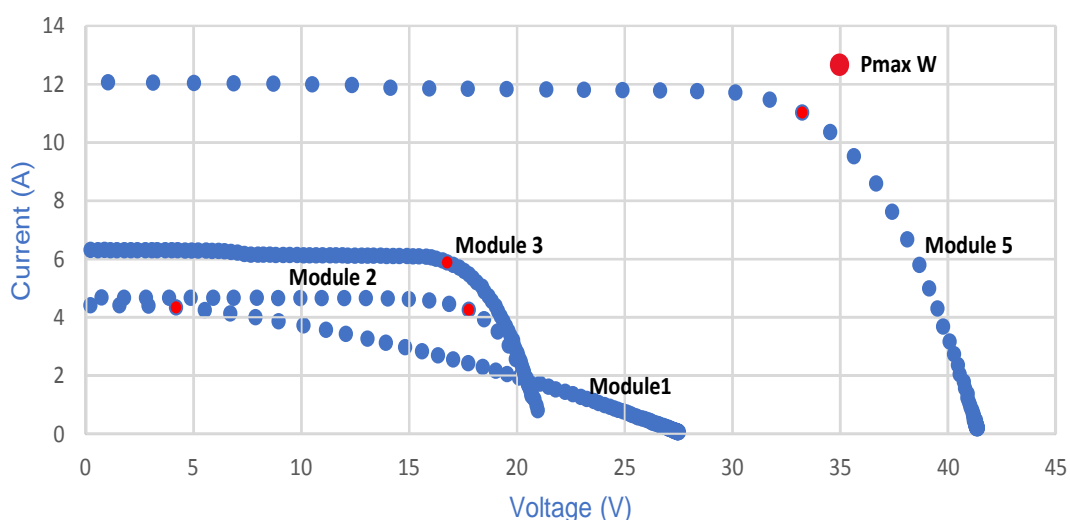


Source (Own Elaboration)

3.2 Photovoltaic performances

Figure 31 show the I-V curve of the module 1, 2, 3 and 5. The I-V curve represents the values of intensity on the Y axis and voltage on the X axis. These tests were executed more than 10 times at each recorded time. Evidencing the instability of the module 1 as in the electroluminescence test. The module obtained a maximum power of 44 W with an efficiency of 3.49%. In the I-V curve of module 2, the improvement in its performance is notorious, due to the correct union in the welding union process. The fall of the curve is prolonged at the point of maximum power. The values reached in Pmax (W) were 101.2 W with an efficiency of 8.21 %. For module 3, the value of the maximum power obtained was 99.6 W with an efficiency of 12.67%. A notable difference in module 5 is its high efficiency. With a maximum power reaching 378 W and an efficiency of 20.90%. Li *et al.*,1997., mentioned the average efficiency has a parameter of 15–17%.

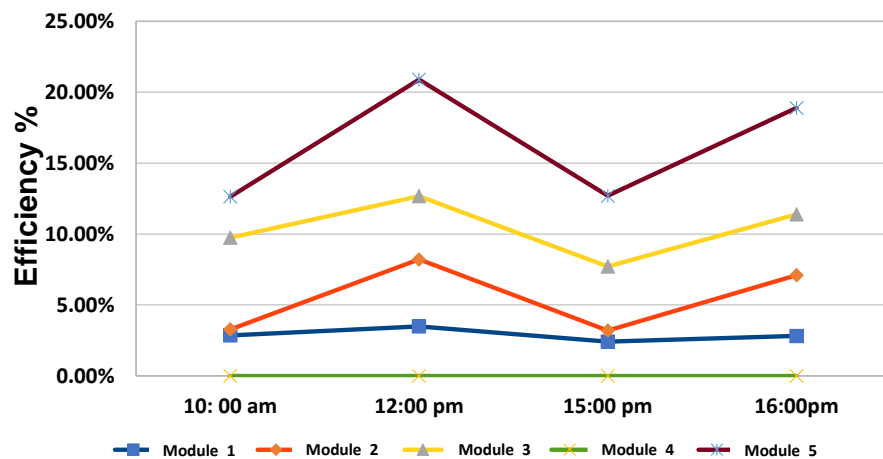
Figure 31 I-V curve Module 5



Source (Own Elaboration)

Figure 40 present the 5 modules with different irradiations. The first record was at 10:00 in the morning with a solar irradiation of 650 W/m^2 . The second record was an irradiation 1000 W/m^2 during noon, the maximum point of each module was achieved. In addition, the information in each aspect increased. The record in the irradiation at 550 W/m^2 at 15:00, losses were obtained in each result. Finally, we were able to observe a slight increase on each module at 16:00 with an irradiation at 800 W/m^2 . In general, the day has two hours of maximum irradiation, at 12:00 pm and 16:00 pm. We have a variation with respect to the course of the day, we must consider the presence of clouds, wind or objects that interfered at the time of each reading. The module with the highest efficiency is module 5, the standard average: 15% - 17% while module 3 manufactured with quality standards does not exceed 13%. However, the Shingled prototype was the module with the smallest difference in each time change and irradiation.

Figure 32 Efficiency of the modules in time zone Jocotitlan



Source (Own Elaboration)

3.3 Shadow moment test

The behavior of a photovoltaic module under different circumstances is reflected in its power and efficiency, the "Shadow Moment" test is a test that is not governed by any standardized norm, but it is a problem that affects the installations of photovoltaic modules. A large part of the companies dedicated to manufacturing carry out this type of test, carrying out two scenarios that lead to overheating and loss of current flow in the photovoltaic modules.

- Obstruction of a cell.
- Obstruction of 20% of each photovoltaic module.

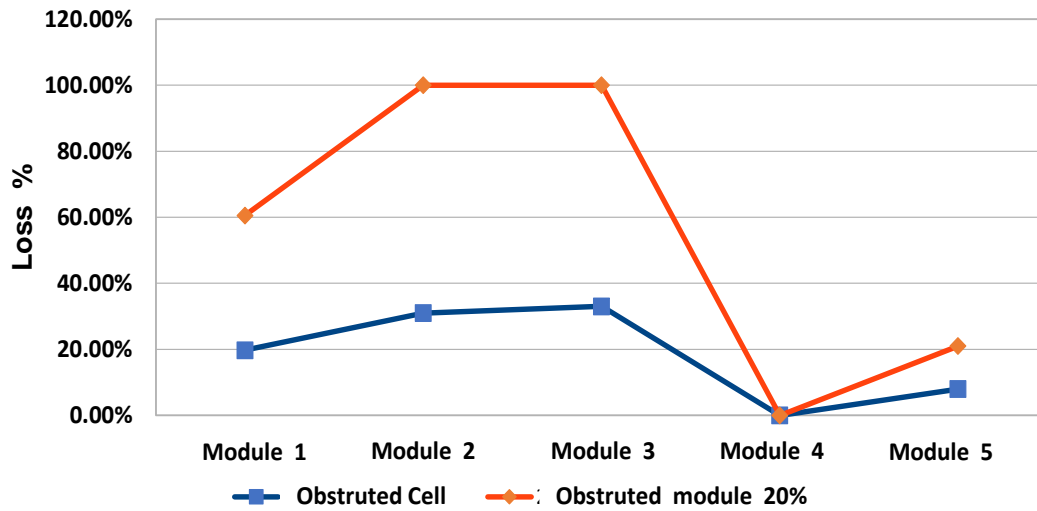
The table 2 and figure 33 shows all the modules flow in a continuous circuit connected in series, any interruption of this flow can have detrimental effects on its operation. The analyze that modules 1 and 5 connected with electrically conductive adhesives are better because they have lower percentages in the presence of a clogged cell. However, when we change the 20% shadow angle on each module, we will have a total loss in power and efficiency in module 2 and 3 (Assoa and Levrard 2020).

Table 2 Efficiencies in partial shades

No.	Module 1	Module 2	Module 3	Module 4	Module 5
Irradiation	1000 W/m^2 .	1000 W/m^2 .	1000 W/m^2 .	1000 W/m^2 .	1000 W/m^2 .
Pmax (W)	43.95 W	101.2 W	99.06 W	-	377 W
1 Cell obstruction	35.22 W -19.75 % Efic.	69.01 W -30.98 % Efic.	66.37 W -33.01 % Efic.	-	346.84 W -8 % Efic.
20 % Module obstruction	17.36 W -60.53 % Efic.	0 W 100 % Efic.	0 W -100 % Efic.	-	297.83 W -21 % Efic.

Source (Own Elaboration)

Figure 33 Cell and module obstruction test

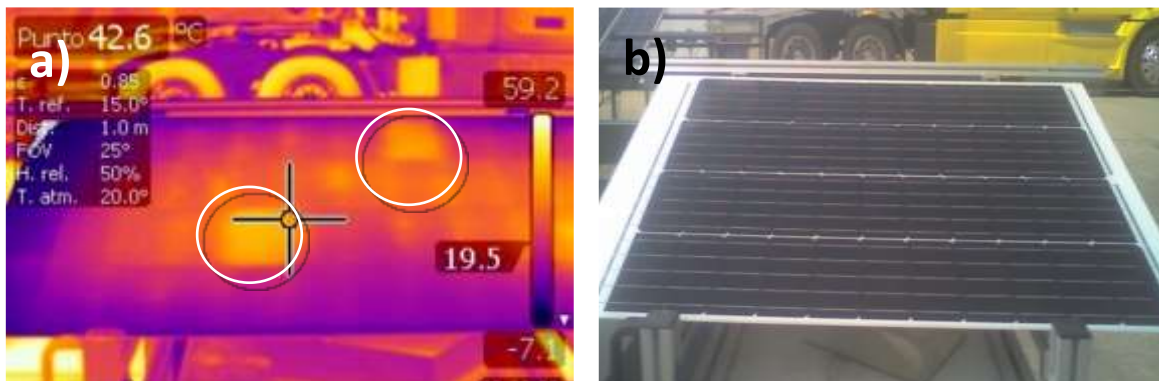


Source (Own Elaboration)

3.4 Thermographic performance

Figure 34 of module 1 shows two areas with hot spots at 43°C, this was due to excess adhesive material applied.

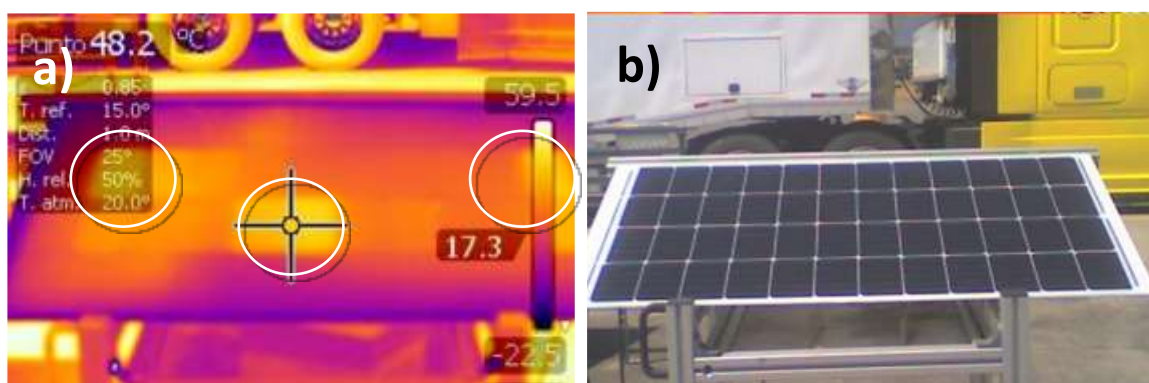
Figure 34 Thermographic testing a) with Infrared and b) without infrared image module 1



Source (Own Elaboration)

Figure 35 shown the Module 2 with infrared image with the presence of several hot spots around 48 °C, the presence of these areas marks the defects in its structure, broken cells, and micro-cracks due to the stresses exerted by the welding process.

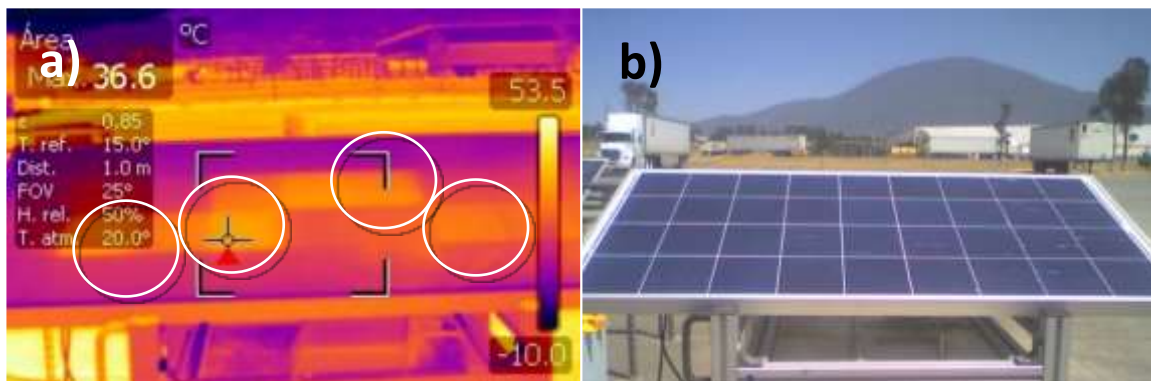
Figure 35 Thermographic testing a) with Infrared and b) without infrared image module 2



Source (Own Elaboration)

Module 3, the electroluminescence image, does not present any broken cells or micro-cracks, but since low-efficiency cells were used, the module has little resistance to temperature, as can be seen in figure 36, the areas of overheating are too many.

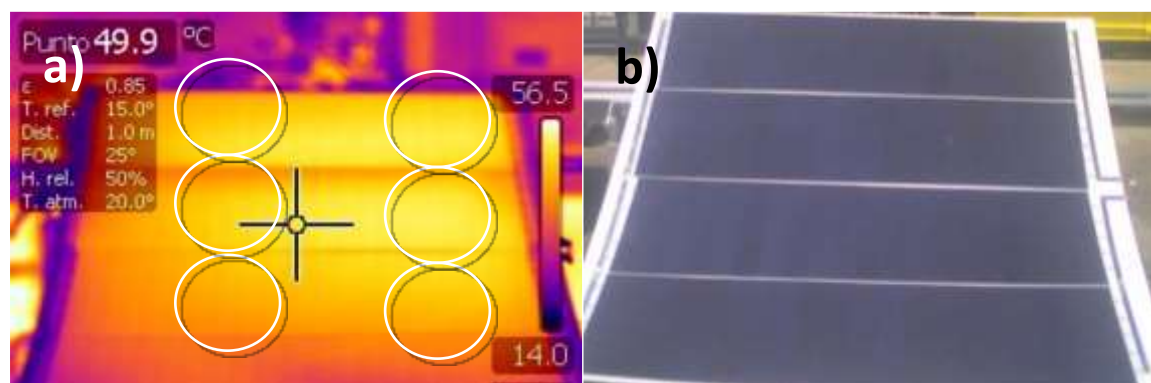
Figure 36 Thermographic testing a) with Infrared and b) without infrared image module 4



Source (Own Elaboration)

Figure 37 shows the module 4 something that in the previous tests did not present any sign of its status, however, in this thermographic test we were able to observe an increase in the operating temperature higher than the other modules. The fact of not using tempered glass and occupying a transparent EVA sheet increases the temperature because it is not dissipating heat.

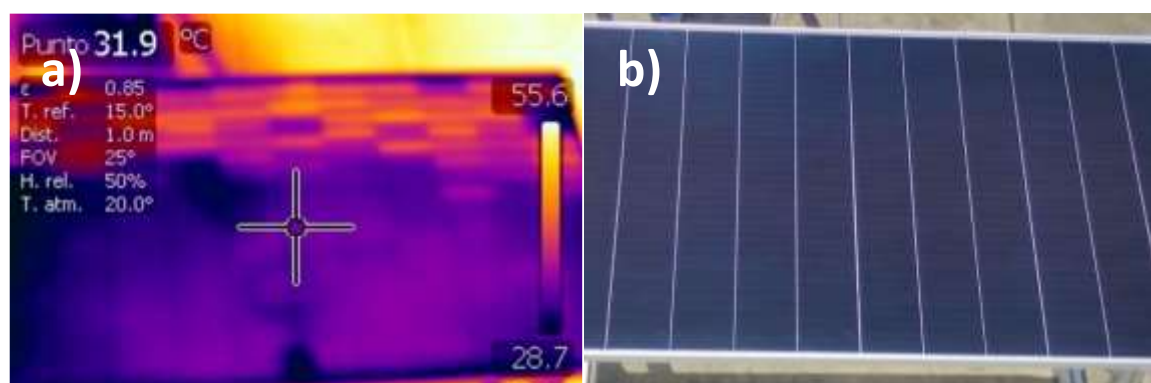
Figure 37 Thermographic testing a) with Infrared and b) without infrared image module 4



Source (Own Elaboration)

Figure 38 shown the module 5 is a reference of the objective to be achieved with the use of the electrically conductive adhesive, but it did not obtain any loss of power or efficiency.

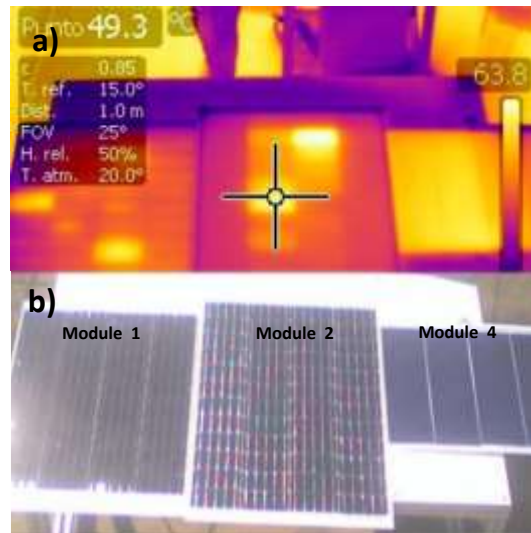
Figure 38 Thermographic testing a) with Infrared and b) without infrared image module 5



Source (Own Elaboration)

Finally, you can see in figure 39 the comparison of module 1 and 2, in which module 2 has a greater number of hot spots and module 4 has overheating throughout its entire structure.

Figure 39 Infrared image (Module 1, 2 y 4)



Source (Own Elaboration)

4. Acknowledgments

We thank the authors to TecNM-TEJJo and participating manufacturing industry.

5. Conclusions

The research conclusion is that electrically conductive adhesives improve power, efficiency, and aesthetics in the superimposition of the cells, a lower rate of broken cells, and micro-cracks, in addition to releasing mechanical stresses in temperature changes. The temperature limits efficiency losses due to partial shading in photovoltaic systems, the choice of adhesive for use in manufacturing and replacement of the welding process was Loctite 8282 adhesive. All this was achieved, but not in the proper way because, in the manufacturing process, the handling, the arrangement of the strings, and the cells are not adequate for a massive process.

The data obtained in each test reflect that the shingled technology is promising. In the inspection process, they show that electrically conductive adhesives prevent fractures of the solar cells and the generation of micro-cracks, however, it is necessary to consider that the cells used are not the correct ones for this technology, the cells with the correct screen printing for manufacturing can be seen in figure 7 to obtain a better performance on the readings carried out, the testing must be carried out in a controlled space.

6. Reference

Anderson G. L. and Macon D. J. (2021). 5-Properties of adhesives, In Woodhead Publishing Series in Welding and Other Joining Technologies, Adhesive Bonding, Second Edition, Woodhead Publishing, 2021,133-155.

<https://www.sciencedirect.com/science/article/abs/pii/B9780128199541000022?via%3Dihub>

<https://doi.org/10.1016/B978-0-12-819954-1.00002-2>

Aparicio M. P., Pelegrí J. S., Sogorb T. and Llario V. (2012). Modeling of Photovoltaic Cell Using Free Software Application for Training and Design Circuit in Photovoltaic Solar Energy, IntechOpen, 50-60.

<https://www.intechopen.com/chapters/41233>

<http://doi.org/10.5772/51925>

- Assoa Y.B. and Levrard D. (2020). A lightweight triangular building integrated photovoltaic module, *Applied Energy*, Volume 279, 115816. <https://www.sciencedirect.com/science/article/abs/pii/S0306261920312964?via%3Dihub>
<https://doi.org/10.1016/j.apenergy.2020.115816>
- Aradhana R., Mohanty S. and Nayak S. K. (2020). A review on epoxy-based electrically conductive adhesives, *International Journal of Adhesion and Adhesives*, Volume 99, 2020, 102596. <https://www.sciencedirect.com/science/article/abs/pii/S0143749620300580?via%3Dihub>
<https://doi.org/10.1016/j.ijadhadh.2020.102596>
- Beaucarne B. (2016). Materials Challenge for Shingled Cells Interconnection, *Energy Procedia*, Volume 98, 115-124. <https://www.sciencedirect.com/science/article/pii/S1876610216310487?via%3Dihub>
<https://doi.org/10.1016/j.egypro.2016.10.087>
- Dhimish M. and Holmes V. (2012). Solar cells micro crack detection technique using state-of-the-art electroluminescence imaging, *Journal of Science: Advanced Materials and Devices*, Volume 4, Issue 4, 499-508. <https://www.sciencedirect.com/science/article/pii/S2468217919302345?via%3Dihub>
<https://doi.org/10.1016/j.jsamd.2019.10.004>
- Elsayed H., Picicco M., Dasan A., Kraxner J., Galusek D. and Bernardo E. (2020). Glass powders and reactive silicone binder: Application to digital light processing of bioactive glass-ceramic scaffolds, *Ceramics International*, Volume 46, Issue 16, Part A, 25299-25305. <https://www.sciencedirect.com/science/article/pii/S0272884220319957?via%3Dihub>
<https://doi.org/10.1016/j.ceramint.2020.06.323>
- Guo Z., Lu W., Zhang Y., Zhou J., and Sun D., (2023) MXene fillers and silver flakes filled epoxy resin for new hybrid conductive adhesives, *Ceramics International*, Volume 49, Issue 8, 2054-12060. <https://www.sciencedirect.com/science/article/abs/pii/S0272884222044509?via%3Dihub>
<https://doi.org/10.1016/j.ceramint.2022.12.055>
- Li L. and Morris J. E. (1997). Electrical conduction models for isotropically conductive adhesive joints," in *IEEE Transactions on Components, Packaging, and Manufacturing Technology: Part A*, Vol. 20, 1, 3-8. <https://ieeexplore.ieee.org/document/558537>
<https://doi.org/10.1109/95.558537>
- Malik M. H., Grosso G., Zangl H., Binder A. and Roshanghias A. (2021). Flip Chip integration of ultra-thinned dies in low-cost flexible printed electronics; the effects of die thickness, encapsulation and conductive adhesives, *Microelectronics Reliability*, Volume 123, 2021, 114-204. <https://www.sciencedirect.com/science/article/pii/S0026271421001700?via%3Dihub>
<https://doi.org/10.1016/j.microrel.2021.114204>
- Oh W., Park J., Jeong C., Park J., Yi J. and Lee J. (2020). Design of a solar cell electrode for a shingled photovoltaic module application, *Applied Surface Science*, Volume 510, 145420. <https://www.sciencedirect.com/science/article/abs/pii/S0169433220301768?via%3Dihub>
<https://doi.org/10.1016/j.apsusc.2020.145420>
- Pander S. H. and Schulze M. E. (2014). Mechanical Modelling of Electrically Conductive Adhesives for Photovoltaic Applications, Conference: 29th European Photovoltaic Solar Energy Conference and Exhibition, 3399 – 3406. <https://userarea.eupvsec.org/proceedings/EU-PVSEC-2014/5DV.3.39/>
<https://doi.org/10.4229/EUPVSEC20142014-5DV.3.39>
- Saeedi I. A., Chalashkanov N., Dissado L. A., Vaughan A.S. and Andritsch T. (2022). The nature of the gamma dielectric relaxation in diglycidyl ether Bisphenol-A (DGEBA) based epoxies, *Polymer*, Volume 249, 124861. <https://www.sciencedirect.com/science/article/abs/pii/S0032386122003482?via%3Dihub>
<https://doi.org/10.1016/j.polymer.2022.124861>

Sharma D., Mehra R. and Raj B. (2021). Comparative analysis of photovoltaic technologies for high efficiency solar cell design, *Superlattices and Microstructures*, Volume 153, 106861. <https://www.sciencedirect.com/science/article/abs/pii/S0749603621000598?via%3Dihub>
<https://doi.org/10.1016/j.spmi.2021.106861>

Springer M. and Bosco N. (2020). "Linear viscoelastic characterization of electrically conductive adhesives used as interconnect in photovoltaic modules", *Progress in Photovoltaics: Research and Applications*, Vol. 28, 7, 659-681. <https://onlinelibrary.wiley.com/doi/abs/10.1002/pip.3257>
<https://doi.org/10.1002/pip.3257>

Svarc J. (2020, March 20). "Panel Solar Construction. *Clean Energy Review* [Online blog] <https://www.cleanenergyreviews.info/blog/solar-panel-components-construction>

Tonini D., Cellere G., Bertazzo M., Fecchio A., Cerasti L., and Galiazzo M. (2018). Shingling Technology For Cell Interconnection: Technological Aspects and Process Integration, *Energy Procedia*, Volume 150, 36-43. <https://www.sciencedirect.com/science/article/pii/S1876610218305502?via%3Dihub>
<https://doi.org/10.1016/j.egypro.2018.09.010>

Xiao G., Liu E., Jin T., Shu S., Wang Z., Yuan G., and Yang X. (2017). Mechanical properties of cured isotropic conductive adhesive (ICA) under hygrothermal aging investigated by micro-indentation, *International Journal of Solids and Structures*, Volumes 122–123, 81-90. <https://www.sciencedirect.com/science/article/pii/S0020768317302597?via%3Dihub>
<https://doi.org/10.1016/j.ijsolstr.2017.06.003>

Chapter 6 Raspberry Pi and grovepi with Python: Sensors, actuators and interfaces

Capítulo 6 Raspberry Pi y grovepi con Python: Sensores, actuadores e interfaces

CORONA-SÁNCHEZ, Ernesto^{*1}, NAMIGTLE-JIMENEZ, Jesús^{1,2}, MASTACHE-MASTACHE, Jorge Edmundo^{1,2} and LÓPEZ-RAMÍREZ, Roberto²

¹Universidad de Ixtlahuaca, Facultad de Ingeniería

²TecNM/Tecnológico de Estudios Superiores de Jocotitlán

ID 1st Author: *Ernesto, Corona-Sánchez* / **ORC ID:** 0009-0004-8828-3400

ID 1st Co-author: *Jesús, Namigtle-Jiménez* / **ORC ID:** 0000-0002-0908-4592, **CVU CONAHCYT ID:** 624757

ID 2nd Co-author: *Jorge Edmundo, Mastache-Mastache* / **ORC ID:** 0000-0001-6104-6764, **CVU CONAHCYT ID:** 544943

ID 3rd Co-author: *Roberto, López-Ramírez* / **ORC ID:** 0000-0001-8341-3684, **CVU CONAHCYT ID:** 233228

DOI: 10.35429/H.2023.5.86.110

E. Corona, J. Namigtle, J. Mastache and R. López

*jesus.namigtle@tesjo.edu.mx

R. López (AA.) Engineering and Architecture in the Northern part of the State of Mexico. Handbooks-TI-©ECORFAN-Mexico, Estado de México, 2023

Abstract

Currently we have seen the launching and distribution of a wide variety of programmable boards, from the well-known Arduino to boards such as Raspberry Pi, Orange Pi, SparkFun RedBoard Artemis, among others. Each one of them presents differences not only in design but also in the language used to work with them, memory capacity, processor type, etc. Another characteristic that distinguishes them is in the extensions and complements such as hats, sensors and actuators that enhance their use. The cards are a fundamental element in the development of projects focused on robotics, monitoring systems, IoT technology applications to name a few, which is why this chapter will delve into one of the extensions compatible with Raspberry Pi, GrovePi+. This add-on presents advantages when using humidity, temperature, light, air quality sensors, as well as actuators of different types. In addition, graphical interfaces will be implemented taking advantage of the Python3 distribution available in Raspberry Pi; in this way, elements that maximize the use of the hat can be used. This with the purpose that the user can understand and manipulate the types of ports available (analog and digital mainly), presenting the Grove family modules from a didactic point of view.

Monitoring, GrovePi+, Raspberry Pi, Interfaces, Programming

Resumen

Actualmente se ha visto el lanzamiento y distribución de una gran variedad de tarjetas programables, desde el reconocido Arduino hasta tarjetas como Raspberry Pi, Orange Pi, SparkFun RedBoard Artemis, entre otras. Cada una de ellas presenta diferencias no sólo en el diseño sino también en el lenguaje utilizado para trabajar con ellas, capacidad de memoria, tipo de procesador, etc. Otra característica que las distinguen está en las extensiones y complementos como hats, sensores y actuadores que potencian su uso. Las tarjetas son un elemento fundamental en el desarrollo de proyectos enfocados en robótica, sistemas de monitoreo, aplicaciones tecnológicas IoT por mencionar algunas, es por ello que en este capítulo se profundizará en una de las extensiones compatibles con Raspberry Pi, GrovePi+. Este complemento presenta ventajas a la hora de utilizar sensores de humedad, temperatura, luz, calidad del aire, así como actuadores de distinto tipo. Además, se implementarán interfaces gráficas aprovechando que la distribución Python3 está disponible en Raspberry Pi; de esta forma se pueden utilizar elementos que maximicen el uso del hat. Esto con la finalidad de que el usuario pueda entender y manipular los tipos de puertos disponibles (analógicos y digitales principalmente), presentando los módulos de la familia Grove desde un punto de vista didáctico.

Monitoreo, GrovePi+, Raspberry Pi, Interfaces, Programación

1 Introduction

Over the years, research in different areas of engineering has presented systems in which a programmable card is indispensable, either for data acquisition and processing purposes, for a control phase, as a means of communication with the cloud, etc. However, several cards have a high cost in the market and come to need extensions, devices or add-ons that require specific libraries, present incompatibility or simply consume a high amount of resources being undesirable the addition of new components. Therefore, GrovePi+ being a Raspberry Pi compatible add-on can be a good option to work with modules of different functions without exceeding the resources it has. It is a hat that provides analog, digital and serial ports that are used to connect basic electronic components, as well as actuators linked to a single Python-based library for manipulation. The purpose of this work is to show the user how to use some elements through simple code segments providing enough tools to make small control systems.

Short introduction to Raspberry Pi

A Raspberry pi can be considered from the user's point of view, a kind of mini-computer that allows you to perform various projects thanks to the functions it can provide. It consists of a board, a processor, different types of pins and connection ports. This board, launched by the Raspberry Pi foundation (its first model) in 2012 has had variants over time, however, it can be narrowed down into 2 models; A and B. You can also find other models that although they can be differentiated by the size or the addition of its keyboard (as for example the Raspberry Pi 400) maintain the same architecture in their models A and / or B.

Raspberry Pi OS or also known as Raspbian is the official operating system of the board. This Linux distro (Linux distribution) is based on Debian, optimized to run on ARM hardware.

Figure 1 Raspberry Pi 3B+ (Kurniawan A.)



Raspberry Pi hardware

The models that provide the most features to the user are models A and B, and the main difference between them is in the USB connection. Model A versions consume less power and do not have an Ethernet port, unlike model B versions which do.

A standard Raspberry board consists of the following components:

- RAM memory.
- Processor(CPU)
- Graphics Processor (GPU)
- Ethernet connection.
- GPIO interface
- XBEE socket (wireless communication)
- UART (Serial Interface)
- Power supply connection.
- Connection for external hardware (microSD memory)

Where, the microSD memory is necessary for storage and booting of the Pi board. From the point of view of a Windows user the microSD would be the hard disk of the PC. Los Distintos Modelos de Raspberry Pi.

Table 1 presents a summary of the various versions and models of the Raspberry Pi board, highlighting the improvement that has brought model after model, positioning this board as one of the most versatile and economical in the market.

Table 1 Raspberry Pi boards comparison

Model	RPI 3	RPI2	RPI B+	RPI A+	RPI ZERO	RPI B	COMPUTE
Characteristics	Performance /Wi-Fi /Bluetooth/ Ethernet	Performance /Ethernet	Ethernet	Price	Price /Size	Original	Integration /eMMC
Price	\$35	\$35	\$25	\$20	\$5+	\$25	\$40
Processor*	BCM2837 quad core Linux ARMv7	BCM2836 quad core Linux ARMv7	BCM2835 Linux ARMv6	BCM2835 Linux ARMv6	BCM2835 Linux ARMv6	BCM2835 Linux ARMv6	BCM2835 Linux ARMv6
Speed	1.2GHz	500MHz	700MHz	700MHz	1GHz	700MHz	700MHz
Memory	1GB	1GB	512MB	256MB	512MB	512MB	512MB
Typical Power	2.5W (up to 6.5W)	2.5W (up to 4.1W)	1W (up to 1.5W)	1W (up to 1.5W)	1W (up to 1.5W)	1W (up to 1.5W)	1W (up to 1.5W)
USB Ports	4	4	4	1	1OTG	2	via header
Ethernet	10/100 Mbps Wi-Fi and Bluetooth	10/100 Mbps	10/100 Mbps	none	none	10/100 Mbps	none
Storage	micro-SD	micro-SD	micro-SD	micro-SD	micro-SD	SO	4GB eMMC
Video	HDMI Composite	HDMI Composite	HDMI Composite	HDMI Composite	mini-HDMI composite	HDMI RCA video	HDMI via edge TV DAC via edge
Audio	HDMI digital audio and analog stereo via a 3.5mm Jack (where available)						
GPU	Dual Core VideoCore TV Multimedia Co-Processor at 250MHz (24 GFLOPS)						
Camera (CSI)	yes	yes	yes	yes	no	yes	CSI x 2 via edge
Display (DSI)	yes	yes	yes	yes	no	yes	DSI X 2 via edge
GPIO header	40 pins	40 pins	40 pins	40 pins	40 pins	26 pins	48 pins via edge
Usage	General-purpose computing and networking. High-performance interfacing. Video streaming	General-purpose computing. High-performance interfacing. Video streaming	General-purpose computing. Internet connected host. Video streaming.	Low cost general-purpose computing. Standalone electronics interfacing applications.	Low cost small profile standalone electronics interfacing projects.	General-purpose legacy applications. Internet connected host.	Suitable for plugin into user-created PCB's using a DDR2 SODIMM connector. Open-source breakout board available.

(Molloy, D., 2019)

Raspbian for robots

Raspbian for Robots is a Raspbian-based operating system created by the company Dexter Industries, intended for Raspberry Pi-based robot kits. This OS contains the embedded software to connect to GoPiGo, BrickPi, GrovePi or Arduberry and program. Programming environments such as Scratch and Python are already available with several test scripts ready to just run.

Grovepi+

Grove Pi+ is either an add-on or a frame/hat designed for the Raspberry Pi board, where the communication between the two is via an I2C interface. All GrovePi+ modules connect to universal Grove connectors consisting of 4-pin cables. Functional Grove modules with analog and digital signals are connected directly to the ATMEGA328 microcontroller in GrovePi. The microcontroller acts as an interpreter between the Raspberry Pi and the Grove sensors that send, receive and execute commands sent by Raspberry Pi.

In addition, Grove Pi allows Raspberry Pi to directly access some Grove sensors since Raspberry Pi has an I2C bus and a serial bus. The latter can be directly connected to the sensors through the I2C ports and the USART port.

This is a hat that has gained relevance in recent years due to its use in various projects such as weather stations (Bell, C., 2021) whose main modules are based on the Grove family of sensors from seeed studio. Among other noteworthy applications is the air quality monitoring system implemented with IoT (Balasubramaniyan, C., 2016), a project that managed to effectively monitor the air remotely and thus raise the possibility of covering a larger area in future work.

In the different projects that have been carried out with this hat, the ease with which the different Grove modules are connected and managed has been observed. Deepening in the code part, Python turns out to be the language with which it can be better interacted allowing that it does not have difficulties with the handling of sensors and actuators.

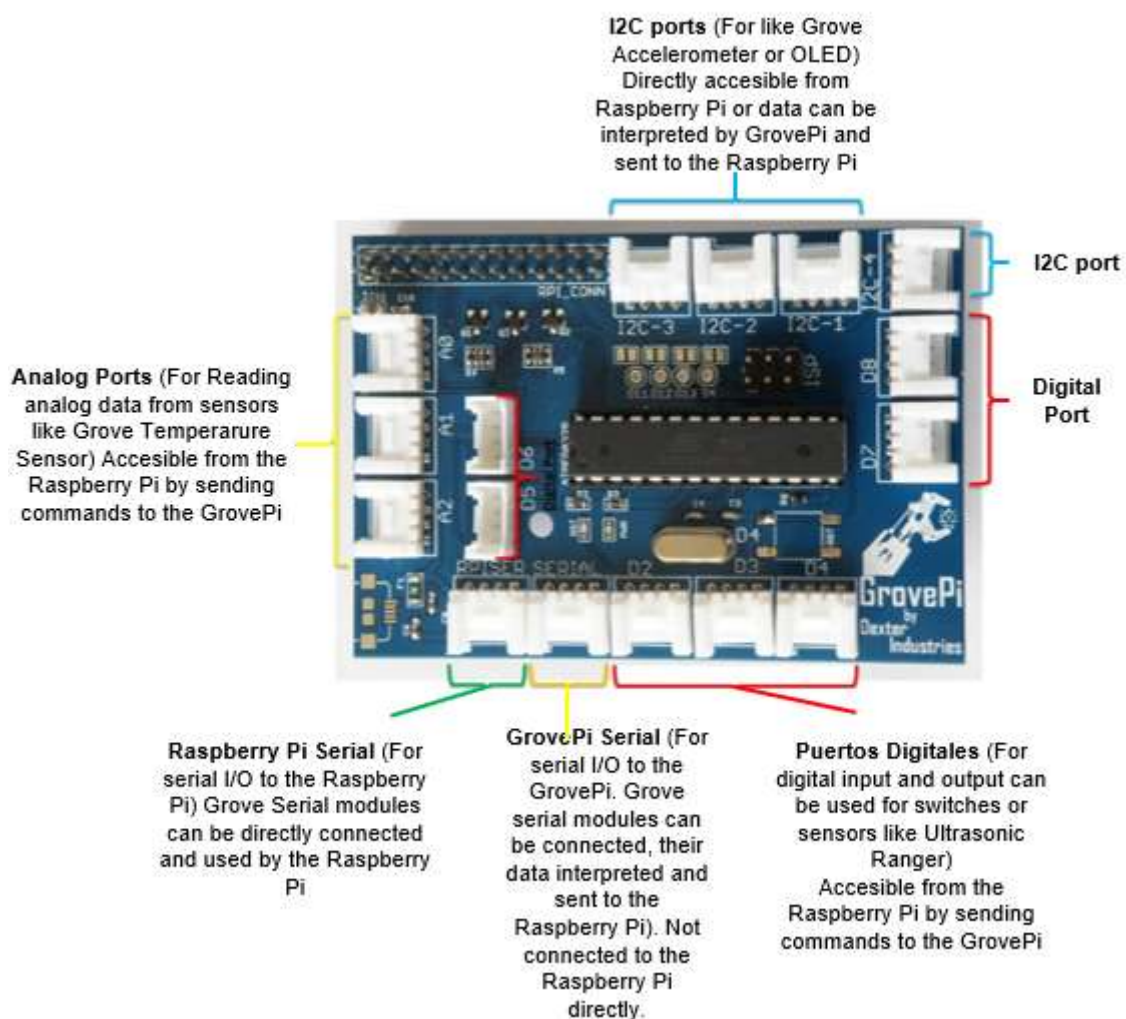
It is important to emphasize that it is thanks to the Raspbian for Robots distribution that it is possible to use GrovePi+, since it is impossible to download the repository containing the dependencies and libraries for its use from other distributions.

GrovePi+ Port Layout

Image 2 shows the way the ports are distributed and the type of each one of them. This hat provides digital (7), analog (3), I2C (3), Grove serial (1), Raspberry Pi serial (1) ports in addition to the power (5v) and ground (GND) pins.

Between the ports already mentioned you can also find 2 rows of pins (26), these pins can be used normally as if you were only working with Raspberry Pi, so you get the most out of both Raspberry and Grove Pi+ pins.

Figure 2 GrovePi+ ports (Dexter Industries)



Python

Raspberry Pi has generally been seen to be used in applications based on Python, an open source programming language with a short history when talking about GrovePi+.

Brief historical context

Python is a programming language widely used in web applications, software development, data science and machine learning (ML). Some of the reasons for using it are its efficiency and ease of learning, in addition to being able to run on several different platforms. Created by Guido Van Rossum in 1989 and released its first version in 1991 (Python 0.9.0), it included notable features such as some data types and error handling functions.

The second version (Python 1.0), released in 1994, contained new functions related to data list processing, assignment, filtering and reduction. This was followed by Python 2.0 in 2000, which provided the programmer with support for Unicode characters and a shorter way to traverse a list. The third version (Python 3.0) was released in December 2008, providing among the most outstanding improvements the print function, support for number division and error handling.

It is a language that has not yet been fully exploited in addition to having a rising popularity in recent years, and it is not for less, since it has been used in various projects involved with IoT. With this, development boards based on this language have raised alternatives according to the needs of users.

Among the works that relate the use of the language, we can find the guide for the management of programmable cards (Gonzales, R., 2021) supported by JavaScript, development and management of prototypes such as the FoamPi (Wright, H. C., Cameron, D. D., & Ryan, A. J.) whose objective is temperature monitoring of chemicals and even, it has been implemented in the field of environmental engineering by developing a software assembled in Python (Mg, I. Y. M. M. L. 2019) that helped to maintain the level of health in the ecosystem studied using the Tennat methodology. So, taking into account this kind of 'projects, Python still has a lot to offer in different research areas.

Main characteristics of the language

Python is an interpreted language, that is, it directly executes the code line by line. If there are errors in the program, its execution is stopped. This makes it easier for the programmer to find irregularities. It is a dynamically typed language, so it is not necessary to define the type of variable when writing the code since Python automatically determines what type it refers to at runtime. It is a high-level language, so the programmer does not have to worry about its underlying functionalities such as architecture and memory management. Object-oriented, Python considers everything as an object, but it can also support other types of programming.

IDE Thonny

Thonny is one of the IDEs originally born to program in Python on a computer that has been gradually incorporating support for Micropython. It allows working with boards such as Micro Bit, and those containing the ESP8266 and ESP32. It can also be used to program in Circuit Python.

This environment is also very easy to use and has more options and tools than other IDE's, although many of them work only when using the PC version of Python.

A very interesting feature included in the latest version is the possibility to record and update the board firmware internally from Thonny without using ESPTOOL.

It is an open source development created at the University of Tartu in Estonia and is very active, so it will surely continue to introduce new features as time goes by. It is available for Windows, Mac and Linux.

Talking a little bit about the workspace view, in *image 3* you can see the basic elements that compose the development environment. In this view you can locate the main icons; button to create a new program, open files, save button, script execution, debug button and sub-functions (skip, enter, exit and resume) as well as the stop/restart button.

In addition to the submenus (file, edit, view, run, tools and help), Thonny provides a wizard that helps the user to improve the structure of the scripts he develops, providing recommendations that can improve the debugging of the program.

The console is fundamental in environments intended to execute programming codes and Thonny is not far behind, as can be seen in *image 3*.

Figure 3 Thonny development environment



GrovePi

In order to work with the GrovePi+ hat it is necessary to install an exclusive library for it. Using the Raspberry Pi command terminal.

This library is mainly used for handling sensors, since GrovePi+ has several ports it is necessary to install it to be able to correctly manipulate each one of them.

Initially, the GrovePi+ shell must be placed on the Raspberry Pi. Then start the command terminal and type the *command 1*. This command creates a folder where the library will be stored.

```
mkdir ~/Dexter
```

Command 1. Creation of main folder

The newly created folder is then entered using the following line as specified in *command 2*.

```
cd /home/pi/Dexter
```

Command 2. Access to the newly created folder

For the next step you must have an active connection to an internet network, since the GrovePi repository provided by Git counter in *command 3* will be downloaded. When the download is finished, a new folder named GrovePi will be created.

```
git clone https://github.com/DexterInd/GrovePi
```

Command 3. Download from grovepi repository

Then, the "Script" folder is accessed as shown in *command 4*.

```
cd /home/pi/Dexter/GrovePi/Script
```

Command 4. Access to the script folder.

The next step is to start the installation script with the *command 5*, where the packages used by GrovePi+ will be downloaded, confirm by pressing "y" and wait for the end of the download. At the end of the download the Raspberry Pi will restart.

```
bash ./update_grovepi.sh
```

Command 5. Installation of dependencies

Installation

To check that the script was installed correctly you must check if the Raspberry Pi is able to detect the GrovePi+ hat by typing the *command 6*.

```
sudo i2cdetect -y 1
```

Command 6. Check

The way to check that the installation was successful is to observe an "04" in the output as shown in *image 4*. The grovepi library is essential because it is through it that the GrovePi+ ports can be used, allowing analog and digital readings, serial communications, and thus take advantage of the Python language with instructions that are very reminiscent of the Arduino syntax.

Figure 4 GrovePi+ detection

```

pi@dex: ~/Desktop/GrovePi/Script
File Edit Tabs Help
Best match: cffi 1.11.5
Processing cffi-1.11.5-py3.5-linux-armv7l.egg
cffi 1.11.5 is already the active version in easy-install.pth

Using /usr/local/lib/python3.5/dist-packages/cffi-1.11.5-py3.5-linux-armv7l.egg
Searching for pycparser==2.18
Best match: pycparser 2.18
Processing pycparser-2.18-py3.5.egg
pycparser 2.18 is already the active version in easy-install.pth

Using /usr/local/lib/python3.5/dist-packages/pycparser-2.18-py3.5.egg
Finished processing dependencies for grovepi==1.4.1
pi@dex:~/Desktop/GrovePi/Script $ sudo i2cdetect -y 1
sudo: i2cdetect: command not found
pi@dex:~/Desktop/GrovePi/Script $ sudo i2cdetect -y 1
 0  1  2  3  4  5  6  7  8  9  a  b  c  d  e  f
00:  -- 04  --  --  --  --  --  --  --  --  --  --  --  --  --
10:  --  --  --  --  --  --  --  --  --  --  --  --  --  --  --
20:  --  --  --  --  --  --  --  --  --  --  --  --  --  --  --
30:  --  --  --  --  --  --  --  --  --  --  --  --  --  --  --
40:  --  --  --  --  --  --  --  --  --  --  --  --  --  --  --
50:  --  --  --  --  --  --  --  --  --  --  --  --  --  --  --
60:  --  --  --  --  --  --  --  --  --  --  --  --  --  --  --
70:  --  --  --  --  --  --  --  --  --  --  --  --  --  --  --
pi@dex:~/Desktop/GrovePi/Script $

```

Tkinter

Tkinter is a library that provides the user with a platform-independent set of windowing tools. It uses the tkinter package and its extension tkinter.tix in addition to the tkinter.ttk modules. Where, the tkinter package can be seen as an object-oriented layer on top of tcl/tk. It is worth noting that tkinter is already included in Python 3 integrated in the Raspian for Robots operating system.

Some of the generalities of this library are the following:

tcl is a dynamic interpreted programming language like Python.

Tk is a package implemented in C that adds custom commands to create and manipulate GUI widgets.

ttk is a new family of Tk widgets that offers a better experience on different platforms.

Having understood the main function of the Liberator tkinter, in this section some simple examples of how to make interfaces from the Thonny IDE will be made.

The first example is the random number generator. For this, the tkinter and Random libraries must be included (the latter is necessary to be able to generate the numbers).

As can be seen in *code segment 1*, once the libraries are placed in the header there is a function called "update", responsible for generating the number (between 1 and 1000), in addition to publishing it in the interface (line 7).

It is also observed in line 11 the command that repeats the function in a tempo of 500ms, it is thanks to this instruction that the number change can be shown in the interface. If it is not specified, it is not updated on the screen.

It is important to say that in the update function, the line `text2.config` contains different parameters; `text`, which is intended to place a string type character string, `font`, which serves to detail the font type and size that will have the text, `bg`, which specifies the background color and foreground to detail the color of the text font. These parameters are fundamental in the design of an interface, so the user must take each and every one of them into account.

From line 13 to 17 you can find the creation of the main window called `window`, named "Generator", the height and width dimensions, as well as the background color, which in this case is `Orchid4`.

Another important part of the main interface are the Labels, generally used to display messages in a certain space of the main window (lines 19 to 23, 25 and 26) and which also need parameters for their design.

Buttons are also an essential part of the interfaces since they can be used to display customized functions; from lines 28 to 34 there is a button with the design parameters that were used for the case of window and labels, however, 2 new fields can be found; `border` and `command`.

`border` emphasizes the design of the button and `command` points to the "update" function. In short `border` customizes the width of the button border and `command` the function that the program will perform when the button is clicked.

Code segment 1. Tkinter window

```

1 import tkinter as tk
2 import random
3
4 def actualizar():
5     num_al=random.randint(1, 1000)
6     texto2.config(text="" + str(num_al),
7                 font=("Arial", 14),
8                 bg="orchid4",
9                 foreground="white")
10    ventana.after(500, actualizar)
11
12 ventana=tk.Tk()
13 ventana.title("Generator")
14 ventana.config(width=250,
15               height=200,
16               bg="orchid4")
17
18 texto1=tk.Label(text="Number: ",
19                font=("Arial", 14),
20                bg="orchid4",

```

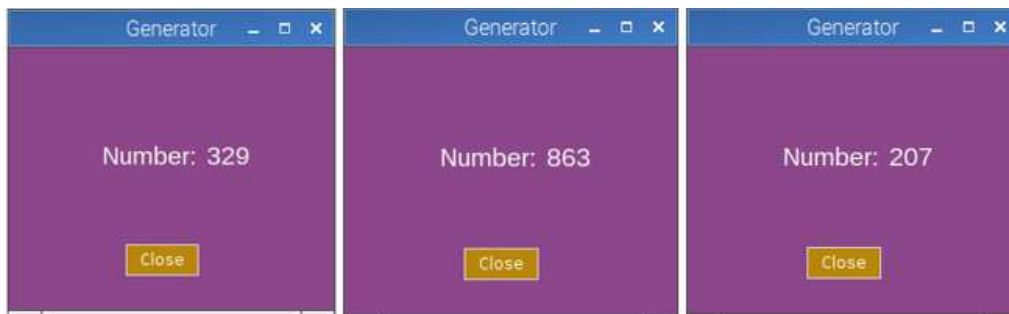
```

21         foreground="white")
22 texto1.place(x=70, y=70)
23
24 texto2=tk.Label(text="0")
25 texto2.place(x=150, y=70)
26
27 Boton=tk.Button(ventana,
28                 text="Close",
28                 command= ventana.destroy,
29                 bg="darkgoldenrod",
30                 foreground="white",
31                 border=0)
32 Boton.place(x=90, y=150)
33
34 ventana.after(500, actualizar)
35 ventana.mainloop()

```

In this way, the result of compiling the program can be seen in *image 5*. In it, 3 windows can be distinguished, which show the different values carried out by the generator. This does not mean that code segment 1 creates 3 windows, but only 1 window, and the values are taken after the time interval specified in the code (500 ms).

Figurer 5 Final screen (3 transitions)



Having shown a way to display a random value in a small interface in tkinter, the next step is to use the analog channels of the GrovePi+ in conjunction with a graphical window.

For this example, we need to connect two Grove modules; the light sensor and the potentiometer (also known as angle rotary sensor). Where the potentiometer will be connected to the analog port A0 and the light sensor to port A1 of the GrovePi+.

As presented in *code segment 2*, the potentiometer is identified as `potentiometer = 0` and `light_sensor = 1` referencing the GrovePi+ ports. For the proposed program we again make use of the `grovepi` library, in addition to importing all the library modules for the interface.

The `after` method is used again in order to carry out the update for the potentiometer and light sensor values. The functions `def light` and `def pot` are in charge of obtaining the values of each one.

Unlike the first interface that was made in this example we will implement the use of `LabelFrame`, an element provided by tkinter to create custom frames. From line 26 to 44, 2 `LabelFrame`s are coded with their respective geometric editor (grid method), however, it is obvious at first glance that it has not been fully customized by the parameters of each label. This will mark the limits of the frames with the main window of the interface.

Other parameters that can be highlighted from the code are `padx` and `pady`. These elements determine the size of the frame inside the main (root) window.

Code segment 2. Interface focused on variables

```

1 import tkinter as tk
2 from tkinter import *
3
4 potentiometer=0
5 light_sensor=1
6
7 def luz():
8     val1=grovepi.analogRead(light_sensor)
9     texto3=Label(contenedor1,text="" + str(val1)).place(x=10, y=15)
10    contenedor1.after(500, luz)
11
12 def pot():
13     val2=grovepi.analogRead(potentiometer)
14     texto4=Label(contenedor2, text="" + str(val2)).place(x=10,y=15)
15     contenedor2.after(500, pot)
16
17 root=tk.Tk()
18 root.title("Main Interfaz")
19 root.config(bg= "orchid4")
20
21 contenedor1=LabelFrame(root,
22     text= "Light Sensor",
23     fg= "Blue",
24     padx=65,
25     pady=65)
26 contenedor1.grid(row=0,
27     column=0,
28     padx=15,
29     pady=15)
30 contenedor2=LabelFrame(root,
31     text= "potentiometer",
32     fg= "Blue",
33     padx=65,
34     pady=65)
35 contenedor2.grid(row=0,
36     column=1,
37     padx=15,
38     pady=15)
39
40 texto1=tk.Label(contenedor1,
41     text= "Value: ").pack()
42 texto3=tk.Label(contenedor1,
43     text= "0").place(x=10, y=15)
44 texto2=tk.Label(contenedor2,
45     text= "Value: ").pack()
46 texto4=tk.Label(contenedor2,
47     text= "0").place(x=10, y=15)
48
49 root.after(500, luz)
50 root.after(500, pot)
51 root.mainloop()

```

Matplotlib

It is a library that helps the user to plot data in figures (or Figure), it contains one or more Axes (Area where the points can be specified in terms of XY or XYZ coordinates in case of 3D graphics) and a variety of methods that can give dynamism to the graphics. The easiest way to create a figure with axes is using `pyplot.subplots` where it is important to note that in order to display the figure you must call the `plt.show()` method.

The above interfaces can be complemented with graphics by using the `matplotlib` library. However, the Raspbian for Robots operating system lacks dependencies that slow down the installation of the library through `pip`, that is why we choose to use an alternative method as shown in *command 7*.

This command must be run from the terminal, if you try to install from the Thonny package manager is very likely not allowed and only manages to remove dependencies linked to the grovepi library.

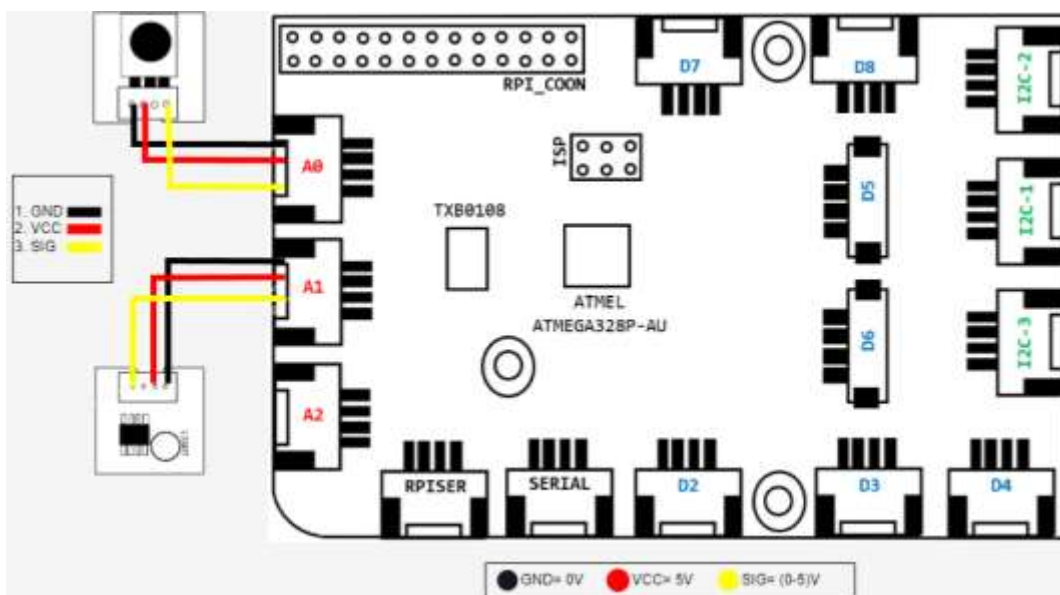
```
sudo apt install python3-matplotlib
```

Command 7 Matplotlib installation

For this circuit you need the potentiometer and the light sensor again, the potentiometer must be connected to channel A0 and the light sensor to channel A1 of GrovePi+ as shown in *image 6*. Remembering that GrovePi+ contains 3 analog ports you can change the connection order of the modules (if required), keeping in mind that you must additionally change the configuration in *code segment 3*.

From figure 6, as it is the first connection diagram seen in this work, it is necessary to mention that the color code was established according to the Grove Cable.

Figure 6 Connection diagram



Once the compatible library has been downloaded, the program is presented in code segment 4. It has the function of plotting the readings of a potentiometer and the light sensor (grove rotary angle sensor & grove light sensor).

In the code you can see the different sections that conform it: functions in charge of providing the sensor readings and functions that draw the lines of the graph according to the value obtained from the code blocks `read_pot` and `luminosidad`.

The way in which the graphs will be presented will be by separate windows, in this case we do not use Tkinter, only Matplotlib. It should be noted that the program is comprised of 3 instructions that, enclosed in the while loop, carry out the plotting of the 2D lines in a continuous manner.

Going deeper into the functions `grafico(frame)` and `grafico1(frame)`, the `append` method is used as the main element in the assignment of values to the `x_data`, `y_data`, `x1_data` and `y1_data` arrays, which makes efficient data processing possible. These functions are a fundamental part of the trafication process since lines 56 and 57 contain the instructions that make possible the update of values; `FuncAnimation(figure, graph, interval=400)` and `FuncAnimation(figure1, graph1, interval=400)` besides containing the same update interval (400 ms) point to their respective space or "plot" and to the function of the variable they represent (`grafico` focuses on the potentiometer and `grafico1` on the light sensor).

Code segment 3 Creation of graphics

```

1 from tkinter import *import time
2 import grovepi
3 import matplotlib.pyplot as plt
4 from datetime import datetime
5 from matplotlib import pyplot
6 from matplotlib.animation import FuncAnimation
7
8 plt.style.use('ggplot')
9 x_data=[]
10 y_data=[]
11 x1_data=[]
12 y1_data=[]
13
14 figure= pyplot.figure()
15 line, =pyplot.plot_date(x_data, y_data, '-')
16
17 figure1= pyplot.figure()
18 line1, =pyplot.plot_date(x_data, y1_data, '-')
19
20 potentiometer = 0
21 light_sensor = 1
22
23 grovepi.pinMode(potentiometer,"INPUT")
24 grovepi.pinMode(light_sensor,"INPUT")
25
26 time.sleep(5)
27
28 def grafico(frame):
29     x_data.append(datetime.now())
30     pase=lectura_pot()
31     y_data.append(pase)
32     line.set_data(x_data, y_data)
33     figure.gca().relim()
34     figure.gca().autoscale_view()
35     return line,
36
37 def grafico1(frame):
38     x1_data.append(datetime.now())
39     sensorluminoso=luminosidad()
40     y1_data.append(sensorluminoso)
41     line1.set_data(x1_data, y1_data)
42     figure1.gca().relim()
43     figure1.gca().autoscale_view()
44     return line1,
45
46 def lectura_pot():
47     sensor_value = grovepi.analogRead(potentiometer)
48     return(sensor_value)
49
50 def luminosidad():
51     sensor_value1 = grovepi.analogRead(light_sensor)
52     return (sensor_value1)
53
54 while True:
55     try:
56         animation2= FuncAnimation(figure, grafico, interval=400)
57         animation= FuncAnimation(figure1, grafico1, interval=400)
58         pyplot.show()
59     except IOError:
60         print ("Error")

```

XlsxWriter

XlsxWriter is an open source Python API for writing files in the Excel 2007+ XLSX file format. With the API, you can write text, formulas, numbers and hyperlinks to multiple worksheets. In addition, the API allows you to insert charts, merge cells, format cells, apply filters, validate data, insert PNG/JPEG/BMP/WMF/EMF Figures, use multi-format strings and more.

XlsxWriter provides more Excel functions than any of the alternative Python modules. In addition, it provides a high accuracy rate when creating new Excel files; in most cases, files produced with XlsxWriter are 100% equivalent to files produced by Excel.

From this description, in this section the "Recording" of data implementing an analog sensor will be performed.

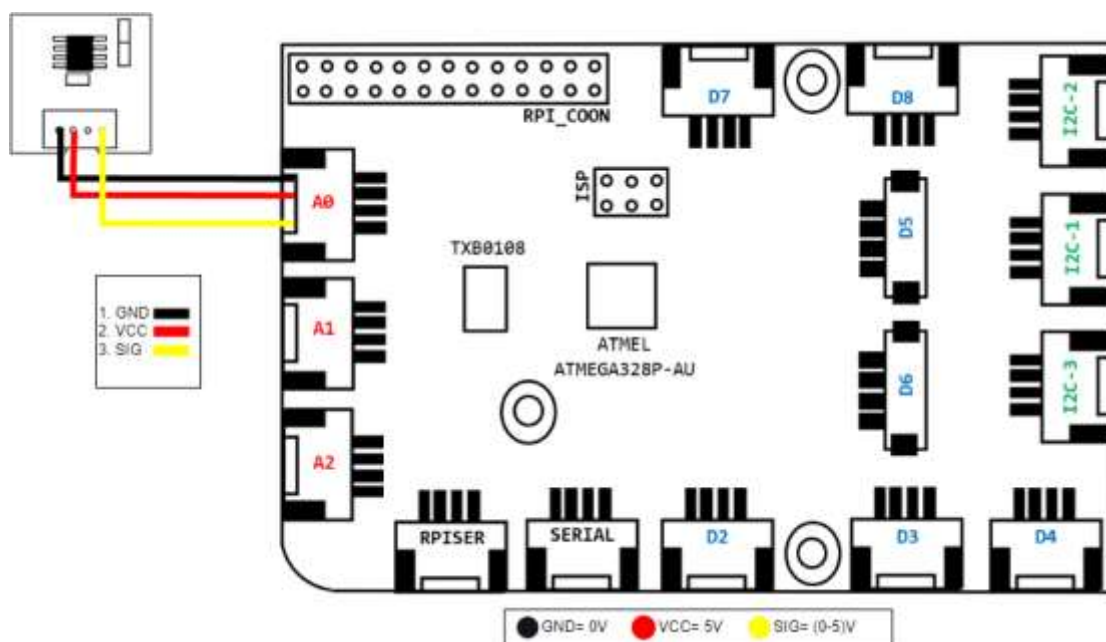
Initially it is necessary to install the library, for this we use pip, with the *command 8* executed from the terminal.

```
pip install XlsxWriter
```

Command 8 Xlsxwriter installation

The sensor to be used will be the temperature sensor as shown in *Figure 7*.

Figure 7 Connection diagram



Once the connection has been made, the program for this activity is the one seen in *code segment 4*. It is in this code that a class is presented that has the objective of obtaining values from various sensors, thus providing an alternative to the usual `grovepi.analogRead()` instruction provided by the `grovepi` library. Highlighting that it favors the compilation of the program in terms of time.

Some of the lines that are indispensable in the elaboration of the script are described:

The XlsxWriter library requires specific syntax for file creation, saving and saving. Line 11 describes how to create the file and gives the option to name it. Line 12 adds spreadsheets to the file.

Line 15 contains an instruction which involves the execution of *code segment 5* yielding the temperature value.

To store data the instruction `hoja.write` can be displayed in lines 18 and 19 and as arguments the location (row, column, data to be stored).

In order to save the file, line 25 contains the instruction `archivo.close()`.

The for loop performs the storage of the temperature value 50 times, therefore, the final file will contain 2 rows; one for the timestamp and one for the temperature value.

Code segment 4. Data storage with Xlsxwriter

```

1 import grovepi
2 import dht11_modulo
3 import time
4 import xlsxwriter
5
6 i=0
7 h=0
8 temperatura=0
9 grovepi.pinMode(temperatura,"INPUT")
10
11 archivo=xlsxwriter.Workbook('GrabadoDeLecturas.xlsx')
12 hoja=archivo.add_worksheet()
13
14 for c in range (0,50):
15     val2=dht11_modulo.lectura_pot(temperatura)
16     hora=time.strftime("%X")
17     hoja.write(i,1,val2)
18     hoja.write(h,0,hora)
19     print(val2)
20     i=i+1
21     h=h+1
22     time.sleep(3)
23
24 archivo.close()

```

Another thing that can be added from the class of *code segment 5* is the versatility of adding or changing sensors in this section, eliminating a possible problem (if it is the case of changing the type of sensor) of having to resort to the main program and look for the lines to change it.

For this it is more advisable to have a class intended only for sensors.

Code segment 5 Class that obtains sensor readings

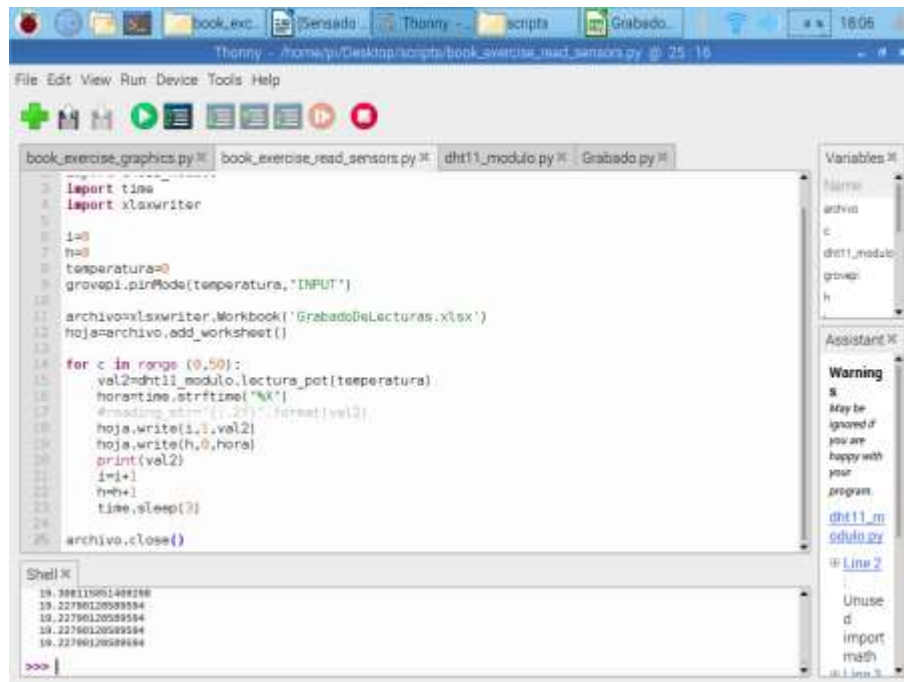
```

1 import grovepi
2 import math
3 import time
4
5 def lectura_hummodulo():
6     sensor_value2= grovepi.analogRead(moisture_sensor)
7     return (sensor_value2)
8
9 def lectura_lummodulo():
10    sensor_value1= grovepi.analogRead(light_sensor)
11    return (sensor_value1)
12
13 def lectura_pot():
14    sensor_value= grovepi.analogRead(temperatura)
15    return (sensor_value)

```

Figure 8 shows a first execution of the code in which the temperature values can be observed in the console, in order to check the data with those of the final file. Since the main program only takes 50 values, it provides a way to check the veracity of the data by comparing the data printed in the Thonny console with those saved in the Excel file.

Figure 8 Console result



```

1 import time
2 import xlswriter
3
4 i=0
5 h=0
6 temperatura=0
7 grovapi.pirNode(temperatura,"INPUT")
8
9 archivo=xlswriter.Workbook('GrabadoDeLecturas.xlsx')
10 hoja=archivo.add_worksheet()
11
12
13
14 for c in range (0,50):
15     val2=dht11_modulo.lectura_pot(temperatura)
16     hora=time.strftime("%X")
17     #reading_str="{:1.2f} - {}".format(val2)
18     hoja.write(i,1,val2)
19     hoja.write(h,0,hora)
20     print(val2)
21     i=i+1
22     h=h+1
23     time.sleep(2)
24
25 archivo.close()

```

Shell

```

19.388115951489188
19.22796120589554
19.22796120589554
19.22796120589554
19.22796120589554

```

Variables

Warning
May be ignored if you are happy with your program

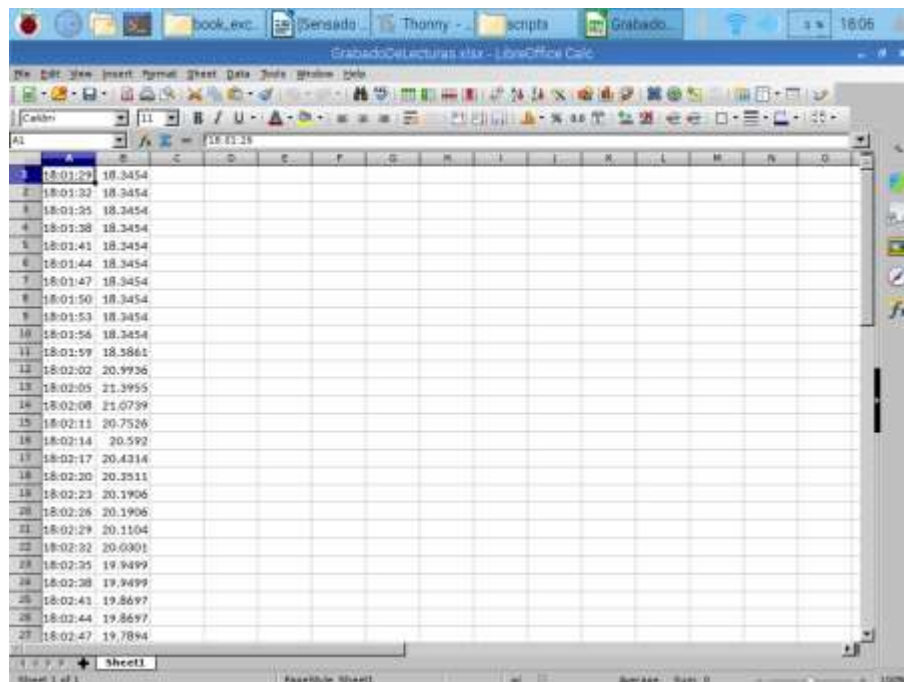
dht11_m
odule.py

Unuse
d
import
math

Now it is time to open the generated file, in order to find it just open the folder where the main program is hosted. Reviewing the file you can find the data of the Figure 9.

The type of data with which each reading was saved are 2; time and string. This feature must be taken into account because, if you plan to use this data to insert graphs or perform calculations, the string data belonging to the temperature (Column B) will have to be converted into an integer or floating data type. In this way it is possible to develop a tool very similar to Data Streamer (Excel add-in whose function is to capture data acquired by the Arduino in serial form).

Figure 9 View to final file



Time	Temperature
18:01:29	18.3454
18:01:32	18.3454
18:01:35	18.3454
18:01:38	18.3454
18:01:41	18.3454
18:01:44	18.3454
18:01:47	18.3454
18:01:50	18.3454
18:01:53	18.3454
18:01:56	18.3454
18:01:59	18.5861
18:02:02	20.9936
18:02:05	21.3955
18:02:08	21.0739
18:02:11	20.7526
18:02:14	20.592
18:02:17	20.4316
18:02:20	20.3911
18:02:23	20.1906
18:02:26	20.1906
18:02:29	20.1104
18:02:32	20.0901
18:02:35	19.9499
18:02:38	19.9499
18:02:41	19.8697
18:02:44	19.8697
18:02:47	19.7894

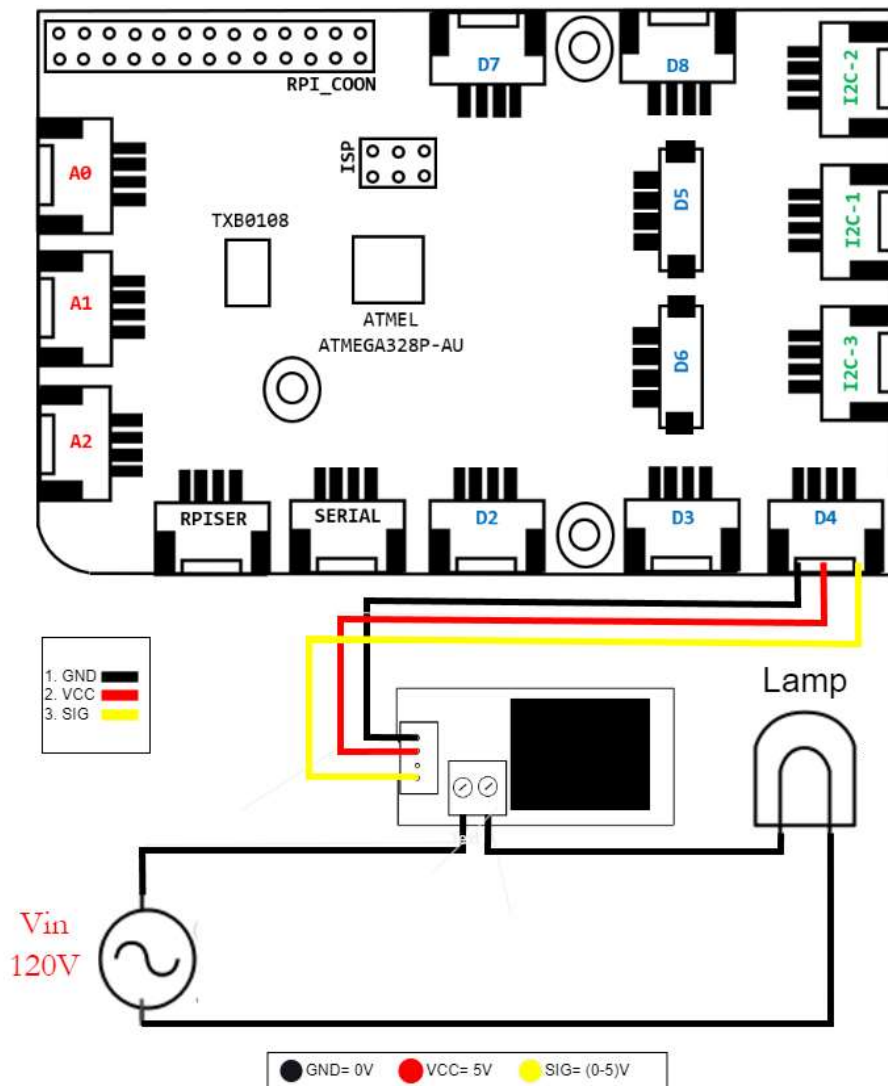
Circuits with actuators and other components

Relay

This is a basic circuit whose objective is to demonstrate the use of the relay. It is important to emphasize that in case of not having the Grove module, a generic relay can replace it without any problem, although it is necessary to have a Grove Cable for a correct communication with the GrovePi+ hat.

As shown in Figure 10, the relay must be connected to port D4 of GrovePi+ and the bulb must be open in one of its two connections.

Figure 10 Connection diagram



In code segment 6 you can see how the program only outputs values of 0 and 1 (0v and 5v) for 2 second intervals. 2 seconds the relay will let the light bulb turn on and 2 seconds will turn it off in an infinite loop thanks to the while loop.

Despite being a relatively short code, it has the virtue of being very understandable as if it were an Arduino. It can be noticed that the number of libraries to use are much less than in previous circuits. And it could even be very easily related to a switch on and off an LED. The instruction that allows this state switching is located in line 10 and 14 through `grovepi.digitalWrite()`.

Code segment 6 Use of the relay module

```

1 import time
2 import grovepi
3
4 relay = 4
5
6 grovepi.pinMode(relay,"OUTPUT")
7
8 while True:
9     try:
10        grovepi.digitalWrite(relay,1)
11        print ("on")
12        time.sleep(2)
13
14        grovepi.digitalWrite(relay,0)
15        print ("off")
16        time.sleep(2)
17
18    except KeyboardInterrupt:
19        grovepi.digitalWrite(relay,0)
20        break
21    except IOError:
22        print ("Error")

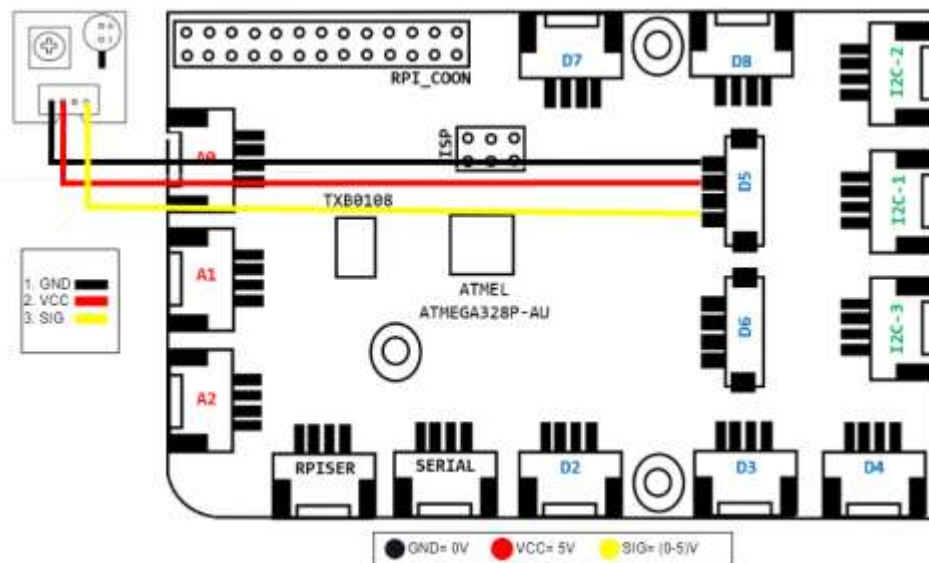
```

PWM

The PWM pulse has several uses, from speed control of a motor to a variable frequency drive and even being part of a digital PID controller. That is why in this section we present a simple code that demonstrates its operation using the Grove led pack.

The connection of this circuit is limited to use a single module, being a PWM it is important to consider using a digital port of the GrovePi+ with the ability to throw a pulse of this type. As can be seen in Figure 11, port D5 is the one chosen.

Figure 11 Connection diagram



As for the program, code segment 7 provides a quick way to display the PWM by means of 2 for loops. With them it will be possible to observe in the physical assembly how the LED changes the brightness level continuously up and down thanks to the described while loop.

It should be remembered that a PWM pulse is between values from 0 to 255, although the changes are visible in shorter values and with longer delays, that is why the voltage will only be varying with values between 0 and 20.

Code segment 7 PWM operation

```

1 import time
2 from grovepi import *
3
4 led = 5
5 z=0
6 pinMode(led,"OUTPUT")
7
8 while True:
9   for i in range(0,20):
10    z+=1
11    analogWrite(led,z)
12    print(z)
13    time.sleep(0.1)
14   for j in range(0,20):
15    z-=1
16    analogWrite(led,z)
17    print(z)
18    time.sleep(0.1)

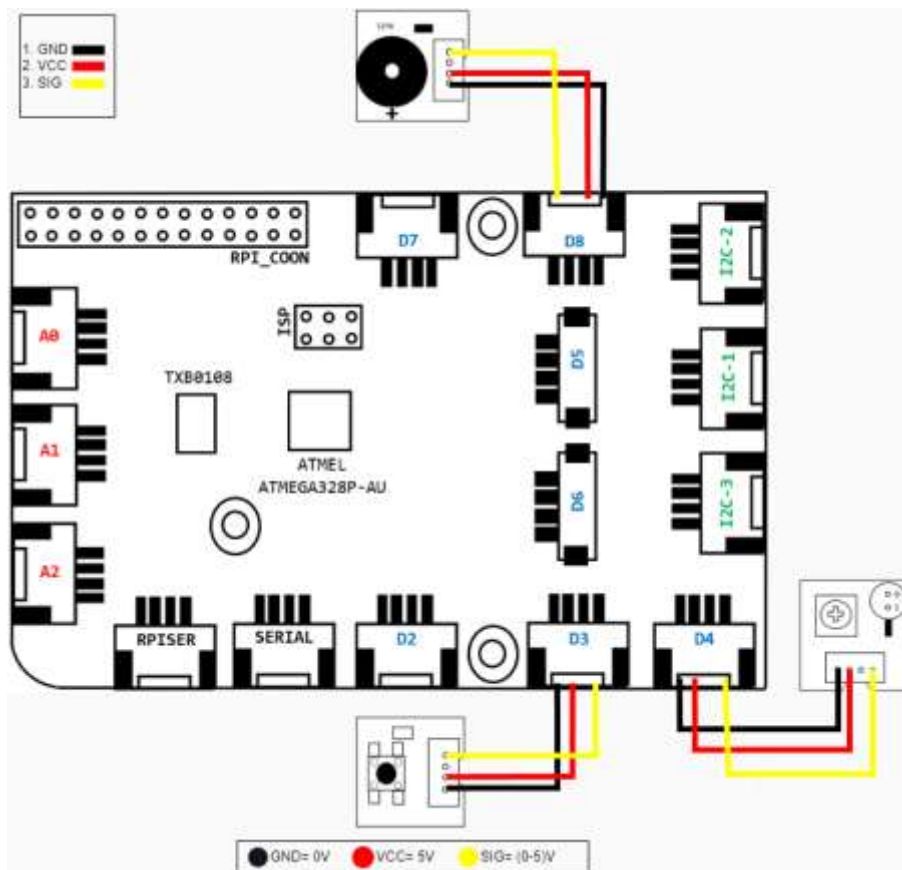
```

Buzzer

For this circuit we will make use of 3 components, the buzzer module, a button and the led pack. Each time the button is pressed, the buzzer will have to emit sound and at the same time the led will have to be in high state.

In the diagram of Figure 12 it can be seen how only digital channels are used due to the nature of the modules to be used. The buzzer must be connected to channel D8, the led to D4 and the button to D3.

Figure 12 Connection diagram



In the code segment 8 above you can see how the while loop encompasses the operation of the circuit by means of a conditional if-else. The if key compares if the input status coming from the button is high (button pressed), if it is true both the buzzer and the led will be activated.

Code segment 8. Control of the buzzer module

```

1 import time
2 import grovepi
3
4 buzzer = 8
5 button = 3
6 led = 4
7
8
9 grovepi.pinMode(button,"INPUT")
10 grovepi.pinMode(buzzer,"OUTPUT")
11 grovepi.pinMode(led,"OUTPUT")
12
13 while True:
14     try:
15         if(grovepi.digitalRead(button)==1):
16             grovepi.digitalWrite(buzzer,1)
17             grovepi.digitalWrite(led,1)
18         else:
19             grovepi.digitalWrite(buzzer,0)
20             grovepi.digitalWrite(led,0)
21
22     except IOError:
23         print ("Error")

```

CD motor control

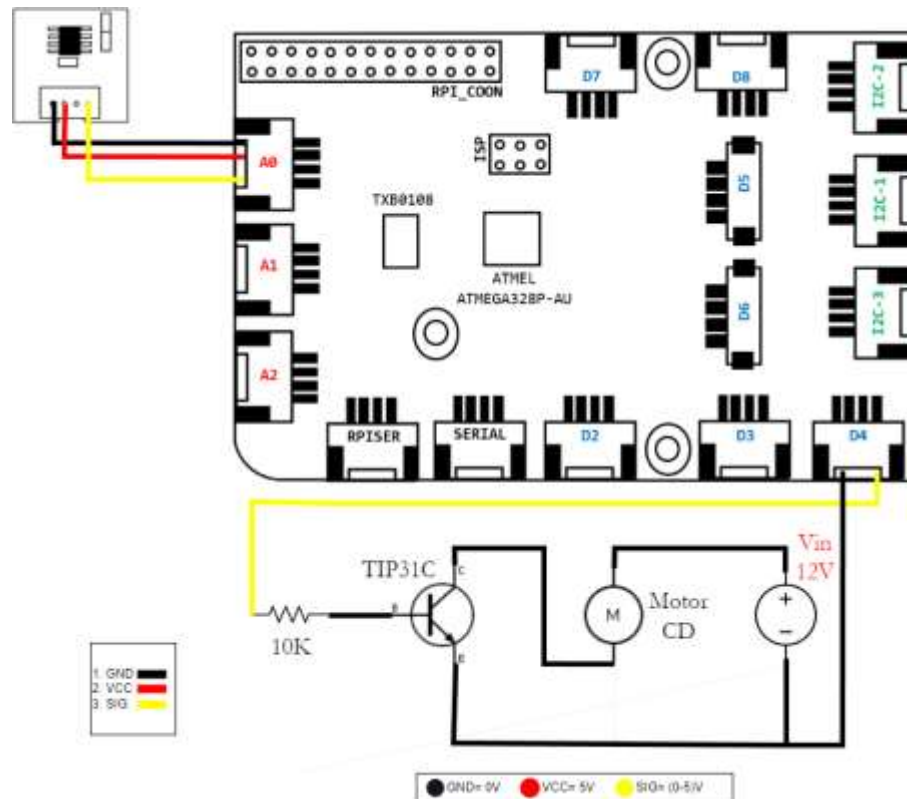
For this circuit another electrical component is presented, the transistor. Since the motor to be used is one of 12V and is of direct current, it is required to compensate the consumption current, that is why the tip31C will be used taking into account that it is a BJT in Darlington arrangement.

As can be seen in *Figure 13*, the circuit requires the following components;

- GrovePi+
- Protoboard.
- Grove Temperature Sensor v1.2
- Resistor 10k
- Tip31C
- Motor 12v DC
- 12v charger / Voltage source.

The ports to be used are A0 and D4.

Figure 13 Connection diagram



According to code segment 9, the motor will be triggered every time the temperature sensor reaches values above 20° C in addition to printing the current value being detected on the console. A while loop is used in this case for constant temperature monitoring.

Code segment 9 DC motor control

```

1 import time
2 import grovepi
3 from grovepi import *
4
5 led = 4
6 temperature=0
7
8 pinMode(led,"OUTPUT")
9 pinMode(temperature,"INPUT")
10
11 while True:
12     val=grovepi.temp(temperature,'1.2')
13     print(val)
14     if(grovepi.temp(temperature,'1.2')>20):
15         analogWrite(led,255)
16     else:
17         analogWrite(led,0)

```

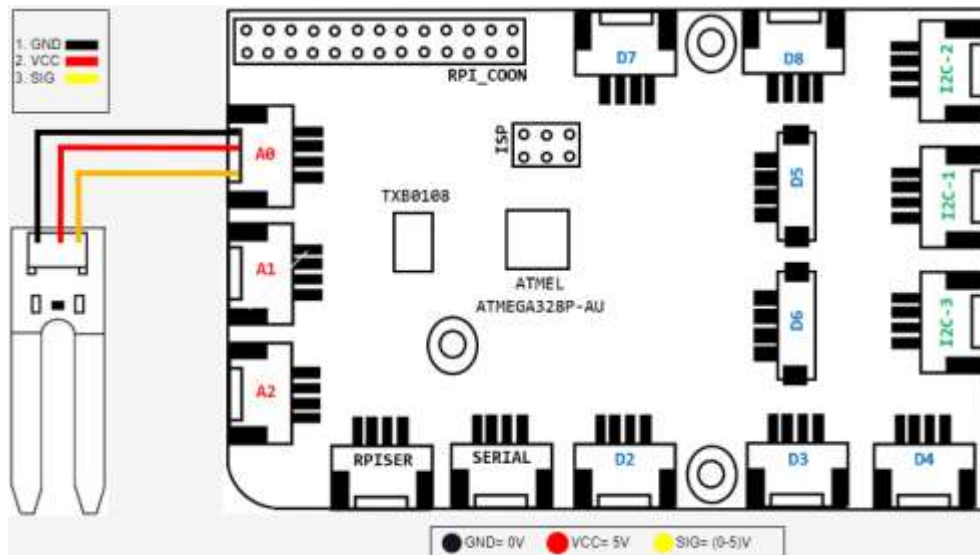
Grove moisture sensor

This is a circuit widely used as far as GrovePi+ is concerned, since only the soil moisture sensor and the base program provided by Dexter Industries are needed.

Since it is an analog sensor, it can be used in any of the 3 ports provided by the GrovePi+, in this case the A0 channel will be used as shown in Figure 14.

One of the things to keep in mind about the humidity sensor is that when placing it in the plant, care must be taken not to completely submerge the module, respecting the division between the electrodes and the connection port.

Figure 14 Connection diagram



Returning to the interfaces, this monitoring will be complemented with a small window in which the value recorded by the humidity sensor can be observed (*code segment 10*). So at this point the structure of the program can be repetitive since the bases of the potentiometer and light sensor interface are taken. For this interface only 1 single label (line 19) will be taken as a reference.

In *code segment 10* there is also a block that involves the use of Figures. Being the first time that these design elements are used in this work, it is important to keep in mind that both the format of the illustrations and their dimensions must be respected in order not to generate irregularities in the final window. As for the format, the ideal format to work with is the jpg, while the dimensions may vary depending on the measures assigned to the main window (root), if the Figure is larger in resolution compared to the main interface, the latter will be covered by the Figure to be placed on top of any element (buttons, frames or labels). If the format is not the right one, compilation errors will occur or it will simply not be displayed in the window. In the code, lines 36, 37 and 38 load an illustration that will serve as an icon to give a better presentation to the window. The Figure is instantiated with the variable "img" and positioned with the function place().

Code Segment 10 Moisture monitoring

```

1 import tkinter as tk
2 from tkinter import *
3 import grovepi
4
5 hum=0
6
7 grovepi.pinMode(hum,"INPUT")
8
9 def humedad():
10     val1 = grovepi.analogRead(hum)
11     texto3=Label(contenedor1,
12     text="" + str(val1)).place(x=10,y=15)
13     contenedor1.after(500, humedad)
14
15 root=tk.Tk()
16 root.title("Plant")
17 root.config(bg="orchid4")
18
19 contenedor1=LabelFrame(root,
20     text="Soil Moisture",
21     fg="blue",
22     padx=65,
23     pady=65.)
24 contenedor1.grid(row=0,
25     column=0,
26     padx=15,
27     pady=15)

```

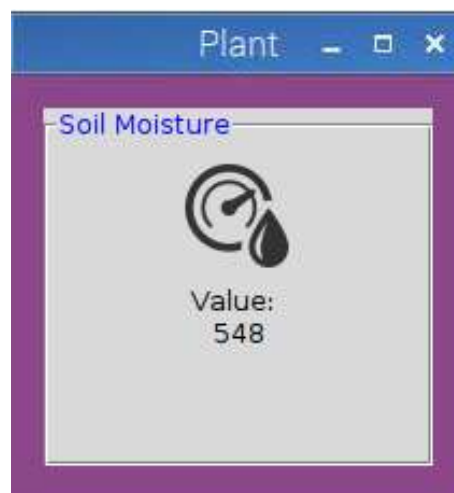
```

28
29 texto1=tk.Label(contenedor1,
30     text="Value: ").pack()
31
32 texto3=tk.Label(contenedor1,
33     text="0").place(x=10,y=15)
34
35 img=tk.PhotoFigure(file="hum.png")
36 lbimg=tk.Label(root, Figure=img)
37 lbimg.place(x=80,y=40)
38
39 root.after(500, humedad)
40 root.mainloop()

```

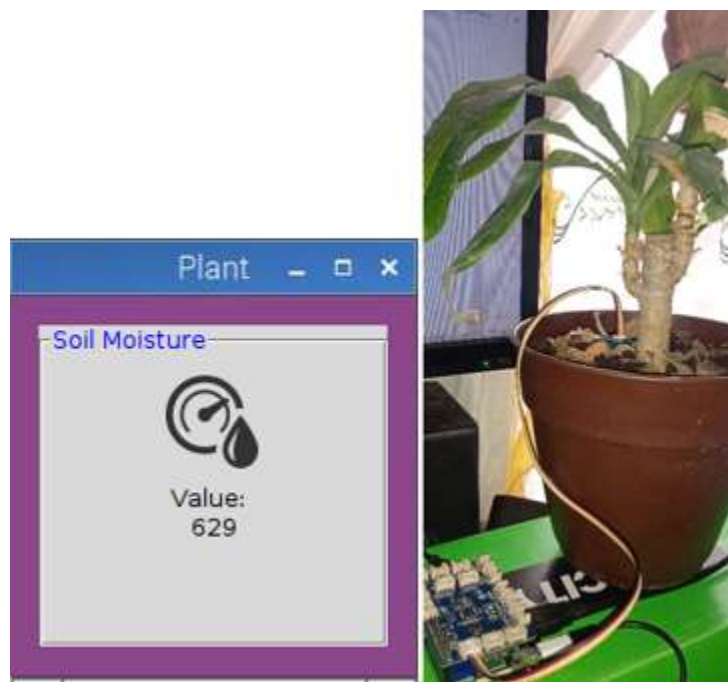
It is important to mention that the value presented in Figure 15 is for an unwatered plant. In this way we have a reference value with which to make a comparison later on.

Figure 15 Window for plant monitoring



When the plant is irrigated, in Figure 16 the value changes to 626 obtaining a very small change for the range of values that the sensor comprises (0 to 1024). This circuit has possibilities to be complemented with a DC motor that has the function of a water pump with the help of the relay, thus implementing the automatic control depending on the state of the plant

Figure 16 Humidity level after adding water



Acknowledgments

This paper would not have been possible without the support of the Universidad de Ixtlahuaca CUI and the TecNM campus Jocotitlán, who mainly provided the material seen during this work.

Conclusions

During the present work the use of different Grove modules was approached, with this it was possible to implement both the control and the visualization through simple graphical interfaces taking advantage of the benefits offered by Python. Implementing analog sensors with the graphical windows represents an alternative for similar desktop applications, demonstrating that the graphics have a relatively fast update time, the ease of programming the control of the components and the wide variety of libraries that Python has, allowing the addition of more features without aggressively consuming Raspberry Pi resources.

In terms of programming, the grovepi library is of great help to the user by providing understandable instruction lines that allow manipulating different actuators as can be seen in the motor control circuit on CD. In conclusion, the use of GrovePi+ is a suitable alternative to make visualization and control interfaces that depending on the robustness of the system needed by the user, the use of the different ports and Python will be less effort compared to other hats that work with C programming.

References

- ¿Qué es Python? - Explicación del lenguaje Python - AWS. (n.d.). Amazon Web Services, Inc. <https://aws.amazon.com/es/what-is/python/>
- Anicai, C. y Shakir, MZ (marzo de 2023). IoT and Machine Learning Enabled Estimation of Health Indicators from Ambient Data. IEEE. <https://doi.org/10.1109/WCNC55385.2023.10119030> En 2023, IEEE Wireless Communications and Networking Conference (WCNC) (págs. 1-6). IEEE.
- Balasubramaniyan, C., & Manivannan, D. (2016). IoT Enabled Air Quality Monitoring System (AQMS) using Raspberry Pi. Indian Journal of Science and Technology, 9(39). <https://doi.org/10.17485/ijst/2016/v9i39/90414>
- Bell, C. (2021). *Beginning IoT projects: Breadboard-less Electronic Projects*. Apress.
- Creating, viewing, and saving Matplotlib Figures — Matplotlib 3.7.2 documentation. (n.d.). <https://matplotlib.org/stable/users/explain/figures.html#figure-explanation>
- D BÜCH, D., B., & M ESCH, M., E. (2023). A Testbed for Smart City Applications and Architectures. IEEE. <https://doi.org/10.1109/COINS57856.2023.10189229>. In 2023, International Conference on Omni-layer Intelligent Systems (COINS) (págs. 1-6). IEEE.
- Getting Started with Ubuntu Core for Raspberry Pi 3. (n.d.). (n.p.): PE
- Gonzalez, R. (2021, December 15). Guía para manejo de tarjetas programables con Python y JavaScript para Internet de las Cosas. URI: <http://repositorio.uts.edu.co:8080/xmlui/handle/123456789/8235>
- GrovePi Port description. (2017, March 21). Dexter Industries. <https://www.dexterindustries.com/GrovePi/engineering/port-description/>
- Ltd, A. P. (2023). API Python de código abierto para hojas de cálculo de Google crear y compartir hojas de cálculo. Aspose Pty. Ltd. <https://products.fileformat.com/es/spreadsheet/python/xlsxwriter/#:~:text=XlsxWriter%20es%20una%20API%20de,en%20varias%20hojas%20de%20trabajo.>
- Mg, I. Y. M. L. (2019, August 1). Determinación del caudal Ecológico en la Microcuenca del Río Cutuchi mediante el método de Tennant en Python, periodo 1988 – 2014. <http://repositorio.utc.edu.ec/handle/27000/6107>

Paguayo. (2022). ¿Que es Raspberry Pi? - Raspberry Pi. Raspberry Pi. <https://raspberrypi.cl/que-es-aspberry/>

Pawar, S., Kelkar, S., Khire, N., Khairnar, T. y Kharabe, M. (marzo de 2023). AQI Monitoring and Predicting System. IEEE. <https://doi.org/10.1109/ESCI56872.2023.10099645>. In 2023, IEEE International Conference on Emerging Smart Computing and Informatics (ESCI) (págs. 1-6). IEEE.

Press. Molloy, D. (2019). Raspberry Pi® a fondo para desarrolladores. España: Marcombo.

tkinter — Python interface to Tcl/Tk. (n.d.). Python Documentation. <https://docs.python.org/3/library/tkinter.html#architecture>

Vila, M., Sancho, M. R., & Teniente, E. (2023, March). Monitoring, IoT Devices, and Semantics. IEEE. <https://doi.org/10.1109/PerComWorkshops56833.2023.10150279>. In 2023 IEEE International Conference on Pervasive Computing and Communications Workshops and other Affiliated Events (PerCom Workshops) (pp. 309-312). IEEE.

Wright, H. C., Cameron, D. D., & Ryan, A. J. (2022). FoamPi: an open-source Raspberry Pi based apparatus for monitoring polyurethane foam reactions. *HardwareX*, 12, e00365. <https://doi.org/10.1016/j.ohx.2022.e00365>

Chapter 7 Biosorbents and biomaterials: Application in the environment and in the health sector

Capítulo 7 Los biosorbentes y biomateriales: Aplicación en el medio ambiente y en el sector salud

SALAZAR-PERALTA Araceli, BERNAL-MARTÍNEZ Lina Agustina and SÁNCHEZ-OROZCO Raymundo

Tecnológico Nacional de México, Tecnológico de Estudios Superiores de Jocotitlán, Materials and Chemical Engineering División, Carretera Toluca Atlacomulco km 44.8, Ejido de San Juan y San Agustín, Jocotitlán, México.

ID 1st Author: *Araceli, Salazar-Peralta* / **ORC ID:** 0000-0001-5861-3748, **Researcher ID Thomson:** U-2933-2018, **CVU CONAHCYT ID:** 300357

ID 1st Co-author: *Lina Agustina, Bernal-Martínez* / **ORC ID:** 0000-0002-4922-043X, **CVU CONAHCYT ID:** 173701

ID 2nd Co-author: *Raymundo, Sánchez-Orozco* / **ORC ID:** 0000-0003-0006-1711, **CVU CONAHCYT ID:** 169684

DOI: 10.35429/H.2023.5.111.122

A. Salazar, L. Bernal and R. Sánchez

*araceli.salazar@tesjo.edu.mx

R. López (AA.) Engineering and Architecture in the Northern part of the State of Mexico. Handbooks-TI-©ECORFAN-Mexico, Estado de México, 2023

Abstract

The objective of this work is to carry out an analysis of the studies using sustainable materials with terms of biosorbents and biomaterials, the biosorbents applied in the environment are mentioned, mainly those applied in water, with the purpose of carrying out an analysis in the removal of different types of both organic and inorganic contaminants, mentioning the factors that are involved during the biosorption process, such as the effect of the pH value, type of material, temperature, pore size, to name a few, as well as its application in different studies. In the case of biomaterials, the biological, chemical, physical, among others, are described, mentioning the classification and applications of these biomaterials in different case studies, finally the conclusions are mentioned where it is highlighted that a large part of the reported studies have been carried out in a lot, so it is necessary to carry out more research focused on all the factors that worsen biosorption but on a pilot, industrial scale and considering economic processes with a focus on recovering the biosorbent and having better environmental sustainability. In biomaterials they are essential to improve human health and quality of life, but what stands out is that it is necessary to focus on the determining factors for the acceptance of new biomaterials for this type of applications is their useful life.

Biomaterials, Environmental Pollution, Sustainability, Processes

Resumen

En este trabajo tiene como objetivo realizar un análisis de los estudios utilizando materiales sustentables con términos de biosorbentes y biomateriales, se mencionan los biosorbentes aplicados en el medio ambiente principalmente los aplicados en agua, con la finalidad de realizar un análisis en la remoción de diferentes tipos de contaminantes tanto orgánicos como inorgánicos, mencionando los factores que involucran durante el proceso de la biosorción como por ejemplo el efecto del valor de pH, tipo de material, temperatura, tamaño de poro, por mencionar algunos, así mismo su aplicación en diferentes estudios. Para el caso de los biomateriales se describen las propiedades biológicas, químicas, físicas, entre otras, mencionando la clasificación y las aplicaciones de estos biomateriales en diferentes casos de estudio, finalmente se mencionan las conclusiones donde se destaca que gran parte de los estudios reportados se han llevado a cabo en lote, por lo que es necesario realizar más investigación enfocada a todos los factores que afectan a la biosorción pero en escala piloto, industrial y considerando procesos económicos con enfoque de recuperar el biosorbente y tener mejor una sustentabilidad ambiental. En los biomateriales son indispensables para mejorar la salud humana y la calidad de vida, pero lo sobresaliente es que hay que enfocarse a los factores determinantes para la aceptación de nuevos biomateriales para este tipo de aplicaciones es su tiempo de vida útil.

Biomateriales, Contaminación Ambiental, Sustentabilidad, Proceso

1 Introduction

Biosorption is the ability of a biomass to remove organic or inorganic species in water, soil and air, through a mechanism of physicochemical sequestration (Akar *et al.*, 2015). There are two types of biomass, live (fungus, algae, bacteria) and dead (agricultural, wood or wool waste). The use of dead biomass is frequently applied in this type of process, because it does not need maintenance conditions; whereas, the use of live biomass requires nutrients and biomass toxicity is likely to occur when in contact with contaminants, however, its potential in the removal of contaminants is recognized (Park *et al.*, 2010). To consider an effective biosorbent, it must meet the properties of low cost, little processing, abundant naturally or as a waste product (Bulut and Tez, 2007), high efficiency, affinity (in terms of equilibrium and kinetics), stable (mechanically and chemically), with the possibility of recycling (Kleinübing *et al.*, 2011), that does not produce secondary compounds, short operating time (Morosanu *et al.*, 2017), metal recovery (Das *et al.*, 2014) and environmentally friendly (Nagy *et al.*, 2017), it is worth mentioning that the biosorption capacity depends on the active sites of the material and the nature of the type of contaminant to be removed (Taty-Costodes *et al.*, 2003), because in the active sites, there are functional groups such as carboxyls, xylanes, hydroxyl, carbonyl, amino and phenolic compounds to mention the most important (Lodeiro *et al.*, 2006; Han *et al.*, 2006; Pehlivan *et al.*, 2008).

On the other hand, the science of biomaterials in recent years has been developing with the incorporation of biologically active compounds, these have gone from being merely implantable devices, designed to replace the loss of a biological function, to become multifunctional and complex interfaces with a dynamic behavior in the interaction with the body and capable of activating the innate regenerative potential of living beings. Around 2700 types of medical devices considered biomaterials have been developed. At present, the science and engineering of biomaterials are multidisciplinary activities that, both in the field of research and development, as well as in industry and clinical and environmental application, occupy an increasing number of highly qualified people. Biomaterials combine medicine, biology, physics, chemistry, tissue engineering, materials science and environmental science.

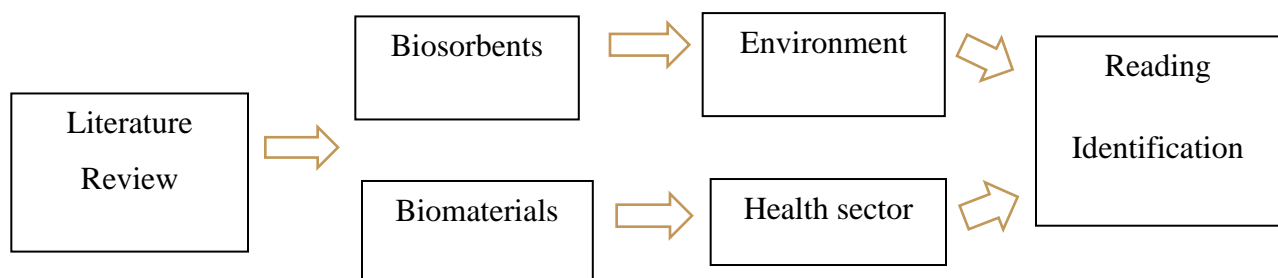
For this reason, this research mentions the study of different materials called biosorbents for the removal of organic and inorganic pollutants that in a certain way is an alternative to purify environmental pollution because they promise to be somehow profitable likewise it has been found that modifications of materials with different chemicals increase the removal of contaminants, however, such modifications can increase the cost of biosorbents (Park *et al.*, 2010), taking into account the feasibility and efficiency, as well as optimal operating conditions for the removal of different contaminants that exist in the environment. In this way, the information of several studies carried out on biomaterials applied in the health sector was also considered because they are essential to improve the quality of life due to their wide spectrum of physical, mechanical and chemical properties, to mention a few, as well as today the extensive research, development and applications of different biomaterials has been promoted.

Therefore, this chapter is divided into the following sections: introduction, methodology and results in which it is divided into two sections, the first section mentions biosorbents and the second section biomaterials.

2 Methodology to be developed

A qualitative research was carried out, based on the bibliographic review of documents related to biosorbents and biomaterials at national and international level, as well as their application in the environment and in the health sector. Scientific articles from which data and information were collected were reviewed. The Science Direct and SciELO databases were consulted. Figure 2.1 shows a diagram of the general methodology.

Figure 2.1. Diagram of the methodology



Source of Consultation: Own Elaboration

3 Results

This study will mention biosorbents applied in the area of the environment and biomaterials in the health sector. We will begin to describe the biosorbents applied in the removal of organic and inorganic pollutants present in aqueous solutions (water) and in the second section what is related to biomaterials used in the health sector.

3.1 Biosorbents

Within the environment, a biomaterial helps water, air and soil not to be polluted, since thanks to the toxic and harmful pollutants that exist on the planet they cause global warming to increase and can end life on the planet. Nowadays, research is being developed to help generate biomaterials which are effective and efficient to reduce environmental pollution in water, soil and air.

Biosorbents are natural materials available in large quantities or from certain waste products of industrial or agricultural operations, for application in the bioadsorption process, the material used as biosorbent must meet the following requirements: a) have an availability and as a type of waste, b) easy to obtain and process for a conditioning of the material, and (c) it must be economical and sustainable. Several researchers have investigated various types of materials of biological origin and have proposed bacteria, fungi, algae, plant remains and crustacean residues as biosorbents. These materials have the advantage that they are produced in large quantities, are economical and can have capabilities as adsorbents due to the presence of the active functional groups in their structures (Gallego *et al.*, 2022). In the literature it is reported that adsorbents are divided into three main categories: natural materials, industrial by-products and products of anthropogenic origin.

However, new studies have focused on the use of various materials mainly of organic origin such as sawdust. Particularly for similar materials, it has been pointed out that the bioadsorption capacity is due to the potential amount of organic compounds capable of interacting with contaminants, among which are: tannins, polysaccharides, glycoproteins, heterocyclic compounds, flavonoids etc., of which the functional groups amino, hydroxyl, carboxylate and sulfhydryl, have been associated with the adsorption of various contaminants. In the same way, some research has been reported for the removal of heavy metals and dyes using coffee residues or chitinous residues as biosorbents. These studies indicate the potential of these residues to be used as biosorbents.

On the other hand, there are factors that affect the biosorption process, since it depends on the nature of the substance to be eliminated, the characteristics of the adsorbent and the experimental conditions, which are determinants in the greater or lesser affinity of the adsorbate for the adsorbent. Table 3.1 lists the main factors affecting the biosorption process.

Table 3.1 Factors affecting the biosorption process

Factors	Description
Effect of pH	It affects the capacity of biosorption in aqueous solution, influencing the surface charge of the adsorbent and the way in which the species to be adsorbed are
Surface functional groups	They are responsible for the adsorption sites in a solid, depending on the type of ions present, the characteristics of the surface, the nature of the adsorbate and the pH of the solution.
Pore surface and structure	The biosorption capacity of the solid adsorbent is generally proportional to the specific surface. However, if it is a less porous adsorbent, which has surface functional groups, the interactions may cease to be physical, entering to dominate other mechanisms such as ion exchange and complexation.
Particle size	For a porous solid, particle size is expected to be independent of retention capacity, since most of its surface is in its internal porous structure. However, in some cases the biosorption capacity increases by reducing the particle size, as well as increasing the contact area and accessibility of small molecules.
Nature of adsorbate	Retention is influenced by solubility, molecular weight, and solute particle size. In the biosorption process there must be greater affinity for the biosorbent since it requires a certain attraction between it and the solute, in addition to a repulsion against the solvent.
Effect of temperature	The effect of temperature on biosorption depends on the thermodynamics of the process, generally when the heat of biosorption is negative the reaction is exothermic and the process is favored at low temperatures.
Equilibrium time	It is the time when the biosorbent is saturated. It has been determined that the retention mechanism occurs initially with the migration of the adsorbate from the solution to the surface of the biosorbent, followed by a diffusion process to end in the fixation at the active site.

Source: Own Elaboration

Table 3.2 lists the biosorbents applied in the bioremoval of organic and inorganic pollutants.

Table 3.2. Biosorbents applied in the removal of organic and inorganic contaminants.

Biosorbent	Conditions	% Removal
Activated carbon (Burciaga, 2020)	It is a function of several factors, including pH, temperature and contaminant concentration, where the properties of the adsorbent determine the removal mechanism.	Pb(II): 70.32 mg/g Cr(VI): 169.5 mg/g Hg (II): 25.88 mg/g
Zeolite	Grain size: 2mm PV= 1.0 g/cm ³ Bulk density 2.0 g/cm ³ CIC=138.7 meq/100 g zeolite pH=7.4	Pb (II): 510 mg/g Cu (CI): 170 mg/g Hg (II): 25.88 mg/g SiO ₂ 63 % Al ₂ O ₃ : 11,57 % FeO ₃ : 1.87 % Na ₂ O: 2.39 % H ₂ O: 3.44 % TiO ₂ : 0.45 %
Double network hydrogels	They can be degraded quickly for the elimination of adsorbed species by modifying the pH of the medium.	Cd (II): approx. 180 mg/L. 1 g/L of the biosorbent was quickly reached equilibrium, achieving complete removal of the contaminant.
Chitatan hydrogels coupled with clay minerals.	It exhibited extraordinary mechanical, optical and swelling properties.	Cr(VI): 96 mg/g Cu(II): 172.4 mg/g
Hydrogel reinforced with nanocomposites (assembly of attapulgite on a polyacrylamide matrix).	Acidification Copolymerization Polymerization in suspension.	Recovery of Pb (II) and Cu (II) in aqueous solutions. Cu(II): 69.75 mg/g
Compound hydrogel (Collagen/ chitosan/ cellulose)	Generation of interpenetrated networks by pH modification and cooling and drying cycles.	Cu(II): 145 mg/g
Rice straw (Diaz, 2021)	Particle size: 2mm Density: 1.56 g/cm ³ Bulk density: 0.017 g/cm ³ pH=7.0.	Ca: 1.1-5.8 % P: 0.3-4.3% Na: 0.1-2.5 % Mg: 1.0-3.6%
Sugarcane bagasse	Grain size: 1.5-2mm Bulk density 0.052 g/cm ³ pH=7.88	Lignin (20%) Cellulose (42%) Hemicellulose (25%)
Activated sludge	Grain size: 1.6mm Density 0.55 g/cm ³	Ca: 12 % Yes: 1.5 Mg: 0.8 % Na: 0.15 % P: 1 %
Eggshell (Escobar <i>et al.</i> , 2014)	10 kg of eggshell were collected. Constituted by 2.00; 4.00 and 6.00 g of pre-treated shell (F ₁ , F ₂ and F ₃ , respectively). Placed in constant stirring for 7 h with 500 mL of a Chromium (VI) solution of initial concentration 3.00 ppm	The absorbance in the aliquots was measured, determining the final concentrations of Chromium (VI), obtaining a removal percentage of 5.24% for F ₁ , 34.36% for F ₂ and 24.43% for F ₃ .
Bagasse and rice straw	Higher adsorption capacity at 20 min of contact. Under packaging conditions values of this parameter for COD 67 and 70 mg/g	Removals greater than 95% for sulphides, fats and oils with all materials.
Rice husk	Discontinuous study with 20 min of contact time and 20 g of material biosorption capacities were obtained for Pb, Cu, Ni and Fe of 1.3; 6.6; 8.2 and 40 mg/g.	With an elimination of 22%, 24, 95 and 68%, respectively
Argomena	Grain size: 1.6mm PV=0.98 g/cm ³ Density 2.1 g/cm ³ pH=7.01 Cation exchange capacity (CEC)=40-70 meq/100 g	Zeolite 42 % Phosphate rock 36 % Peat 16 % Urea 2.6 % (NH ₄) ₂ HPO ₄ 1.2 % KCl 2%
Natural cane bagasse	Biosorption capacity less than 7.57 mg/g that was improved up to 86.5% from bagasse modified with H ₃ PO ₄ .	Cu ²⁺ removal of 18.3%
Coffee grounds (Duany, Timosthe, 2022)	Dose of 30 g of coffee grounds, coffee grounds washed with deionized water applying 30 g / L of water.	The removal of cadmium and dissolved lead was 96.54 % and 94.05 % respectively.
Banana peel	Insoluble polymers, it has a high molecular weight, which results from the union of several acids and phenylpropyl alcohols, pulverized in it.	The highest clearance percentage is 80%
Moringa	High efficiency in turbidity reduction	It eliminated up to 85-94% and improved dissolved oxygen (DO). It was observed after treatment as Fe, Cu and Cd, were eliminated up to 98% and Pb 78.1%.
Orange peel	The maximum removal capacity was presented 40 minutes after contact with contaminated water and the maximum biosorption capacity was obtained with a pH of 4.8. Orange peel has an adsorption power for Pb of 99.5% and for Cu (II) has a yield of 36.23 mg / g.	100% removal
Potato pulp (Burciaga <i>et al.</i> , 2020)	1 kg raw pastusa potato A solution containing 1 L of ascorbic acid (1 % w/v, pH 5.0) Stored at - 20 °C for 12 h	Being the contribution by biosorption 35% of total pollutant removal

Source: Own Elaboration

In Table 3.3, biomaterials for the removal of different types of contaminants are mentioned.

Table 3.3 Biomaterials for the removal of contaminants

Biomaterial	Conditions	% Removal
Potato pulp for removal of industrial contaminants (Morales, 2022)	Orange II: PM= 350.32g/mol Solubility= 116g/L at 30°C Total volume of mixture= 6.6 mL t= 0.5 and 1 h The absorbance at 420 nm increased as a function of time to a certain final value, which became stable over the time studied. The maximum absorption peak at 485 nm did not change as a function of pH	pKa=pK ₁ =1.0; pK ₂ =11.4 At the pH studied (5 – 9), the dye was in its undissociated state The molar extinction coefficient at 485 nm was 4.2 ± 0.2 a. u/c mM
Biomaterial for high-performance water-based adhesives (Presti, 2021)	Dopamine hydrochloride (Sigma-Aldrich, >99.9%), anhydrous ferric chloride FeCl ₃ (Sigma-Aldrich, ≥99.99% trace metal base), hydrochloric acid, HCl (Sigma-Aldrich, reactive grade, ≥37%) and sodium carbonate (Na ₂ CO ₃)	The silk fibroin solution (7.3%) was modified with the addition of dopamine hydrochloride at a final concentration of 2 × 10 ⁻³ , 20 × 10 ⁻³ and 200 × 10 ⁻³ m
Agromena (Agrom) (CIP14-184, 2015) (Rodriguez, 2021)	Grain size: 1.6 mm, PV=0.98 g/cm ³ density 2.1 g/cm ³ ; pH=7.01; cation exchange capacity (CEC)=40-70 meq/100 g	Zeolite 42 %; phosphate rock 36 %; peat 16 %; urea 2,6 %; (NH ₄) ₂ HPO ₄ 1,2 %; KCl ₂ %
Product Improver (PM)	Grain size: 1.5-2 mm, pH=7.88	Rice straw, bagasse, activated sludge and urea; N ₁ %; P ₁ ,34 %
Compound hydrogels; 1) Polyacrylamide 2) Carboxymethyl cellulose 3) Chitosan 4) Sodium Alginate/Vinyl	1) Acidification and polymerization in suspension It has great adsorbent capacity, and is simple to reactivate 2) Generation of hydrogels by modification of pH and temperature. High adsorbent capacity and biodegradability 3) Dispersion of the inorganic phase by sonication modifying the pH Simple and efficient functionalization and absorbance	1) Cu (II): 69.75 mg/g 2) Cr (VI): 21.7 mg/g Cd (II): 25.7 mg/g 3) Cu (II): 172.4 mg/g 4) Pb (II): 432.28 mg/g

Source: Own Elaboration

The atmospheric applications within the field of study of biomaterials is broad, since to produce any type of biomaterial a proposal analysis has to be done to verify that the synthesis or creation of this does not affect the environment anymore. This type of analysis serves to avoid less atmospheric emissions in order to try to reduce the damage that occurs from the beginning.

Currently, innovation efforts are focused on improving their properties and reducing their cost, work is being done to overcome the sustainability of these biomaterials, for example; Biopolymers so that they are not only commonly used in packaging, but also become the new star material of contemporary society. On the other hand, 0.4% of world production corresponds to biopolymers, however, its high cost can not fight against the economic, some strategies that are being evaluated to reduce the cost of biopolymers is the use of by-products of the industry as raw material, the design of bioreactors or improvements in processes.

Although water-soluble plastics have been developed or that degrade under the action of light (they contain substances that weaken the bonds of their molecules when receiving light), the degradation is not total.

Another important fact is that they can be produced from renewable resources, their fermentative production uses products derived from agriculture as a source of carbon, because of their origin from renewable sources and because they are biodegradable, they are called "doubly green polymers", however it is important to mention that biopolymers are already used in other sectors, such as automotive and electronics, and are beginning to be used as co-formulants in the chemical industry and as citizens better understand the advantages that biopolymers represent in terms of saving energy resources and reducing pollution, the demand for this type of materials also increases in other sectors.

3.2 Biomaterials

A biomaterial is defined as that natural or synthetic material used to be in contact with a living being, so it must have specific properties to perform its function properly, so it must be biocompatible. They are materials, natural or artificial (man-made), used in the manufacture of devices that interact with biological systems and that are applied in various specialties of medicine either to increase or replace a tissue, organ or a function of the organism. They are systemically and pharmacologically inert, which means that they should not provoke a response in the body and that they do not adversely affect its tissues. They are designed to be incorporated or implanted in a living being, they are able to be in contact with living tissues (muscle, bone, blood, body fluids, etc.) without affecting their properties (depending on what they were designed for). They are used to replace parts of the human body; Example: Unsaturated fatty acids, to treat different diseases and wounds (sutures, catheters, needles, plates, etc.), are also used with diagnostic and storage applications. Depending on the type of biomaterial, they are used for varying periods of time. They can be metallic, ceramic, polymeric or combined (composite).

Properties of biomaterials

To succeed in the application of these biomaterials, properties such as; mechanics, toxicity, surface modification, degradation rate, biocompatibility and corrosion rate and structural design. Table 3.4 mentions the main properties of biomaterials.

Table 3.4 Properties of biomaterials

Property	Description	Example
Biological (Elices, 2020)	It is the result or reaction of a hard or soft tissue against a material.	Cozy and intelligent scaffolding for implants and spare organs.
Chemical (Saenz 2004)	They are the reactions that the material undergoes against pH changes, ionic changes or against electrical stimuli.	Ceramics: Aluminium oxides, Calcium aluminates, titanium oxides, calcium phosphates, carbon. Application in Orthopedics, Dentistry and Veterinary.
Physical	They include the properties of handling, adhesion, dimensional variations (thermal or electrical), etc.	Evaluate external actions such as light, heat, electricity or the application of forces. Type of viscosity of a biomaterial
Mechanical or biomechanical	They are physical properties that appear when a force is exerted on the material (ductility, hardness, elasticity, tensile strength, fatigue resistance). In this type of properties, it will depend on the type of device to be manufactured.	A hip replacement must be strong and rigid; Material to replace a tendon should be strong and flexible; Heart valve should be flexible and hard; Dialysis membrane should be strong and flexible; Joint cartilage replacement should be soft and elastic. These materials have high elasticity and can be deformed long before they break, for example, an elastic band.
Thermoplastic	They can be melted and molded repeatedly when heated and then cooled and solidified while maintaining their basic chemical properties. Their ability to be reused and recycled makes them very versatile and easy to process.	Applications such as packaging, pipes, toys, car parts, textiles, among others.
Toxicity	It consists of the identification and quantification of adverse effects associated with exposure to physical agents, chemical substances and other situations.	Effects that occur in tissues by contact with released biomaterials and can occur independently or associated, for example, the adverse effect resulting from contact with a xenobiotic (Laygre, 1995). Adverse reactions may be allergic or non-allergic.
Biocompatibility	It is the description and characterization of a reproducible response by biological tissue or relative to the materials used. From the development of biomaterials according to the response of the organism there are 4 types: Inert. Implantable materials that generate little or no response Interactive. Implantable materials that generate a specific response Viable. Implantable materials that are treated by the body like normal tissue and are reabsorbed. Reimplantation. Implantable materials consisting of native tissue, developed in vitro from cells obtained from the patient. The compatibility index is also considered, which tells us how suitable or not of that material, to be used as a biomaterial in a living being, taking into account its application.	Dental materials are known to be used on humans for long or short periods of time, are similar to other specialized materials used in orthopedics, cardiovascular surgery, plastic surgery and ophthalmology, are in close contact with various human tissues. For example, in dentistry the following biocompatibility tests are performed: Group I or primary tests. Group II or secondary tests. Group III or evidence of preclinical use. (Anusavice, 1996).
Biodegradability	It is the resistance of a substance to be decomposed into the chemical elements that compose it by the action of living organisms, usually microorganisms, under environmental conditions. The higher the biodegradability; easier to decompose.	In implants, biodegradability is important as it avoids a second surgery to remove the implant, ensures that the biomaterial is chemically stable and has an electrical behavior suitable for its application. A bone fixation plate should do its job for 6 months or more. A heart valve should flex 80 times per min without rupturing for the patient's lifetime (expected to be for 10 years or more). A hip joint should not fail under heavy loads for more than 10 years.

Source: Own Elaboration

Due to the properties and characteristics of biodegradability, it makes them very versatile to be used in many functions of our daily lives.

Applications of biomaterials

Biomaterials have evolved according to the needs and problems generated by the human being, they are very useful since they can be used in different areas. Therefore, they must be evaluated with some specific parameters so that they truly fulfill the function for which they were designed and generate a benefit. It is essential to have a mixture of chemistry, nanotechnology, engineering and design to be able to create a biomaterial that can replace a human need without affecting the environment. (Ramirez *et al.*, 2016) Biomaterials combine medicine, biology, physics, chemistry, sustainable development engineering and materials science. (Duffo, 2012).

In the area of health, biomaterials are those natural or synthetic substances whose mission is to replace a part or some function of our body, in a safe and physiologically acceptable way, can help the proper functioning of the human body, the main types of biomaterials that have been applied in the field of regenerative medicine, include natural and synthetic polymers, bioactive ceramics and composite materials, such as gels and cell matrices, even to grafts improved with stem cells and organ design, as well as other applications of biomaterials include diagnostics (gene sets and biosensors), medical supplies (blood bags and surgical tools), therapeutic treatments (implants and medical devices) and emerging regenerative medicine (skin and cartilage designed by tissue) (Lo Presti *et al.*, 2021). They can be classified in different ways: according to their chemical composition, in biometals, biopolymers, bioceramics, biocomposites and semiconductors; according to their origin, in natural and synthetic. Another more practical way to classify them are implantable devices, which are implanted over time in the human body to replace a function, and non-implantable devices, which include probes and catheters, among others. Table 3.5 lists the classification of biomaterials and Table 3.6 presents the classification of biomaterials by generations in the health sector.

Table 3.5 Classification of biomaterials according to type

According to its origin	According to its nature	Depending on the body's own response
Natural	Metals	Inert
Synthetic	Polymers	Bioactives
	Ceramic	Reimplanted
	Compounds	Biodegradable
	Biopolymers	Non-degradable

Source: Own Elaboration

Table 3.6. Classification of biomaterials through generations in the health sector

Generation	Type of Biomaterial	Application	Example
First	Inert	Replace damaged tissues with minimal receptor toxicity response	Metal implants Dental ceramic materials
Second	Bioactive and biodegradable	Interaction with the biological environment to improve the response, progressively degrading in the new tissue	Bioactive glass Compositos (polymer-ceramic)
Third	Functionalized	They are able to stimulate a cellular response at the molecular level	Biomaterials with extracts Biomaterials with functionalized surface
Fourth	Functionalized and intelligent	Stimulate specific cells to help the body heal itself	Polypyrrole-based biomaterials Biomaterials with hydroxyapatir

Source: Reyes *et al.*, 2019

Table 3.7 presents biomaterials in the health sector and Table 3.8 describes some biomaterials and their use in the health sector.

Table 3.7 Applications of biomaterials in the health sector

Biomaterial	Application
Medical implants	These include heart valves, stents, and grafts; artificial joints, ligaments and tendons; hearing loss implants; dental implants; and nerve-stimulating devices. Methods to promote healing of human tissues, including sutures, clips, and staples for wound closure, and dissolvable dressings.
Regenerated human tissues	As biomaterial supports or scaffolds, bioactive cells and molecules, such as bone regeneration hydrogel and a lab-grown human bladder.
Molecular probes and nanoparticles	They break down biological barriers and aid in cancer diagnosis and therapy at the molecular level.
Biosensors	They are used to detect the presence and amount of specific substances and to transmit that data, such as blood glucose monitoring devices and brain activity sensors.

Source: Own Elaboration

Table 3.8. Uses of biomaterials

Biomaterial	Uses
Titanium alloys	Joint replacement
Stainless steel	Joint replacement
Polyethylene (PE)	Joint replacement
Hydroxyapatite	Repair of bone defects
Teflon, Dacron	Artificial tendons and ligaments
Titanium, Alumina (Al ₂ O ₃), Calcium phosphate (CaPO ₄)	Dental implants
Stainless steel	Fracture fixation plates
Cobalt alloys with chromium	Fracture fixation plates
Polymethylmethacrylate	Bone cement
Stainless steel, Dacron	Heart valves
Teflon, Polyurethane (PUR)	Catheter
Polyurethane (PUR)	Artificial heart
Polyacrylonitrile, cellulose	Artificial kidney
Silicone gum	Ventilators
Hydrogels, silicone-acrylate	Contact lenses
Silicone and collagen composite materials, cellulose, polyacrylonitrile	Insoles for skin repair
Collagen, hydrogel	Cornea
Calcium phosphate ceramics	To repair certain intraosseous defects, they are non-toxic, biocompatible with the body and do not significantly disrupt the levels of calcium and phosphorus in the blood. It is a material classified in bioceramics that are hard and degrade very slowly, it is usually necessary to combine them with biodegradable polymers to achieve better results. This type of implants are used to promote bone recovery in fractures, for example, it has been observed that these biomaterials with mesenchymal stem cells can promote rapid and perfected tissue regeneration in certain animals, a biomaterial is not only a mineral or compound, but a mixture of organic and inorganic elements that try to find the perfect balance to achieve their functionality.
Bioactive crystals	They are ideal for certain regenerative processes at the bone level, their degradation rate can be controlled, they secrete certain ionic materials with osteogenic potential and have a more than correct affinity meeting with bone tissue. For example, studies have shown that some bioactive crystals promote the activation of osteoblasts, bone tissue cells that secrete intercellular matrix that give bone its hardness and functionality.
Resorbable bicortical screws	Resorbable plates and screws based on polylactic and polyglycolic acids, increasingly replace the hard titanium elements that brought so many problems when welding injuries. For example, polyglycolate is a strong, non-rigid material, does not fray and offers good safety as an abutment during suturing. These materials outperform titanium as they cause less patient discomfort, are more economical and do not require surgical removal.
Biomaterial patches	The National Institute of Biomedical Imaging and Bioengineering is developing alginate patches, based on brown algae, as therapeutic sealants to treat lung infiltrations from trauma, surgery, or conditions such as pneumonia and cystic fibrosis. The results of these technologies are promising, as alginate patches respond well to pressures similar to those exerted by the lungs and aid tissue regeneration in these organs so essential for life.
Hydrogel bandage	The use of hydrogel would act as an ideal film to prevent infection and degradation caused by environmental conditions in the wound. In addition, it could be dissolved at the rate of certain controlled procedures and expose the injury without the mechanical stress that this entails, this would improve the hospital stay of patients with severe burns.

Source: Own Elaboration

Another aspect that is of great interest and that today is creating a great impact around the world are bioplastics, however, the price of bioplastics is still high so that they can displace traditional plastics, because of this it is necessary to design strategies to obtain at a similar cost, So the price of biopolymers depends on several factors; production costs, yield of the polymer obtained and processing costs. On the economic front, it is estimated that the global market value of orthopedic biomaterials will reach around US\$26 billion by 2026 and grow at a CAGR of over 10.0% over the forecast time, making this market highly attractive to both researchers and companies looking to provide such solutions to the market. (CIQA).

Acknowledgements

This work has been funded by the Technologic of Studio's Superiors of Jocotitlán and the Secretary of the Ministry of Mexico with the project: Study, evaluation and treatment of pollutants present in environmental matrices through sustainable processes for technological development, PI202022, 2020-2022/2023.

Conclusions

In the application of the biosorbents of any contaminant, it is conditioned by the type of material, pH, temperature and contact time, the type of contaminant must be considered to obtain a better biosorption efficiency, however it is important to mention that according to the bibliographic review a large part of the reported studies have been carried out in batch, Therefore, it is necessary to carry out more research focused on all the factors that affect biosorption, to do it on a pilot scale, industrial and considering economic processes with a focus on recovering the biomaterial and having better environmental sustainability. Therefore, the revised biosorbents and biomaterials can be considered as a treatment alternative for the biosorption of contaminants.

As for biomaterials, they are indispensable to improve human health and quality of life due to the wide spectrum of physical, mechanical and chemical properties, as well as one of the determining factors for the acceptance of new biomaterials for this type of applications is their useful life. Today, biomaterials technology is being focused on composite biopolymers, in such a way that it promotes a great effort to investigate how biomaterials work and how to perfect them.

References

- Anusavice, K.J. Philip's Science of dental materials. Tenth ed. Biocompatibility. (1996), Philadelphia: Saunders Company. 75-99. <https://books-library.net/files/download-pdf-ebooks.org-1533070470MI0P8.pdf>
- Akar Sibel T., Yilmazer D., Celik S., Balk Y. Y. and Akar T. (2015). Effective biodecolorization potential of surface modified lignocellulosic industrial waste biomass. *Chemical Engineering Journal* 259: 286-292. <https://doi.org/10.1016/j.cej.2014.07.112>
- Araujo L., Cabreira V. L., Luan S., C., R., Antonio da S. E., Watanabe T., De Padua F., R. V., (2022). Biosorption of uranium from aqueous solutions by *Azolla* sp. and *Limnobium laevigatum* *Environ sci pollut res* 29:45221–45229. <https://doi.org/10.1007/s11356-022-19128-8>
- Bulut Y. and Tez Z. (2007). Removal of heavy metals from aqueous solution by sawdust adsorption. *Journal of Environmental Sciences* 19 (2): 160–66. http://www.jesc.ac.cn/jesc_cn/ch/reader/create_pdf.aspx?file_no=2007190206
- Burciaga Montemayor N., Claudio Rizo L.F., Martinez Luevano A., Vega Sanchez P., (2020), Composites in hydrogel state with application in the adsorption of heavy metals present in wastewater. <https://doi.org/10.22201/fesz.23958723e.2020.0.211>
- Das D., Vimala R. and Das N. (2014). Biosorption of Zn (II) onto *Pleurotus platypus*: 5-Level Box–Behnken design, equilibrium, kinetic and regeneration studies. *Ecological Engineering* 64: 136–141. <https://doi.org/10.1016/j.ecoleng.2013.12.051>

- Díaz Rodríguez, Y. L. M. (2021). Adsorption Capacity of natural Materials for the treatment of process water from oil activity.
- Duffo, G. (2012). Biomaterials. Obtained from Biomaterials: didactic guide: <https://www.inet.edu.ar/wp-content/uploads/2012/11/biometales.pdf>
- Duany Timosthe, S. (2022). Chemical Technology. Obtained from unconventional bioadsorbents used in the removal of heavy metals. Revision.
- Elices Calafat, M., Biological materials and biomaterials, Royal Academy of Sciences. <https://rac.es/ficheros/doc/9c154482325d90a8.pdf>
- Escobar M., Lobo G., Maza M., Pineda A., Romero L., Velasquez J., De la Rosa Ma. A. (2014). Evaluation of the use of eggshell as an adsorbent substrate for the removal of Chromium (VI) in aqueous solution. <http://revistacvml.jimdo.com>
- Espinoza Martínez A. B., Dávila Mendoza A. J., Ramos de Valle L. F., Biomaterials and their importance in the medical sector Center for Research in Applied Chemistry (CIQA). <http://www.ciqa.mx/Biomateriales.aspx>
- Gallego Ramírez C., Rubio Clemente Ainhoa. Removal of dyes in water from the textile industry through the use of biochar (2022) *Afinidad. Journal of Chemical Engineering Theoretical and Applied Chemistry*, Vol. 79, Num. 596. <https://doi.org/10.55815/401287>
- Han R, Li H., Li Y., Zhang J., Xiao H. and Shi J. (2006). Biosorption of copper and lead ions by waste beer yeast. *Journal of hazardous materials* 137 (3): 1569-1576. <https://doi.org/10.1016/j.jhazmat.2006.04.045>
- Jayakumar R., Rajasimman M. and Karthikeyan C. (2015). Optimization, equilibrium, kinetic, thermodynamic and desorption studies on the sorption of Cu (II) from an aqueous solution using marine green algae: *Halimeda gracilis*. *Ecotoxicology and environmental safety*. *International Journal of Environmental Science and Technology* 121:199-210. <https://doi.org/10.1016/j.ecoenv.2015.03.040>
- Kleinübing S.J., Da Silva E.A., Da Silva M.G.C. and Guibal E. (2011). Equilibrium of Cu (II) and Ni (II) biosorption by marine alga *Sargassum filipendula* in a dynamic system: Competitiveness and selectivity. *Bioresource technology* 102 (7): 4610-4617. <https://doi.org/10.1016/j.biortech.2010.12.049>
- Lygre, H., Aromatic leachables from denture base materials, in Department of dental biomaterials; School of Dentistry. (1995), University of Bergen: Bergen
- Lodeiro P., Barriada J. L., Herrero R. and De Vicente M E Sastre (2006). The marine macroalga *Cystoseira baccata* as biosorbent for Cadmium (II) and lead (II) removal: Kinetic and equilibrium studies. *Environmental pollution* 142(2):264-273. <https://doi.org/10.1016/j.envpol.2005.10.001>
- Marco Lo Presti, Giorgio Rizzo, Gianluca M. Farinola, and Fiorenzo G. Omenetto, (2021), Bioinspired Biomaterial Composite for All-Water-Based High-Performance Adhesives, *Adv. Sci.* 8, 2004786. <https://doi.org/10.1002/advs.202004786>
- Morosanu I., Teodosiu C., Paduraru C., Ibanescu D. and Tofan L. (2017). Biosorption of lead ions from aqueous effluents by rapeseed biomass. *New biotechnology* 39: 110-124. <http://dx.doi.org/10.1016/j.nbt.2016.08.002>
- Morales-Urrea, D. A. (2022). Use of potato pulp as biomaterial for removal. Obtained from Use of potato pulp as biomaterial for removal. <https://doi.org/10.1007/s11356-018-2134-8>
- Nagy B., Manzatu C., Măicăneanu A., Indolean C., Barbu-Tudoran L. and Majdik C. (2017). Linear and nonlinear regression analysis for heavy metals removal using *Agaricus bisporus* Macrofungus. *Arabian Journal of Chemistry* 10: S3569-S3579. <https://doi.org/10.1016/j.arabjc.2014.03.004>

- Park D., Yun Y. S. and Park J. M. (2010). The Past, Present, and Future Trends of Biosorption. *Biotechnology and Bioprocess Engineering* 15(1): 86-102. <https://doi.org/10.1007/s12257-009-0199-4>
- Pehlivan E., Yanik B.H., Ahmetli G. and Pehlivan M. (2008). Equilibrium isotherm studies for the uptake of cadmium and lead ions onto sugar beet pulp. *Bioresource technology* 99(9): 3520-3527. <https://doi.org/10.1016/j.biortech.2007.07.052>
- Pérez Morales (2019). *Environ Sci pollut res* 26:5955-5970. <https://doi.org/10.1007/s11356-018-04097-8>
- Presti, M. L. (2021). Bioinspired Biomaterial Composite for All-Water-Based. Obtenido de Bioinspired Biomaterial Composite for All-Water-Based: <https://doi.org/10.1002/advs.202004786>
- Ramírez A., Benítez J.L., Rojas de Astudillo L. and Rojas de Gáscue B. (2016). *Rev. LatinAm. Metal. Mat.*; 36 (2): 108-130, www.rlmm.org
- Restrepo Ospina DP, Ardila Medina CM. Adverse reactions caused by biomaterials used in prosthodontics. (2010) *Av. Odontoestomatol*; 26 (1): 19-30. <https://scielo.isciii.es/pdf/odonto/v26n1/original2.pdf>
- Reyes Blas I., Olivas Armendáriz, Martel Estrada S. A., Valencia Gómez L.E. (2019) Use of Functionalized Biomaterials with Bioactive molecules in Biomedical Engineering, *Revista Mexicana de Ingeniería Biomedica*, Vol. 40, No. 3. pp 1-20, <https://dx.doi.org/10.17488/RMIB.40.3.9>
- Rodriguez, Y. D. (2021). Adsorption capacity of natural materials.
- Sáenz Ramírez, A. (2004). *Biomaterials, Technology in progress*. Vol. 17 N° 1. Technology underway. Vol. 17 N° 1.
- Taty-Costodes V. C., Fauduet Henri, P. C. and Delacroix A. (2003). Removal of Cd (II) and Pb (II) ions, from aqueous solutions, by adsorption onto sawdust of *Pinus sylvestris*. *Journal of hazardous materials* 105(1): 121-142. <https://doi.org/10.1016/j.jhazmat.2003.07.009>

Instructions for Scientific, Technological and Innovation Publication

[[Title in Times New Roman and Bold No. 14 in English and Spanish]

Surname (IN UPPERCASE), Name 1st Author†*, Surname (IN UPPERCASE), Name 1st Coauthor, Surname (IN UPPERCASE), Name 2nd Coauthor and Surname (IN UPPERCASE), Name 3rd Coauthor

Institution of Affiliation of the Author including dependency (in Times New Roman No.10 and Italics)

International Identification of Science - Technology and Innovation

ID 1st Author: (ORC ID - Researcher ID Thomson, arXiv Author ID - PubMed Author ID - Open ID) and CVU 1st author: (Scholar-PNPC or SNI-CONAHCYT) (No.10 Times New Roman)

ID 1st Coauthor: (ORC ID - Researcher ID Thomson, arXiv Author ID - PubMed Author ID - Open ID) and CVU 1st author: (Scholar-PNPC or SNI-CONAHCYT) (No.10 Times New Roman)

ID 2nd Coauthor: (ORC ID - Researcher ID Thomson, arXiv Author ID - PubMed Author ID - Open ID) and CVU 1st author: (Scholar-PNPC or SNI-CONAHCYT) (No.10 Times New Roman)

ID 3rd Coauthor: (ORC ID - Researcher ID Thomson, arXiv Author ID - PubMed Author ID - Open ID) and CVU 1st author: (Scholar-PNPC or SNI-CONAHCYT) (No.10 Times New Roman)

(Report Submission Date: Month, Day, and Year); Accepted (Insert date of Acceptance: Use Only ECORFAN)

Citation: First letter (IN UPPERCASE) of the Name of the 1st Author. Surname, First letter (IN UPPERCASE) of the First Coauthor's Name. Surname, First letter (IN UPPERCASE) of the Name of the 2nd Co-author. Surname, First letter (IN UPPERCASE) of the Name of the 3rd Co-author. Last name

Institutional mail [Times New Roman No.10]

First letter (IN UPPERCASE) of the Name Publishers. Surnames (eds.) Title of the Handbook [Times New Roman No.10], Selected Topics of the corresponding area © ECORFAN- Subsidiary, Year.

Instructions for Scientific, Technological and Innovation Publication

Abstract (In English, 150-200 words)

Text written in Times New Roman No.12, single space

Keywords (In English)

Indicate 3 keywords in Times New Roman and Bold No. 12

1 Introduction

Text in Times New Roman No.12, single space.

General explanation of the subject and explain why it is important.

What is your added value with respect to other techniques?

Clearly focus each of its features

Clearly explain the problem to be solved and the central hypothesis.

Explanation of sections Chapter.

Development of headings and subheadings of the chapter with subsequent numbers

[Title No.12 in Times New Roman, single spaced and bold]

Products in development No.12 Times New Roman, single spaced.

Including graphs, figures and tables-Editable

In the Chapter content any graphic, table and figure should be editable formats that can change size, type and number of letter, for the purposes of edition, these must be high quality, not pixelated and should be noticeable even reducing image scale.

[Indicating the title at the bottom with No.10 and Times New Roman Bold]

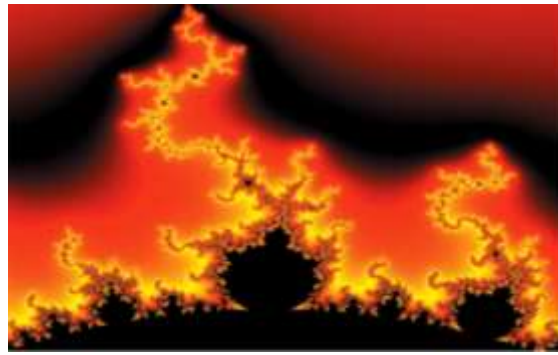
Table 1.1 Title

Variable	Descripción	Valor
V_V	Volumen de Venta	20000
P_V	Postura de venta	490.61
V_C	Volumen de Compra	20000
P_C	Postura de Compra	485.39
p^{Uh}	Precio último Hecho	491.61
V_o	Volumen Operado	1241979
P_u	Precio/Utilidad	0
p^{VL}	Precio/Valor Libro	0
U_a	Utilidad p/Acción	0
V^{La}	Valor Libro p/Acción	0

Source (in italics)

Should not be images-everything must be editable.

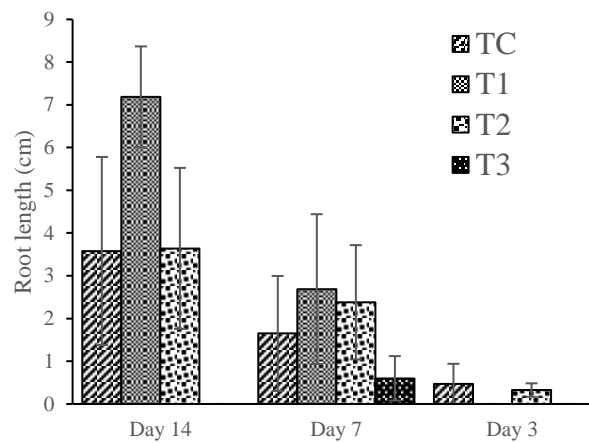
Figure 1.1 Title



Source (in italics)

Should not be images-everything must be editable.

Graphic 1.1 Title



Source (in italics)

Should not be images-everything must be editable.

Each chapter shall present separately in **3 folders**: a) Figures, b) Charts and c) Tables in .JPG format, indicating the number and sequential Bold Title.

For the use of equations, noted as follows:

$$\int_{lim^{-1}}^{lim^1} = \int \frac{lim^1}{lim^{-1}} = \left[\frac{1(-1)}{lim} \right]^2 = \frac{(0)^2}{lim} = \sqrt{lim} = 0 = 0 \rightarrow \infty \quad (1)$$

Must be editable and number aligned on the right side.

Methodology

Develop give the meaning of the variables in linear writing and important is the comparison of the used criteria.

Results

The results shall be by section of the Chapter.

Annexes

Tables and adequate sources

Instructions for Scientific, Technological and Innovation Publication

Thanks

Indicate if they were financed by any institution, University or company.

Conclusions

Explain clearly the results and possibilities of improvement.

References

Use APA system. Should not be numbered, nor with bullets, however if necessary numbering will be because reference or mention is made somewhere in the Chapter.

Use Roman Alphabet, all references you have used must be in the Roman Alphabet, even if you have quoted an Chapter, book in any of the official languages of the United Nations (English, French, German, Chinese, Russian, Portuguese, Italian, Spanish, Arabic), you must write the reference in Roman script and not in any of the official languages.

Technical Specifications

Each chapter must submit your dates into a Word document (.docx):

Handbooks title
Chapter title
Abstract
Keywords

Proceedings sections, for example:

1. *Introduction*
2. *Description of the method*
3. *Analysis from the regression demand curve*
4. *Results*
5. *Thanks*
6. *Conclusions*
7. *References*

Author Name (s)
Email Correspondence to Author
References

Intellectual Property Requirements for editing:

- Authentic Signature in Color of Originality Format Author and Coauthors
- Authentic Signature in Color of the Acceptance Format of Author and Coauthors
- Authentic Signature in Color of the Conflict of Interest Format of Author and Co-authors.

Reservation of Editorial Policy

ECORFAN Handbooks se reserva el derecho de hacer los cambios editoriales requeridos para adecuar la Obra Científica a la Política Editorial del ECORFAN Handbooks. Una vez aceptada la Obra Científica en su versión final, el ECORFAN Handbooks enviará al autor las pruebas para su revisión. ECORFAN® únicamente aceptará la corrección de erratas y errores u omisiones provenientes del proceso de edición de la revista reservándose en su totalidad los derechos de autor y difusión de contenido. No se aceptarán supresiones, sustituciones o añadidos que alteren la formación de la Obra Científica.

Code of Ethics - Good Practices and Declaration of Solution to Editorial Conflicts

Declaration of Originality and unpublished character of the Scientific Work, of Authorship, on the obtaining of data and interpretation of results, Acknowledgments, Conflict of interests, Assignment of rights and distribution

The ECORFAN-Mexico, S.C Directorate asserts to the Authors of the Scientific Work that its content must be original, unpublished and of Scientific, Technological and Innovation content to be submitted for evaluation.

The Authors signing the Scientific Work must be the same that have contributed to its conception, realization and development, as well as the obtaining of data, interpretation of the results, its writing and revision. The Correspondent Author of the proposed Scientific Work will request the form that follows.

Title of the Scientific Work:

- The sending of a Scientific Work to ECORFAN Handbooks emanates the commitment of the author not to submit it simultaneously to the consideration of other serial publications for it must complement the Format of Originality for its Scientific Work, unless it is rejected by the Arbitration Committee, may be withdrawn.
- None of the data presented in this Scientific Work has been plagiarized or invented. The original data are clearly distinguishable from those already published. And you have knowledge of the test in PLAGSCAN if a level of plagiarism is detected Positive will not proceed to arbitrate.
- References are cited on which the information contained in the Scientific Work is based, as well as theories and data from other previously published Scientific Works.
- The authors sign the Authorization Form for their Scientific Work to be disseminated by means that ECORFAN-Mexico, S.C. in its Holding Mexico consider relevant for the dissemination and dissemination of its Scientific Work by giving up its Scientific Work Rights.
- The consent of those who have provided unpublished data obtained by verbal or written communication has been obtained, and such communication and authorship are adequately identified.
- The Author and Co-Authors who sign this work have participated in its planning, design and execution, as well as in the interpretation of the results. They also critically reviewed the paper, approved its final version and agreed with its publication.
- No signature responsible for the work has been omitted and the criteria of Scientific Authorization are satisfied.
- The results of this Scientific Work have been interpreted objectively. Any result contrary to the point of view of those who sign is exposed and discussed in the Scientific Work.

Copyright and Access

The publication of this Scientific Work entails the transfer of the copyright to ECORFAN-Mexico, SC in its Mexico Holding for its ECORFAN Handbooks, which reserves the right to distribute on the Web the published version of the Scientific Work and the making available of the Scientific Work in this format supposes for its Authors the fulfillment of what is established in the Law of Science and Technology of the United States of Mexico, regarding the obligation to allow access to the results of Scientific Research.

Title of the Scientific Work:

Name and surnames of the Contact Author and the Coauthors	Signature
1.	
2.	
3.	
4.	

Principles of Ethics and Declaration of Solution to Editorial Conflicts

Publisher Responsibilities

The Publisher undertakes to guarantee the confidentiality of the evaluation process, it may not disclose to the Arbitrators the identity of the Authors, nor may it reveal the identity of the Arbitrators at any time.

The Editor assumes the responsibility of properly informing the Author of the phase of the editorial process in which the text is sent, as well as the resolutions of Double Blind Arbitration.

The Editor must evaluate the manuscripts and their intellectual content without distinction of race, gender, sexual orientation, religious beliefs, ethnicity, nationality, or the political philosophy of the Authors.

The Editor and his editing team of ECORFAN® Holdings will not disclose any information about the Scientific Work sent to anyone other than the corresponding Author.

The Editor must make fair and impartial decisions and ensure a fair peer arbitration process.

Responsibilities of the Editorial Board

The description of the processes of peer review is made known by the Editorial Board in order that the Authors know the evaluation criteria and will always be willing to justify any controversy in the evaluation process. In case of Detection of Plagiarism to the Scientific Work the Committee notifies the Authors for Violation to the Right of Scientific, Technological and Innovation Authorization.

Responsibilities of the Arbitration Committee

The Arbitrators undertake to notify about any unethical conduct by the Authors and to indicate all the information that may be reason to reject the publication of the Scientific Work. In addition, they must commit to keep confidential information related to the Scientific Work that they evaluate.

Any manuscript received for your arbitration must be treated as confidential, must not be displayed or discussed with other experts, except with the permission of the Editor.

The Referees should conduct themselves objectively, any personal criticism of the Author is inappropriate.

The Arbitrators must express their points of view with clear and valid arguments that contribute to the Scientific, Technological and Innovation of the Author.

The Arbitrators should not evaluate the manuscripts in which they have conflicts of interest and that they have been notified to the Editor before submitting the Scientific Work to evaluation.

Responsibilities of Authors

Authors must ensure that their Scientific Works are the product of their original work and that the data have been obtained in an ethical manner.

Authors must ensure they have not been previously published or are not being considered in another serial publication.

Authors must strictly follow the rules for the publication of Scientific Works defined by the Editorial Board.

Authors should consider that plagiarism in all its forms constitutes unethical editorial conduct and is unacceptable, consequently any manuscript that incurs plagiarism will be removed and not considered for publication.

Authors should cite publications that have been influential in the nature of the Scientific Work submitted to arbitration.

Information services

Indexing - Bases and Repositories

RESEARCH GATE (Germany)

MENDELEY (Bibliographic References Manager)

GOOGLE SCHOLAR (Citation indices-Google)

REDIB Ibero-American Network of Innovation and Scientific Knowledge-CSIC

Publishing Services

Citation and Index Identification H

Management of Originality Format and Authorization

Testing of Handbooks with PLAGSCAN

Evaluation of Scientific Work

Issuance of Certificate of Arbitration

Edition of Scientific Work

Web layout

Indexing and Repository

Publication of Scientific Work

Certificate of Scientific Work

Editing Service Billing

Editorial Policy and Management

143 – 50 Itzopan, Ecatepec de Morelos–Mexico. Phones: +52 1 55 6159 2296, +52 1 55 1260 0355, +52 1 55 6034 9181; Email: contact@ecorfan.org www.ecorfan.org

ECORFAN®

Chief Editor

VARGAS-DELGADO, Oscar. PhD

Executive Director

RAMOS-ESCAMILLA, María. PhD

Editorial Director

PERALTA-CASTRO, Enrique. MSc

Web Designer

ESCAMILLA-BOUCHAN, Imelda. PhD

Web Diagrammer

LUNA-SOTO, Vladimir. PhD

Editorial Assistant

REYES-VILLO, Angélica. BsC

Philologist

RAMOS-ARANCIBIA, Alejandra. BsC

Advertising & Sponsorship

(ECORFAN® -Mexico – Bolivia – Spain – Ecuador – Cameroon – Colombia - El Salvador – Guatemala -Nicaragua-Peru-Paraguay-Democratic Republic of The Congo, Taiwan), sponsorships@ecorfan.org

Site Licences

03-2010-032610094200-01-For printed material ,03-2010-031613323600-01-For Electronic material,03-2010-032610105200-01-For Photographic material,03-2010-032610115700-14-For the facts Compilation,04-2010-031613323600-01-For its Web page,19502-For the Iberoamerican and Caribbean Indexation,20-281 HB9-For its indexation in Latin-American in Social Sciences and Humanities,671-For its indexing in Electronic Scientific Journals Spanish and Latin-America,7045008-For its divulgation and edition in the Ministry of Education and Culture-Spain,25409-For its repository in the Biblioteca Universitaria-Madrid,16258-For its indexing in the Dialnet,20589-For its indexing in the edited Journals in the countries of Iberian-America and the Caribbean, 15048-For the international registration of Congress and Colloquiums. financingprograms@ecorfan.org

Management Offices

143 – 50 Itzopan, Ecatepec de Morelos–México.

21 Santa Lucía, CP-5220. Libertadores -Sucre–Bolivia.

38 Matacerquillas, CP-28411. Morazarzal –Madrid-España.

18 Marcial Romero, CP-241550. Avenue, Salinas 1 - Santa Elena-Ecuador.

1047 La Raza Avenue -Santa Ana, Cusco-Peru.

Boulevard de la Liberté, Immeuble Kassap, CP-5963.Akwa- Douala-Cameroon.

Southwest Avenue, San Sebastian – León-Nicaragua.

31 Kinshasa 6593 – Republique Démocratique du Congo.

San Quentin Avenue, R 1-17 Miralvalle - San Salvador-El Salvador.

16 Kilometro, American Highway, House Terra Alta, D7 Mixco Zona 1-Guatemala.

105 Alberdi Rivarola Captain, CP-2060. Luque City- Paraguay.

69 Street. YongHe district, ZhongXin. Taipei-Taiwan.

43 Street # 30 -90 B. El Triunfo CP.50001. Bogota Colombia



ISBN 978-607-8948-04-8



www.ecorfan.org